Modelling the Interaction between Human Immunodeficiency Virus, Mycobacterium Tuberculosis and the Human Immune System, including the Effects of Drug Therapy

by

Santosh Ramkissoon

Submitted in fulfilment of the academic requirements

for the degree of Master of Science in the

School of Physics

University of KwaZulu-Natal

February 2007

Abstract

Tuberculosis (TB) is the leading cause of death in individuals infected with human immunodeficiency virus (HIV) in several African countries, including South Africa. HIV-positive individuals do not have the immune system resources to keep TB in check and are as much as 30 times more likely to develop active TB than people who are HIV-negative. Many people infected with HIV develop TB as the first manifestation of AIDS and TB accelerates disease progression in HIV-positive individuals. HIV and TB pathogenesis are thus inextricably intertwined so that it is necessary for medical practitioners to have an understanding of the dynamics and treatment of HIV-TB coinfection. At present the question remains as to whether the best time for coinfected individuals to start antiretroviral treatment for HIV is at the beginning, the peak, or after the completion of the TB treatment phase. This dissertation was undertaken with the aim of obtaining some clarity on this question by creating a mathematical model of HIV-TB coinfection and its treatment. This needs an understanding of the biological interactions; therefore the dissertation begins with a discussion of the biological mechanisms of HIV, the human immune system, TB and the drug therapies for each disease. Thereafter a brief introduction to mathematical modelling reviews basic HIV models, which are then modified to include HIV drug therapy. Analyses and simulations of these models were carried out, which yielded some insights into the dynamics of HIV and HIV therapy. Finally HIV-TB coinfection is introduced by reviewing a previously developed model. Based on all the models reviewed, a model for coinfection is developed which includes treatment for HIV and TB. Numerical simulations suggest that, if HIV disease progression is at an advanced stage of the immune system collapsing towards AIDS, with low T-cell count and high viral load, it is necessary to treat for both diseases simultaneously to ensure a positive survival prognosis for the coinfected individual. However, if disease progression is in the early stages of AIDS, with T-cell count and viral load beginning to display signs of the immune system collapse but still at reasonable levels relative to advanced stages, it need not be necessary to treat both diseases simultaneously. TB can be treated first, and upon completion HIV treatment can be initiated thus sparing the coinfected individual from the compounded side-effects and drug-drug interactions which usually result from simultaneous treatment.

Acknowledgements

I would like to express my sincere gratitude to my supervisor, Dr. A.P. Matthews, and cosupervisor, Dr. H.G. Mwambi. They have allowed me the academic freedom to choose the path that my research should take and were always willing to offer their knowledge and guidance. I would also like to express my gratitude to my parents, Anand and Chumpa Ramkissoon, without their support none of this would have been possible.

Declaration

This dissertation represents the original work of the author. In the instances where use has been made of other researchers' work, acknowledgements are duly made. This research has not been previously submitted, in any form, to any other institution.

Mr. Santosh Ramkissoon

4 October 2007

Date

Dr. A.P. Matthews
MSc. Supervisor

2 November 2007

Date

Dr. H.G. Mwambi
MSc. Cosupervisor

2 November 2007

Date

Dedication

To all those who have been affected by HIV/AIDS, directly or indirectly. By facing such adversity we are constantly reminded of the great resilience of the human spirit. Due to the disease one witnesses firsthand the amazing capacity for human compassion of those people who are involved in the fight against HIV/AIDS. Many people all over the world are united in selflessly pooling their resources – be they financial, academic or social – to overcome a common foe.

Contents

Table of Figures

Chapter 1

Introduction

HIV/AIDS represents a multifaceted challenge to society. Its burden is felt not only by the mortality rates associated with the disease, but also in terms of its social and economic impact. In order for humanity to come to terms with this scourge, there needs to be collaboration by the different groups of people who are involved in the fight against the disease. This need is most apparent in the scientific sphere. As an example the collaboration of mathematical and biological scientists has proved successful in revealing features of viral dynamics that were previously unknown. Mathematical models have been used to demonstrate the somewhat counter-intuitive fact that during the asymptomatic stage of HIV disease progression the viral turnover rate is approximately 10 billion HIV virions per day.

Such successes clearly encourage the development of mathematical models to yield insight into the quantitative and qualitative dynamics of disease progression. An area where this insight could potentially be useful is the problem of HIV-TB coinfection. Sub-Saharan Africa in particular has very high HIV-TB coinfection rates. TB is curable in HIV-positive individuals. In fact, if TB is not treated, the HIV disease progression increases in its rapidity and death soon results. Generally, when people are HIV-TB coinfected, their immune system is already well on its way to collapsing towards AIDS. This means that the immune system is in a delicate state; therefore, death could result from either one of the two diseases. Even so, medical practitioners are reluctant to treat both diseases simultaneously due to the adverse compounded side-effects and undesirable drug-drug interactions of combining HIV and TB treatment. This problem is significant enough to warrant the running of medical trials in order to answer the question, when would the optimal point in time be to commence antiretroviral treatment in coinfected individuals? The START trials (STarting Anti-Retroviral Therapy) undertaken by the Centre for the AIDS Programme of Research in South Africa (CAPRISA) in order to

address the issues involving treatment of coinfection seek to ascertain whether the best time to start antiretroviral treatment for HIV-TB coinfected individuals is at the beginning, the peak, or after the completion of the TB treatment phase.

The main aim of the dissertation focuses on this HIV-TB treatment predicament. One might sense that the development of a mathematical model to simulate the treatment of HIV-TB coinfection could lead to some practical insight as to what the best strategy to treat for coinfection is likely to be. Since medical trials such as START are typically time intensive, a mathematical model could offer predictions to medical researchers while they wait for the trials to run its course. Furthermore, once the trials are completed, the model can be evaluated using the clinical data from the trials. Thus the central goal in undertaking this research was to develop a mathematical model to simulate the treatment of HIV-TB coinfection and to test the various strategies used to treat coinfection. By doing this one is able to offer some suggestions, in terms of the model's results, as to what the optimal method of treating for coinfection is likely to be.

One should bear in mind that building and testing such a model requires an interdisciplinary approach. One needs firstly to be familiar with the biological aspects of the dynamics. Thereafter one needs to translate these biological dynamics into mathematical formalism by way of equations, which are then solved computationally in many cases. For this reason the contents of this dissertation can be viewed as having two distinct, but equally important, parts. The first part, Chapters 2 to 4, is devoted to describing the biological underpinnings of Human Immunodeficiency Virus (HIV), Tuberculosis (TB), the human immune system and the treatment therapies for HIV and TB. The second part, Chapters 5 to 8, deals with the mathematical modelling component of the research.

An introduction to the biological aspects of HIV-TB coinfection and its treatment was undertaken to familiarise the reader with the mechanisms of biological interactions of the system to be modelled. However, in attempting to understand the system one should not get bogged down by trying to understand the minute details of the system; rather one

should familiarise oneself with those aspects of the system that would yield insight when translated into mathematical formalism. The above thought is astutely summarised by Albert Einstein [wikiquote.org],

"Things should be made as simple as possible, but not any simpler"

The discussion of the biological aspects of HIV and TB was done with this thought in mind. From a mathematical modeller's point of view one needs only to understand the underlying mechanism by which the observed biological interactions between HIV, TB and the immune system take place. Once these interactions are translated into mathematical formalism they present themselves as nonlinear differential equations. As one finds later in the dissertation, even simple-looking nonlinear differential equations which have simple underlying mechanisms of interaction, can produce exceedingly complex dynamics. Happily for us the converse holds true as well in that the complex immunological dynamics which take place within the human body can be reproduced by simple underlying mechanisms. Therefore, as a mathematical modeller one need not attempt to explain the minute details of the biology, rather one need only understand the underlying mechanisms of interaction which are necessary to build a successful model, a model that yields insight into the immunological dynamics. The nitty-gritty of the biology should be left to the biologist.

However, with that said any person reading the biological account that follows in Chapters 2 to 4 will have a coherent and relevant understanding of the biology of HIV, TB and the immune system. Chapter 2 is dedicated to familiarising the reader with HIV, its transmission routes, molecular structure, characteristics of disease progression, replication cycle, drug therapies and historical accounts of the disease. Chapter 3 deals with describing the human immune system. The functioning and description of the immune system cells that are specifically involved during the pathogenesis of HIV and TB are described. Chapter 4 gives an account of Tuberculosis. A discussion is made of the epidemiological statistics, implications for coinfection with HIV, pathogenic mechanisms and the treatment of the disease.

The second part of the thesis, Chapters 5 to 8, presents the mathematical modelling aspect of the research, where the goal is to create a mathematical model of HIV-TB coinfection with treatment. In order to achieve this objective the following strategy was pursued. Initially the reader is familiarised with the mathematical modelling of biological systems by being introduced to various population models. Population models are relevant to modelling HIV since HIV models are merely in-host population models. This is followed by the review of various HIV models. Some of these HIV models included treatment mechanisms. The modelling of HIV-TB coinfection is then reviewed by the presentation of a previously developed HIV-TB coinfection model. All models reviewed – HIV, HIV with treatment and HIV-TB coinfection – made it possible to build a suite of models that each contained certain desirable mathematical features. Combining these different features separately and together culminated in the development of a final all-inclusive model of HIV-TB coinfection and its treatment.

The strategy outlined above to develop a mathematical model of HIV-TB coinfection is presented in Chapters 5 to 8. Chapter 5 introduces the reader to mathematical biological modelling by simulating and analysing well-known population and predator-prey models. Chapter 6 reviews various HIV models. Model simulations, mathematical analyses and numerical bifurcation analyses are carried out. Mechanisms for simulating HIV treatment are added to the models. Treatment strategies and implication are discussed. Chapter 7 presents a model for HIV-TB coinfection. Simulations and discussions of the various permutations that the model displays are undertaken. The culmination of the dissertation is presented in Chapter 8. A new model is developed by using some of the mathematical structures found in the models that were previously presented. The model contains mechanisms that are able to simulate both the treatment of HIV and TB. Model simulations are carried out to evaluate the dynamics displayed by the model. Thereafter, the various treatment strategies used to treat HIV-TB coinfection are evaluated. The final chapter, Chapter 9, forms the conclusion of the dissertation. This chapter reviews the motivation for the dissertation, the research problems that were posed and the aims and objectives of the dissertation. A summary of the results from the model of HIV-TB coinfection with treatment is made. These results are then used to offer possible suggestions when treating for HIV-TB coinfection.

Chapter 2

Human Immunodeficiency Virus

2.1. Basic Virology

Viruses are pathogens that may cause death and disease to the living organisms that they infect. They are small particles that range in size from about 20 to 300 nano-metres [13, 29], and are probably the least complex of all life forms. In its basic form a virus consists of genetic material in the form of DNA or RNA. This is surrounded by a capsid, which is a casing composed of protein. Further to this it can also be encapsulated by a membrane consisting of a mixture of proteins and fatlike substances that serve to protect the viral genetic material [22]. Viruses are in fact so simple that they do not possess many of the characteristics used to define life. For example they cannot metabolise or reproduce on their own. In order to reproduce a virus must infect a living cell and use its host's biological processes to replicate. Morbidity and mortality, which are associated with viral infection, are only side-effects of the virus' primary reproductive objective.

The virus' life cycle is typically categorised into a few key events. The replication cycle begins with the virus attaching itself to the host cell, thereafter inserting its genetic material into its host. The viral genetic material is then exposed by an uncoating process and viral proteins are produced. These newly produced viral proteins manipulate the host cell to replicate the viral genome. Yet more viral proteins are produced for the coat and membrane of the nascent virus. Finally the virus particles are assembled and the new virions are released from the host cell. The virions may undergo internal structural changes once they have budded from their host cell to form a mature virus capable of causing infection.

2.2. HIV: An Overview

Infection with Human Immunodeficiency Virus (HIV) results in Acquired Immunodeficiency Syndrome (AIDS), which is characterised by a failing immune system and susceptibility to opportunistic infections caused by fungi, bacteria, parasites and other viruses. Due to the collapsing state of the immune system the infected individual has an inability to fight off the constant assault of opportunistic infections, which finally results in death.

Human Immunodeficiency Virus belongs to a category of viruses known as retroviruses [49, 99]. Retroviruses have their genome in the form of RNA which has to be translated into DNA during its lifecycle. This is generally the reverse of what usually occurs during the biological processes found in nature, hence the prefix '*retr*o'. Typically most biological processes proceed from DNA to RNA. In addition to being a retrovirus HIV is also a lentivirus [20, 99]. Lentiviruses are characterised by long incubation periods and long duration of illness. This has grave implications for the epidemiology of the disease since HIV-positive individuals can remain asymptomatic for many years and not know that they are infected, while spreading the disease to many others. HIV infection is spread by the transfer of infected bodily fluids such as blood, semen, vaginal fluid, or breast milk [6], which contain HIV present as free virus or as infected immune cells. Transmission can occur during any process that transfers infected bodily fluids from one individual to another. Typical routes of transmission are unprotected sexual intercourse, sharing of unsterilised hypodermic needles, usually amongst intravenous drug users, blood transfusions and from mother to child during breast feeding and child birth [124, 137].

2.3. HIV Virion Structure

The HIV genome encodes at least nine genes, these are - Gag, Pol, Env, Tat, Rev, Nef, Vif, Vpu and Vpr [99]. The first three genes are structural genes that encode for structural proteins used as building blocks, or are used in the construction of the building blocks, to

form the physical structure of new viral particles. The six remaining genes are regulatory genes, which encode for proteins that regulate the processes that the HIV virion performs, including viral replication by way of manipulation of the host cell's biological processes.

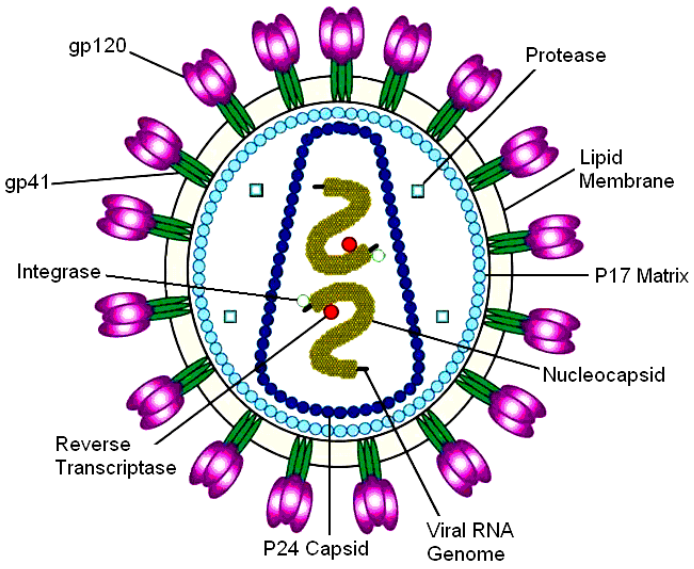

Figure 1: Structure of HIV virion [USA. Fed. Gov.].

A pictorial representation of an HIV virion is shown in figure 1. It is approximately spherical and has a diameter of about 120 nanometers [82]. The HIV virion's outer layer (viral envelope) is composed mainly of a bilayer of phospholipids [114]. Newly formed HIV virions are coated with the phospholipids bilayer as the viral capsid (core) emerges from the host cell during the budding process. The surface of the viral envelop is studded with the gp160 glycoprotein complex [18, 153, 154], which consists of a cap made from the glycoprotein gp120 and a stem made from the glycoprotein gp41. The surface glycoprotein complex enables the HIV virion to bind and subsequently fuse its capsid, including its genetic material, into its host cell [18, 51]. Just below the viral envelope is a matrix composed of the protein p17 [53, 67, 89]. The p17 protein performs important functions throughout the viral life-cycle, including anchoring the glycoprotein gp41 onto the surface of the virus, assisting in viral penetration, transporting the proviral integration complex across the nuclear envelope, and localizing the assembling virion to

the cell membrane [89]. Contained within the p17 matrix is the viral capsid, which is conical in shape and is composed of the protein p24 [1, 19]. The capsid contains the genetic material of HIV in the form of two copies of single-stranded RNA and enzymes such as reverse transcriptase and integrase, which are essential to the viral production process [3, 132].

2.4. HIV Replication Cycle

The replication cycle of HIV can typically be broken down into a number of steps. These steps are listed as: 1. Virion Binding and Capsid Insertion; 2. Reverse Transcription and Integration; 3. Transcription and Translation; 4. Assembly, Budding and Maturation.

2.4.1. Virion Binding and Capsid Insertion

Since HIV virions cannot replicate on their own they need to manipulate the biological processes of their host cells in order to do so. When an HIV virion comes into contact with a cell expressing CD4 on its cell surface, the gp120 glycoprotein spikes that protrude from the surface membrane of the HIV virion bind to the CD4 receptors [26, 32]. This binding induces a conformational change in the gp120/gp41 glycoprotein complex which allows the gp120 glycoprotein to bind to the chemokine coreceptors CXCR4 or CCR5 [36, 38, 51, 146]. This in turn induces an additional conformational change that exposes the gp41 glycoprotein and facilitates the entry of the viral capsid into the host cell [18, 48, 78, 106].

2.4.2. Reverse Transcription and Integration

Once the HIV virion has penetrated the cytoplasm of its host cell an uncoating step leads to the release of the viral RNA from its core [15]. The reverse transcriptase enzyme then copies the viral RNA into DNA [124]. The viral DNA is then transported into the nucleus of the host where the integrase enzyme facilitates the splicing of the viral DNA into the

host cell's DNA [21, 152]. The viral DNA that has been integrated into its host genome is known as a provirus.

2.4.3. Transcription and Translation

In the nucleus of the cell transcription of the cellular DNA into RNA, which are used as blueprints for protein building, takes place. At the same time RNA copies of the viral DNA, which has been spliced into the cellular DNA, are produced [58]. These copies are messenger RNA (mRNA) and travel to the cell's cytoplasm [47], where the Env precursor polyprotein gp160 is synthesized in the endoplasmic reticulum with subsequent post-translational modification of the Env polyproteins occurring at the endoplasmic reticulum and Golgi apparatus to form the gp120/gp41 glycoprotein complex [132]. The Gag and Gag-Pol polyproteins are synthesized in the ribosomes. The Gag polyprotein is the precursor to the matrix, capsid and nucleocapsid proteins [47, 65]. The Gag-Pol polyprotein is the precursor to the matrix and capsid proteins, as well as the protease, reverse transcriptase and integrase enzymes [119]. The polyproteins are transported to the cell membrane where viral assembly takes place.

2.4.4. Assembly, Budding and Maturation

During or after transport of the Gag and Gag-Pol polyproteins to the cell membrane the Gag precursor recruits two copies of the single-stranded viral RNA genome, interacts with the Gag-Pol precursor and assembles into structures lining the inner face of the plasma membrane [47]. The Env glycoproteins, which form the viral envelope spikes, are also incorporated into the assembled structures. The assembled Gag protein complex, which encapsidates the two copies of the viral genome, buds from the plasma membrane, see figure 2, taking some of the membrane with it [132]. At this stage the particles are not yet infectious. They go through a maturation process during which the Gag and Gag-Pol

polyproteins are cleaved by the protease enzyme into the proteins and enzymes that make up a functional HIV virion and triggers the rearrangement of the cleavage products to form mature HIV virions capable of causing infection [59].

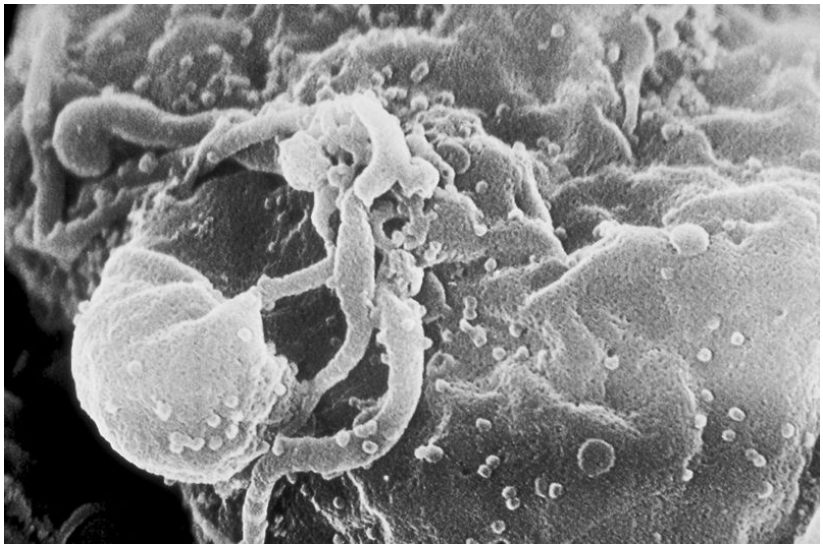

Figure 2: Electron microscope image of HIV virion budding [CDC].

2.5. HIV Disease Progression

The clinical course of HIV infection shown in Figure 3, leading ultimately to AIDS, varies between individuals in terms of viral load, symptoms and duration. However, there are four typical stages during disease progression that an HIV-positive individual experiences. These four stages were classified in 1990 by the World Health Organisation (WHO) [142] and are intended to be a means of establishing disease prognosis in a resource limited setting, such as one would typically find in Sub-Saharan Africa. These stages are classified as: Stage One – Primary Infection, Stage Two – Asymptomatic Infection, Stage Three – Symptomatic Infection, and Stage Four – AIDS. The World Health Organisation revised its classification of the various HIV stages in 2005; however, both classification systems are similar. For the sake of simplicity, as is necessary for mathematical modelling purposes, a review is made of the initial classification system.

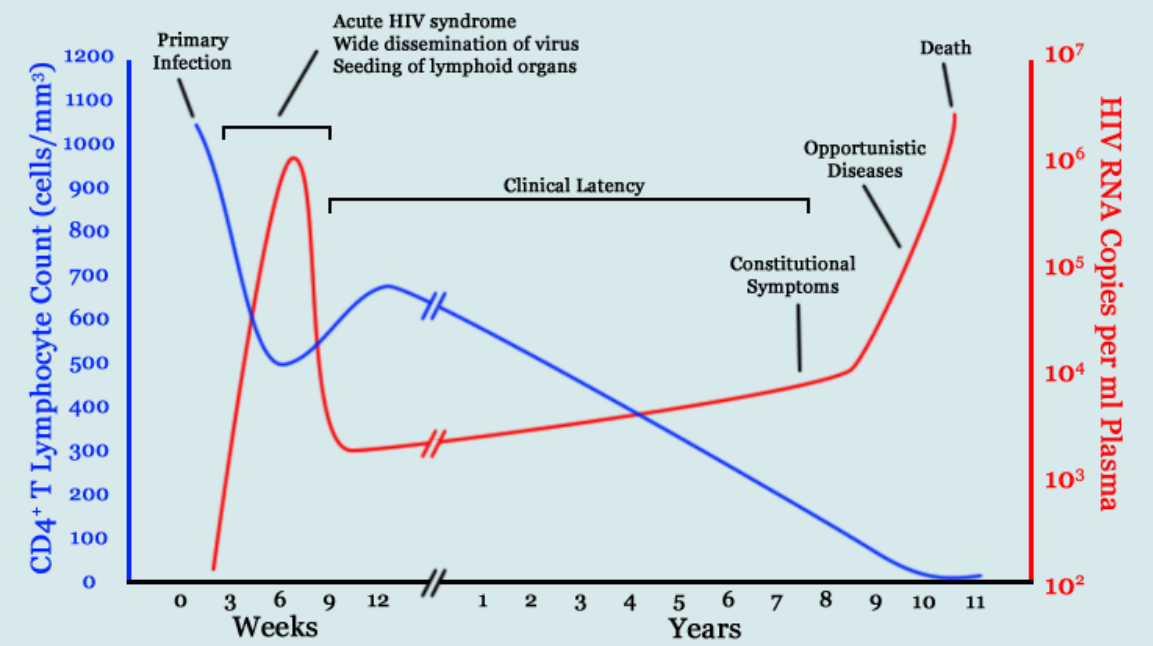

Figure 3: Graph of generalised HIV disease progression [Wikimedia Commons].

2.5.1. Primary Infection

Subsequently to initial infection with HIV viral replication commences in cells expressing CD4 receptors, primarily in $CD4^+$ T cells. Individuals develop high viral loads that typically peak somewhere in the range 10^3–10^5 virions per mm^3 of blood [124], resulting in high numbers of infectious virus and infected cells circulating in the peripheral blood. Within five to six weeks individuals may develop acute HIV syndrome, which is characterised by flu-like symptoms. This lasts for about a week, at which time the immune system mounts HIV specific immune responses, and the individual's flu-like symptoms disappear. This is accompanied by a decrease in the viral load of about one to two orders of magnitude, which is largely due to HIV specific $CD8^+$ T cell immune response; however, a limitation in the number of cells susceptible to HIV infection could also play a part [124, 127]. The $CD8^+$ T cells ability to decrease viral load is an important factor since the rapidity of disease progression is correlated with the level (set point) the viral load settles down to shortly after primary infection [91]. The set point viral load is characterised by being relatively stable over prolonged periods of time due to approximately equal rates of production and clearance of HIV virions.

2.5.2. Asymptomatic Infection

The viral load settling to its set point value signals the onset of the asymptomatic phase. This phase is characterised by clinical latency, shown in Figure 3, during which the HIV-positive individual remain free from any major symptoms. The typical duration of the asymptomatic phase is from 8 to 11 years [93, 129]. However, about 22% of individuals progress to AIDS within 5 years [96] and an estimated 8–15% of individuals will remain free from any AIDS defining illnesses for 20 years [95]. Even though HIV-positive individuals do not show AIDS related symptoms during this phase, the internal dynamics of the disease are not static in that there is a high turnover rate of HIV virions of the order 10^{10} virions per day [107], accompanied by a gradual decline in the $CD4^+$ T cell count [132].

2.5.3. Symptomatic Infection

Characteristic of disease progression through the various stages of HIV is an increase in viral load accompanied by a decrease in $CD4^+$ T cell count [73]. The increase in viral burden is temporally associated with the emergence of viral mutants displaying enhanced pathogenicity [25]. The failing immune system coupled with the high viral loads allows opportunistic infection, which would otherwise be controlled by the immune system, to appear. The diseases and symptoms which characterise WHO stage 3 are: unexplained weight loss of more than 10%, chronic diarrhoea for more than a month, prolonged fever (constant or intermittent) for more than a month, oral thrush, oral hairy leukoplakia, pulmonary tuberculosis and severe bacterial infections (i.e. pneumonia, pyomyositis). An individual in stage 3 of HIV infection would typically be bedridden for up to 50% of the day towards the end of this stage.

2.5.4. AIDS

The final stage of disease progression is characterised by the severe impairment of the immune system with an associated $CD4^+$ T cell count of less than 200 per mm^3 of blood.

As a result a whole host of life-threatening opportunistic infections, c.f. WHO report [142], known as AIDS Related Complexes (ARCs) appear. Without antiretroviral therapy an individual with AIDS would live on average for 9.2 months [93]. The average survival time, using the present treatment strategies, of individuals diagnosed with AIDS, is in excess of 5 years [123].

2.6. HIV/AIDS Drugs and Treatment Strategies

Antiretrovirals, which have been approved to treat HIV, come primarily in two variants [124] – reverse transcriptase inhibitors and protease inhibitors. Protease inhibitors are designed to inhibit the activity of the HIV protease enzyme by preventing it from cleaving the Gag polyprotein into the proteins and enzymes that make up a functional HIV virion. Reverse transcriptase inhibitors are designed to inhibit the HIV reverse transcriptase enzyme from transcribing the viral RNA into DNA, thereby foiling an essential part of the HIV life-cycle. Reverse transcriptase inhibitors fall into two categories, nucleoside analogues or nonnucleoside analogues. Nucleoside analogues function as chain terminators. They are incorporated into the growing DNA molecule by mimicking the structure of the host cell's DNA building blocks and thereby preventing its extension. Since they are structurally different from the host cells DNA when the viral DNA combine with these DNA building blocks they cannot integrate into the host cells DNA. A nonnucleoside analogue on the other hand binds to the HIV reverse transcriptase enzyme and disrupts the enzyme's ability to transcribe the viral RNA into DNA.

In addition to the above-mentioned antiretroviral drugs, there are several drugs in the developmental stage that target other key aspects of the HIV life-cycle. Fusion inhibitors block an HIV virion's ability to fuse with a candidate host cell's membrane, thereby rendering it unable to enter and infect the host cell. Integrase inhibitors disrupt the activity of the HIV integrase enzyme which facilitates the integration of the viral DNA

into the host cell's DNA. Entry inhibitors block an HIV virion's ability to enter a candidate host cell by binding to the CCR5 chemokine coreceptor, a vital mechanism of host cell entry.

Current treatment strategy for HIV is termed HAART (Highly Active Antiretroviral Therapy). There is much debate about the optimal timing during disease progression when HAART should commence. However, HAART is typically commenced when an individual's $CD4^+$ T cell count is less than 200 per mm^3 of blood or when an AIDS-related complex has been identified. HAART has several adverse side-effects; however, this is outweighed by its ability to reduce morbidity and mortality. Nevertheless HAART cannot completely eradicate HIV so treatment is generally continued for the duration of the illness [124]. HAART consists of a combination of at least three drugs belonging to two different classes, typically two nucleoside analogue reverse transcriptase inhibitors and either a protease inhibitor or a nonnucleoside analogue reverse transcriptase inhibitor. By combining these antiretroviral drugs one is able to suppress viral replication to low levels, thereby decreasing viral load and giving the immune system an opportunity to recover. Equally importantly, by slowing down the HIV replication rate, the emergence of drug-resistant HIV mutants is at least delayed if not prevented [124].

2.7. Viral Mutations and Drug resistance

Viral mutations are a consequence of the high HIV virion turnover rate of the order 10^{10} virions per day [107] and the fact that the reverse transcription step, which transcribes the genomic viral RNA into proviral DNA, is highly error prone and lacks proof-reading capabilities [112, 117]. This results in the production of genetically heterogeneous HIV virions, characterised by the appearance of mutant strains of the disease. Genetically heterogeneous HIV virions, called quasispecies, can have up to 15% diversity between them in an HIV-infected individual [88]. Genetic variation is thought to be one of the primary factors which enable HIV to escape eradication by the immune system.

During antiretroviral therapy the selective forces to which the viral mutants are subjected allow the virus to develop drug resistance; moreover HIV drug-resistant strains can be transmitted from one individual to another [148]. HIV mutants, with varying degrees of resistance, have been found for all drugs that have been used, or are being considered for use, as anti-HIV therapy [23]. The emergence of anti-HIV drug resistance is the most common cause of treatment failure. Nevertheless treatment failure due to drug resistance can be reduced by ensuring strict compliance with the antiretroviral administration routine and by using a cocktail of multiple antiretroviral drugs simultaneously, in most cases three drugs, which slows the replication rate of the virus, thereby curtailing the mutation rate.

2.8. Origin of HIV

HIV seems to be a zoonotic infection crossing species from African chimpanzees to human beings [52, 63] establishing two different strains of the disease. HIV-1 and HIV-2 are genetically distinct and crossed from different chimpanzee subspecies [80]. HIV-1 is responsible for the global HIV pandemic; therefore all references to HIV in this dissertation pertain to HIV-1 unless otherwise explicitly stated. HIV-1 is closely related to a strain of Simian Immunodeficiency Virus, classified as SIV_{cpz}, harboured by the Pan Troglodytes Troglodytes chimpanzees native to West Equatorial Africa [52]. The geographic location of origin of HIV-1 is most likely the Democratic Republic of Congo. Infected individuals in that country have a constant and extremely high genetic diversity of HIV-1 stemming from the likelihood that the disease was present there for the longest period, having more time to mutate relative to anywhere else on the globe [134, 135]. Estimates of the timescale of SIV_{cpz} crossing species into human beings, introducing the HIV-1 disease, place the event around 1930 [80, 121].

The HIV-2 strain is less virulent and not as easily transmissible as HIV-1 and is largely confined to West Africa [83]. Like HIV-1, however, HIV-2 is also closely related to a strain of Simian Immunodeficiency Virus, classified as SIV_{sm}, harboured by the Sooty

Mangabey monkeys indigenous to West Africa [52]. A reconstruction of the HIV-2 lineage puts the likely location of SIV_{sm} crossing species to establish the HIV-2 disease in the West African country of Guinea-Bissau around 1940; however, the disease only experienced rapid exponential growth, establishing itself as an epidemic, during the period 1955–1970 [111]. This period coincides with Guinea-Bissau's war for independence which most likely created the social conditions necessary for the rapid spread of the disease [83].

2.9. History of HIV

The earliest cases of HIV on record are plasma samples taken in 1959 of a man in the Democratic Republic of Congo [155], tissue samples of an American teenager who died in Saint Louis in 1969 [103] and tissue samples of a Norwegian sailor who died around 1976 [72]. It was, however, only in 1981 that the disease was clinically diagnosed and its existence brought to the attention of the global medical community when a group of homosexual men in Los Angeles, San Francisco and New York were afflicted by rare diseases caused by the suppression of the immune system [101].

In 1969, when the disease was initially introduced into the United States of America, it was unable to take off. Possible reasons for this could be that the disease needed carriers who engaged in frequent sexual intercourse with large numbers of partners in order to establish itself as an epidemic, a condition that was likely met by the homosexual population that initially carried the disease. By 1982 there were over 800 cases of AIDS in the United States. It spread from the initial homosexual population to haemophiliacs, who received blood derived products from donors, intravenous drug users, and the heterosexual population.

With the disease rapidly spreading, the search was now on to identify its causative agent. In 1983 Luc Montagnier and his team, working at the Pasteur Institute in Paris, identified the presence of a retrovirus in the lymph node tissue obtained from infected

individuals [4]. Soon afterwards Robert Gallo and his team, working at the National Institute of Health in Bethesda, Maryland, were also able to identify the retrovirus from infected patients [50, 122]. In addition the team at the NIH was able to multiply the retrovirus in continuous culture and was thereby able to develop a specific test for the disease [110]. This was a significant step which now gave health workers the ability to accurately diagnose the status of infected individuals and identify contaminated blood samples.

Since then there has been a wealth of research performed on the disease and numerous important features of the retrovirus' structure and dynamics have been established. Nevertheless there is still no vaccine or cure for the disease and there remains much research to be done in order to improve our understanding of the disease so that a vaccine or cure may be developed.

Chapter 3

Human Immune System

3.1. Immune System: An Overview

The immune system consists of organs, tissues and cells that function as an integrated unit to protect the body by overcoming infection due to pathogens such as viruses, bacteria, fungi and parasites. The immune system consists of the lymph vessels, lymph nodes, thymus, spleen, bone marrow and an elaborate network of interacting white blood cells [29]. At a fundamental level the immune system defence can either be adaptive or innate.

The adaptive immune system response is specific in that it adapts the immune response to maximise its effectiveness to eliminate a specific pathogen. After the immune system has eliminated the pathogen, it develops immunological memory whereby it is able to launch a quicker and more effective defence against the pathogen if it subsequently reappears.

The innate immune system response is nonspecific. It does not differentiate between the different types of pathogens that initiate the immune response. Thus it deals with all pathogens in a generic way. As a consequence of its generic manner, even for pathogens it has encountered before, the innate immune system does not develop immunological memory. Previous exposure to the pathogen would not be of any added advantage during future encounters.

3.2. Immune System Cells

White blood cells are the major protagonist of the immune system's defence against foreign substances (antigens). There are various subcategories amongst white blood cells that perform important functions in a healthy immune system. Foremost among these are the lymphocytes, which are made up of B cells and T cells, as well as the phagocytes, namely the macrophages.

3.2.1. B cells

B cells are produced in the bone marrow. They are able to recognise antigens that invade the body. B cells have antibody molecules on their cell surface that are able to identify localised regions, known as antigenic determinants, found on the surfaces of antigen molecules. The antigen binding site, found on specific regions on the antibody molecule, binds to an antigen if the antigenic determinant and the antigen binding site have complementary shapes and fit like a lock and key. The ability to combine the protein subunits that make up the antibody molecule in a vast number of different ways ensures that the antibody molecule binds to almost any antigen entering the body.

When the diverse array of B cells, each with differing antibody molecules on their cell surface, encounter an antigen only the B cell with the antibody molecule that best fits the antigenic determinant of the given antigen is activated to divide and form clones. This process, called clonal selection, ensures a high specificity for antibody-antigenic binding. Adding further to the specificity of the process is somatic mutation, whereby antibodies with slightly differing shapes are produced and might have a greater binding affinity to the given antigen. Variants that bind better have a stronger signal to multiply, thus replicating more rapidly and effectively outcompeting the other B cells that do not have as high a specificity. This process, called affinity maturation, ensures optimal specificity of the antibody-antigen binding. The stronger replication signal that accompanies the dynamics of greater specificity also ensures that large numbers of antibodies are

produced only when the body needs them. Furthermore in subsequent encounters with the given antigen the immune system is able to launch a faster and more effective attack due to some clones becoming long-lived memory cells.

B cells release their antibody molecules into the blood. The antibodies mark the pathogen for elimination by other immune cells such as, for example, phagocytes and the complement system of blood enzymes. The antibodies might even be able to neutralise the pathogen on their own by forming a coating so dense that it effectively prevents the pathogen from reproducing or invading target cells.

3.2.2. T cells

T cells are produced in the bone marrow, but undergo a maturation process in the thymus where they develop into functional immune cells that are differentiated according to the various tasks that each subcategory of T cells is required to carry out. The $CD8^+$ T cells are the killer cells, while the $CD4^+$ T cells are the helper cells. They are differentiated by the CD (cluster of differentiation) glycoprotein T cell receptor on their cell surface, either CD4 or CD8.

Vital to the proper functioning of the immune system is its ability to differentiate between self and nonself, ensuring it does not mount an immune response against its own cells and tissues by falsely identifying them as foreign, as is the case during autoimmune disease. The task of differentiating between self and nonself lies with the T cells.

When a virus infects a T cell, it undergoes antigen processing whereby the cell processes the viral proteins into smaller fragments, known as peptides. Parts of the peptides are then bound on the cell surface to the Major Histocompatibility Complex (MHC) molecules. T cell receptors bind to these MHC-peptide complexes; however, the interaction has a high degree of specificity and binding only occurs according to fit, analogously to the lock and key mechanism. During the T cell maturation process in the thymus, cellular peptides of immune system cells form MHC-peptide complexes that are presented to the

T cells for binding. Those T cells that are adequately able to bind to the MHC-peptide complexes are allowed to survive. The remaining T cells die by apoptosis, a process of programmed self destruction of cells. This mechanism of identifying T cells that are able to bind to MHC-peptide complexes is known as positive selection. However, in order to ensure that the T cell do not mistake normal cellular peptides for pathogenic peptides, the T cells also undergo negative selection. During negative selection those T cells that bind only weakly with self MHC-peptide complexes are allowed to survive. The rest of the T cells, which bind too strongly with the self MHC-peptide complexes, also undergo apoptosis in order to avoid autoimmune disease. T cells that survive the positive and negative selection processes can mature to $CD4^+$ or $CD8^+$ T cells, which are differentiated by the class of MHC molecule on antigen presenting cells to which their receptors bind. $CD8^+$ T cell receptors bind to MHC class one (MHC-1), while $CD4^+$ T cell receptors bind to MHC class two (MHC-2).

3.2.2.1. $CD8^+$ T cells

The $CD8^+$ T cells are cytotoxic. If a cell is infected by a virus, the cell processes the viral proteins into antigenic peptide fragments and transports them to the cell surface where they are bound to MHC-1. The MHC-peptide complexes are presented on the cell surface. $CD8^+$ T cells with the correct specificity are able to bind to the MHC-peptide complex and kill the infected cells by the release of perforins, proteins that cause death to the cell by puncturing its cellular membrane [14]. Once the $CD8^+$ T cells are activated they undergo clonal expansion, producing more $CD8^+$ T cells of the same specificity ready to kill the remaining virally infected cells. $CD8^+$ T are also equipped with chemicals and defence mechanisms that can inhibit infected cells from replicating or infecting other cells.

3.2.2.2. $CD4^+$ T cells

The $CD4^+$ T cells cannot by themselves kill infected cells. Nevertheless they do have an important role to fulfil in terms of regulating and optimising the various aspects of

cell-mediated immunity, for example $CD4^+$ T cells are necessary for the proliferation of activated $CD8^+$ T cells. They also fulfil a crucial role when establishing an antigen specific antibody immune response. Antigen Presenting Cells (APC), such as macrophages and B cells, internalise pathogens and present antigenic peptides bound to MHC-2 on their cell surface, which are then recognised by $CD4^+$ T cells. $CD4^+$ T cells of the correct specificity that are able to bind to the MHC-peptide complex ensure that the B cells are able to distinguish between self and nonself, while signalling to the B cells to increase its numbers via clonal expansion and produce more antibodies for the given antigen.

3.2.3. Macrophages

Macrophages are phagocytes that engulf and digest antibody-bound pathogens and other debris, such as dust, dead cells and tissue. Macrophages are derived from monocytes, white blood cells produced in the bone marrow that mature through a series of changes to become a macrophage. As is the case with B cells, macrophages are also antigen presenting cells. Subsequently to digesting an antigen they break the antigen down into smaller peptide fragments and present the antigenic peptides bound to MHC-2 on their cell surface. Circulating T cells are then able to recognise this MHC-peptide complex and become activated to mount a specific immune response against the antigen, which includes the stimulation of B cells to produce more antibodies for the given pathogen. Antibody-coated pathogens are cleared more easily by the immune system. This antigen-specific immune response strengthens the ability of the immune system to overcome the pathogen.

Chapter 4

Tuberculosis

"We cannot win the battle against AIDS if we do not also fight TB. TB is too often a death sentence for people with AIDS. It does not have to be this way."
– Nelson Mandela, XV International AIDS conference, Thailand 2004

4.1. Tuberculosis: An Overview

Tuberculosis (TB) is a contagious disease which typically results from being infected with the bacteria *Mycobacterium tuberculosis*, which is a rod-shaped bacillus [29].

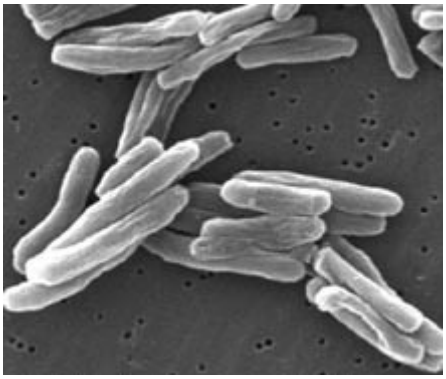

Figure 4: Electron microscope image of *Mycobacterium tuberculosis* [CDC].

TB is one of the oldest known diseases, with evidence of infection found in the vertebra of Stone Age Man and Egyptian mummies; as well as in records from ancient Greece, Rome, India, China and medieval Europe [55, 94, 98]. TB infection is spread through the air. It occurs by the inhalation of aerosol bacilli of its causative agent. TB commonly infects an individual's lungs. This form of TB is known as Pulmonary Tuberculosis. As a

result of active infection granulomas subsequently develop at infected sites in the lungs. These granulomas consist predominantly of aggregates of T cells and TB infected macrophages [68]. Granulomas undergo cell death, referred to as necrosis. Lung cavitation can result from necrosis due to the destruction of lung tissue. TB infection is not only confined to the lungs. Infection in other organs and tissues does occur as a result of bacilli migration via infected dendritic cells and peripheral blood.

4.2. Tuberculosis Epidemiology

TB is a major public health problem in most of the developing world. In Sub-Saharan Africa the problem is aggravated by the fact that TB is the main opportunistic disease of HIV [34, 40, 61]. As data became available, the World Health Organisation was able to make estimates for HIV-TB epidemiology for 2000, then 2002 and recently for 2004. Estimates for 2000 showed that TB infections attributable to HIV in WHO African member states was about 31%, with South Africa estimated to have had 2 million of the global total of 11 million HIV-TB coinfected individuals [27]. The 2002 estimates for HIV prevalence amongst adult TB patients revealed that Southern Africa faced grim prospects, with Zimbabwe (75%) and South Africa (60%) ranking amongst the worst affected [144]. Estimates for 2004 showed coinfection prevalence for the African continent increased to about 33%, with Southern African countries still faring poorly – Swaziland (81%), Botswana (77%), Lesotho (76), Zimbabwe (68%), Namibia (61%), South Africa (60%), Zambia (54%) and Malawi (52%) all being severely affected [145].

4.3. Tuberculosis-HIV Coinfection

Many people infected with HIV develop TB as the first manifestation of AIDS. HIV-positive individuals do not have the internal immune system resources to keep TB in check. In fact they are more than 20 times likely to develop active TB than people who are HIV-negative as the suppression of the immune system worsens [115]. Studies have shown that the host's immune response to the TB bacterium enhances HIV replication

and might accelerate the natural progression of the HIV infection [57, 97, 149]. In addition HIV can also accelerate disease progression in TB infection [31]. Therefore without treatment dually-infected individuals succumb to coinfection at a rapid rate.

4.4. Tuberculosis Pathogenesis

The etiological agent of TB is *Mycobacterium Tuberculosis*, first identified in 1882 by Robert Koch [79]. *Mycobacterium Tuberculosis* is an intracellular pathogen primarily infecting macrophages. TB infection begins when an uninfected individual inhales aerosol droplets containing *Mycobacterium Tuberculosis*. TB bacilli are expelled from the lungs of infected individuals when they cough. Once the bacilli are airborne they are inhaled by other individuals and typically get lodged in their alveoli, the tiny air sacs of the lung where gaseous exchange of oxygen and carbon dioxide take place [56]. Here the pathogen is engulfed and ingested by alveolar macrophages. Normally once pathogens have been phagocytosised by macrophages, they are transported to the macrophage's lysosomes, where digestive enzymes break down and destroy the pathogen. However, it seems that *mycobacteria* may be able to block their delivery to the lysosomes enabling them to survive within the macrophages and start to replicate [68]. The ability of bacilli to evade the initial nonspecific immune response depends upon various factors. These include the state of the immune system, where diseases like HIV may inhibit immune responses, as well as the virulence factor of the *mycobacteria* [125]. The more virulent strains of TB are characterised by greater transmissibility and produce greater morbidity and mortality in infected individuals.

The replication of bacilli within the macrophages attracts blood monocytes that mature into macrophages and ingest the released bacteria. During this stage in disease progression symbiosis occurs between bacteria and macrophages, with neither population eliminating the other. Bacteria continue replicating while blood-derived macrophages continue arriving. Macrophages that have ingested the *mycobacteria* process and present *mycobacterial* antigens to T lymphocytes. Two to three weeks after infection cell-

mediated immunity develops with the arrival of antigen-specific T lymphocytes that intensifies the immune response and activates macrophages to kill the intracellular *mycobacteria* [133]. In addition to the activated cell-mediated response the immune system also initiates an inflammatory response. The inflammatory response serves to inhibit dissemination of the *mycobacteria* by encapsulating *mycobacteria* infected macrophages, activated macrophages, and T cells within granulomas. The granulomas subsequently develop central areas of necrosis which kill most of the *mycobacteria*; however, the pathogen is almost never totally eradicated. Nevertheless, the vast majority of the TB-harbouring population, approximately 90% of TB infected individuals, are able adequately to contain the bacteria and do not progress to any symptoms of active TB [46]. In fact it is estimated that latent TB may be carried by a third of the global population [42]. From the remaining 10% of infected individuals the immune systems of approximately 5% are not able to adequately contain the bacteria and active TB results within a year of infection, with the other 5% going on to develop active TB at some later stage in life [139]. Immunosuppression, such as infection with HIV, greatly increases the risk of reactivation of latent TB amongst previously infected individuals. Under these conditions granulomas can become liquefied and are able to serve as a rich medium for the revived bacteria to replicate prodigiously [125].

4.5. Tuberculosis Treatment

The treatment of TB aims to cure patients of the disease, prevent death from active TB, prevent relapse of TB, decrease disease transmission and prevent development of acquired drug resistance [143]. In order to achieve these aims a combination of anti-TB drugs are used. The most widely used first-line treatment anti-TB drugs are Isoniazid, Rifampin, Pyrazinamide and Ethambutol. A typical treatment regimen involves taking Isoniazid, Rifampin, Pyrazinamide and Ethambutol for two months, then Isoniazid and Rifampin for the next four months. It is essential to maintain a strict adherence to the

drug intake regime as skipping a treatment or not completing the full course could result in a multidrug resistant strain of TB. Multidrug resistant TB takes longer to treat, treatment is more expensive, side-effects associated with the treatment are greater and treatment success rates are smaller.

In order to avoid such complications a TB control strategy has been developed from the collective best practices, clinical trials and programmatic operations of TB control over the past two decades [126]. This strategy, known as Directly Observed Treatment Short-course (DOTS), is widely regarded as being the most effective strategy for treating TB and is recommended by the World Health Organisation. The South African Department of Health has also adopted the DOTS strategy to treat TB by implementing its core features [126], which involve sputum smear microscopy to detect infectious cases among people attending health care facilities with symptoms of TB, standardised short-course anti-TB treatment with direct observation of treatment, an uninterrupted supply of TB drugs and a standardised recording and reporting system which allows assessment of treatment results.

4.5.1. Antituberculosis Drugs

4.5.1.1. Rifampicin

Rifampicin may be bacteriostatic, by inhibiting the multiplication of bacteria, or bactericidal, in that it kills bacteria. The bacteriostatic or bactericidal action of Rifampicin depends on the susceptibility of the bacterial species and the concentration of the drug. In the case of *M. tuberculosis* Rifampicin is bactericidal. In particular it possesses early bactericidal activity against active and semidormant bacterial populations, producing a sterilizing effect [71, 130]. Rifampicin inhibits the action of DNA-dependent RNA polymerase [17, 70], which is the enzyme that promotes the synthesis of RNA using a DNA or RNA template, thereby leading to the suppression of RNA synthesis and the subsequent translation to proteins in susceptible bacteria.

4.5.1.2. Ethambutol

Ethambutol is used in the initial phase of TB treatment primarily to prevent drug resistance to Rifampicin [7]. Ethambutol is generally considered to have a bacteriostatic effect on *M. tuberculosis* when used at typical doses during TB treatment [5]. The exact mechanism of interaction between Ethambutol and *M. tuberculosis* is still unknown; however, several hypotheses have been advanced. The most prominent amongst these theories propose that ethambutol interferes with the biosynthesis of arabinogalactan, a constituent of the *mycobacterial* cell wall [37]. A further theory suggests that Ethambutol acts as a chelating agent, capable of forming bonds with metals, and disrupts and deactivates one of several metal-containing enzyme systems in the nucleic acid structures of *mycobacteria* [90].

4.5.1.3. Isoniaziad

Isoniazid is bacteriostatic against dormant and semidormant *mycobacteria* and bactericidal against rapidly dividing *mycobacteria*. Its primary use stems from its potent early bactericidal action against actively dividing *mycobacteria*. Isoniazid's therapeutic mechanism results from its ability to inhibit the synthesis of mycolic acids, a major constituent of the *mycobacterial* cell wall [140]. Isoniazid inhibits the biosynthesis of mycolic acids by specifically targeting the enzyme InhA, which is essential to the biosynthesis process [118]. Mycolic acids form a lipid shell, which serves to determine permeability properties at the cell surface. They endow several unique characteristics to *M. tubeculosis* and are important to the growth, survival and pathogenicity of the *mycobacteria* [113].

4.5.1.4. Pyrazinamide

The concomitant use of Pyrazinamide with the other anti-TB drugs plays a unique role in shortening TB therapy from the previous 9–12 months to 6 months [151]. Pyrazinamide exerts its therapeutic effects by inhibiting the synthesis of fatty acids in *M. tuberculosis*

by disrupting the activity of the enzyme fatty acid synthetase I [156]. The drug is converted into its active form, pyrazinoic acid, by the *M. tuberculosis* enzyme pyrazinamidase. Pyrazinamidase, and consequently pyrazinamide, are only active at an acidic pH [150]. Once in its active form the drug shows bactericidal activity against *M. tuberculosis*, including bacilli within macrophages, presumably because of its acidic intracellular ph [5]. Its importance within the anti-TB drug regime stems from its sterilizing ability of dormant and semidormant tubercle bacilli, which are unaffected by other drugs [69, 151].

Chapter 5

Mathematical Biology

Mathematics can be applied to various systems in nature in order to gain qualitative and quantitative insight into the system. One can use mathematics to develop a model of the system, as has been the case in this dissertation where the aim was to develop a mathematical model of the interaction between HIV, TB and the human immune system, including the effects of drug therapy.

Many systems found in nature can be modelled by nonlinear coupled differential equations. Mathematical modelling is an iterative process in which one refines the model by successive iterations. The steps involved in modelling natural phenomena, as can be seen in Figure 5, are studying the phenomena, formulating a mathematical model of the phenomena, solving the model analytically or computationally, analysing and interpreting the solution, using the results to make predictions and gain insights about the phenomena and testing the validity of the insights and predictions.

Before a mathematical model is formulated one has to construct a verbal model of the underlying mechanisms of interaction of the system. One must then identify and understand the various parameters and variables that make up the system. Thereafter, one can combine the parameters and variables to form mathematical equations that follow certain rules, which according to our experience and knowledge, govern the system. Often in order to make the equations mathematically tractable one has to simplify and generalise these rules. Thus in essence most mathematical models are only idealised approximations of the phenomena being studied. The model does not necessarily have to reproduce exactly what happens in nature. It needs only to reproduce the salient features of the system so that one is able to approximate its future behaviour, as well as make quantitative estimates of the different parameters that govern the system.

After the initial steps of studying the system and building the mathematical model have been completed, the next step is to find solutions to the equations. In general one cannot solve the equations analytically; therefore one has to resort to computational techniques. After solving the equations an analysis of the solution/s can be undertaken. This analysis can be used to make predictions and gain insights into the system. The predictions and insights that the model yields can then be tested on the system itself. If the predictions and insights do not agree well with observations or experimental results from the system, the iterative loop of Figure 5 must be traversed once again in order to refine and enhance the model's ability to depict reality.

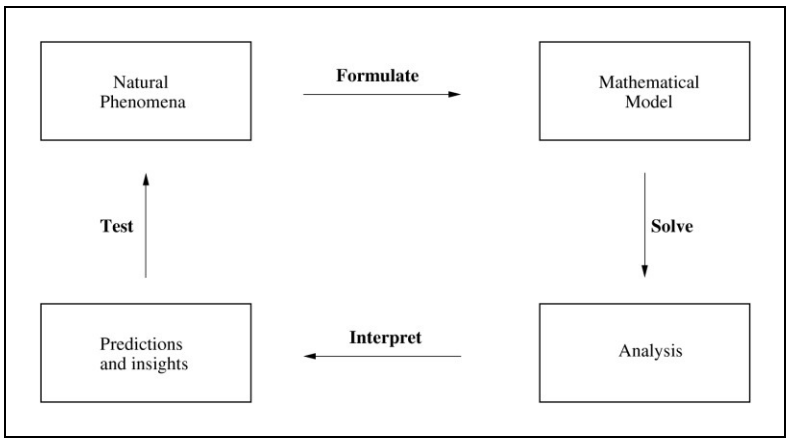

Figure 5: Flowchart of mathematical model development [128].

5.1. Population Models

Population models are of interest when modelling the interaction of the immune system with pathogens such as HIV and TB. This is simply because one can think of the pathogen and the immune system cells as interacting populations and then model how coexistence affects each population. Such models can be useful in attempting to explain what factors in the form of model parameters, such as drug therapy and frequency and duration of therapy, eliminate or at least contain the pathogen population at low levels, while maintaining the cell population of the immune system at adequate levels. Alternatively, as would be relevant in HIV modelling, one can gauge what factors

facilitate the rapid onset of AIDS, characterised by an increase in the HIV virion population and decrease in the cell population of the immune system, so that one can take the necessary preventative measures in order to negate these factors.

5.1.1. Fibonacci Sequence

A forerunner of population models dates back to 1202 when the Italian mathematician Fibonacci published a problem about the breeding of rabbits. The question Fibonacci posed was the following, "How many pairs of rabbits can be produced from a single male/female pair assuming that the rabbits only reproduce after their first month and thereafter produce a male/female pair regularly at the end of every month without any rabbits dying?"

The model that simulates rabbit breeding based on the Fibonacci assumptions is given by a recursive relationship [43] and generates the famed Fibonacci sequence.

$$R_N = R_{N-} + R_{N-} \quad \forall \text{ ntegers } N \geq ?, \tag{1}$$

where R_N denotes the number of rabbit pairs alive at the end of month N. The initial conditions are given by $R_0 =$, since there is only one pair of rabbits at the beginning, and $R_1 =$, since the initial pair only start reproducing after the first month. Applying the initial conditions and solving recursively for eqn. (1) one obtains the Fibonacci sequence: 1, 1, 2, 3, 5, 8, 13, 21, 34, 55, 89, 144, 233, …

The Fibonacci sequence representation of the growth curve of the rabbit population is plotted in Figure 6 over the period of a year. One notes from the steep curve that the rabbit population increases quite rapidly. Even a simple mathematical model such as the

Fibonacci sequence demonstrates its value by being able to predict, even if one did not have any prior knowledge, the rapid growth of a rabbit population with no environmental restrictions.

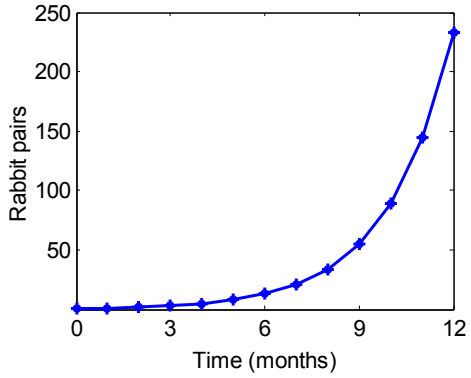

Figure 6: Plot of Fibonacci sequence representing growth of rabbit population.

5.1.2. Predator-Prey Model

Modelling the interaction of HIV or TB with immune system cells takes the form of an in-host population model. More specifically the population model is a predator-prey type model. This type of model assumes the existence of interacting species in which a subset of the population, known as the predators, kills other members of the population, known as the prey. In the context of modelling the interaction of pathogens with immune system cells one finds that, since one subset of the population is killed by another subset of the population, one can simulate the interaction using predator-prey type models [33].

5.1.2.1. Lotka-Volterra Equations

One of the benchmark predator-prey models is called the Lotka-Volterra model. It was proposed by the Italian mathematician Vito Volterra in 1926 to explain variations in the shark and fish populations in the Adriatic Sea after World War One [138]. A similar model was previously independently developed by the American biophysicist Alfred J. Lotka in 1925 [87]. The model is formulated in the following manner.

Suppose there are two species that coexist in a given habitat. Assume that these species are rabbits (R), which are the prey, and wolves (W), which are the predators, and that the following assumptions hold.

i. *The birth rate of rabbits is proportional to the rabbit population with proportionality constant* α.
ii. *The primary cause of rabbit deaths is due to wolves and rabbits are killed by wolves at a rate* β *which is proportional to the rabbit and wolf populations. This follows from the fact that the more wolves and rabbits there are, the greater the likelihood that a rabbit will encounter a wolf and be killed by it.*
iii. *The birth rate of wolves is proportional to the wolf population and the availability of food (rabbit population) with proportionality constant* μ.
iv. *The death rate of wolves is proportional to the wolf population with proportionality constant* γ.

Combination of the above assumptions and then translation into mathematical formalism yield the following system of coupled ordinary differential equations.

$$\frac{dR}{dt} = \epsilon - \beta W \tag{2a}$$

$$\frac{dW}{dt} = \iota W - \cdot V \ . \tag{2b}$$

Parameters α, β, γ and μ are all positive. The first and second terms in eqn. (2a) are due to assumptions *i* and *ii* respectively, whereas the first and second terms in eqn. (2b) are due to assumptions *iii* and *iv* respectively.

Mathematical Analysis

One can analyse the Lotka-Volterra model qualitatively by linearising the system close to the equilibrium points. This is accomplished by computing the Jacobian matrix at the equilibrium points. The Jacobian (**J**) is given by

$$\mathbf{J} = \begin{pmatrix} \alpha & \beta W & -\beta R \\ \mu W & & \mu R - \gamma \end{pmatrix}. \tag{3}$$

By equating eqn. (2a) and eqn. (2b) to zero and solving for R and W one finds that the system has equilibrium points at

$$(R, W) = (0,0) \text{ and } \left(\frac{\gamma}{\mu}, \frac{\alpha}{\beta}\right). \tag{4}$$

The Jacobians at the equilibrium points are

$$\mathbf{J} = \begin{pmatrix} \alpha & 0 \\ 0 & -\gamma \end{pmatrix} \text{ at } (0,0) \tag{5a}$$

$$\mathbf{J} = \begin{pmatrix} 0 & \dfrac{-\beta\gamma}{\mu} \\ \dfrac{\mu\alpha}{\beta} & 0 \end{pmatrix} \text{ at } \left(\frac{\gamma}{\mu}, \frac{\alpha}{\beta}\right). \tag{5b}$$

In order to find the eigenvalues (λ of the linearised system at the equilibrium points one must solve the characteristic equation at those equilibrium points.

$$\det(\mathbf{J} - \lambda\mathbf{I}) = \det\begin{pmatrix} \alpha - \lambda & 0 \\ 0 & -\gamma - \lambda \end{pmatrix} = (\alpha - \lambda)(-\gamma - \lambda) = 0 \text{ at } (0,0) \tag{6a}$$

$$\det(\mathbf{J} - \lambda\mathbf{I}) = \det\begin{pmatrix} -\lambda & -\beta\gamma/\mu \\ \mu\alpha/\beta & -\lambda \end{pmatrix} = \lambda^2 + \alpha\gamma = 0 \text{ at } \left(\frac{\gamma}{\mu}, \frac{\alpha}{\beta}\right). \tag{6b}$$

Solving for λ in eqns. (6a) and (6b) one obtains

$$\lambda = \alpha \quad \lambda = -\alpha \text{ at } (0,0) \tag{7a}$$

$$\lambda_1 = -i\sqrt{\alpha\gamma}, \quad \lambda_2 = -i\sqrt{\alpha\gamma} \text{ at } \left(\frac{\gamma}{\mu}, \frac{\alpha}{\beta}\right). \tag{7b}$$

From eqn. (7a) one notes that $(R,W) = (0,0)$ is saddle point, whereas from eqn. (7b) one sees that the point $(R,W) = \left(\frac{\gamma}{\mu}, \frac{\alpha}{\beta}\right)$ is a centre. Biologically speaking $(R,W) = (0,0)$ is a trivial equilibrium point because both the predator and prey populations are zero. On the other hand $(R,W) = \left(\frac{\gamma}{\mu}, \frac{\alpha}{\beta}\right)$ is more interesting. One can confirm that it is indeed a centre by analysing graphical solutions of the Lotka-Volterra equations. As an example substitute into eqn. (2)

$$\alpha = 0.08, \beta = 0.001, \gamma = 0.02, \mu = 0.00002. \tag{8}$$

Eqn. (2) now becomes

$$\frac{dR}{dt} = 0.08R - 0.001RW \tag{9a}$$

$$\frac{dW}{dt} = 0.00002RW - 0.02W. \tag{9b}$$

The equilibrium solutions to eqn. (9) are given by substituting eqn. (8) into eqn. (4).

$$(R, W) = (0,0) \text{ and } (1000,80). \tag{10}$$

Computational Analysis

One can analyse eqn. (9) by drawing its slope field, as has been done in Figure 7a, where the point $(R, W) = (1000,80)$ can clearly be seen to be an equilibrium point. Moreover by graphing a few typical solutions (phase trajectories) onto the slope field one obtains Figure 7b, which is the phase portrait of the Lotka-Volterra system. Figure 7b graphically confirms the theoretical observation that the equilibrium point $(R, W) = (1000,80)$ is a centre. Numerical solutions to the initial value problem $R = 1000$ and $W = 40$ for eqn. (9) are plotted in Figure 8a and Figure 8b for the rabbit and wolf populations.

a. Slope field

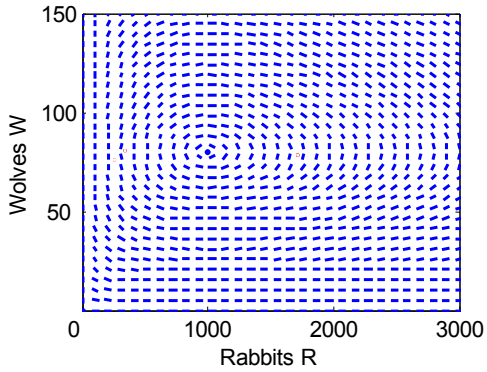

b. Slope field with phase trajectories

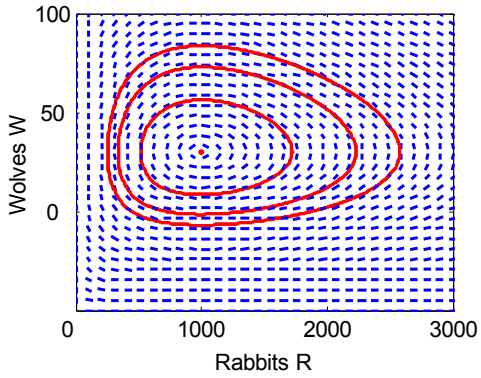

Figure 7: Slope field and phase portrait of the Lotka-Volterra system. Notice that the system has cyclic trajectories and a centre at the point $(R, W) = (1000,80)$.

a. Rabbit population

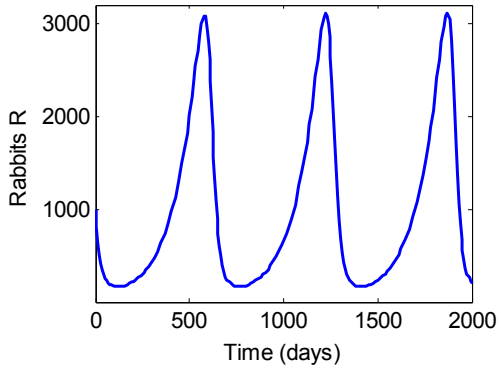

b. Wolf population

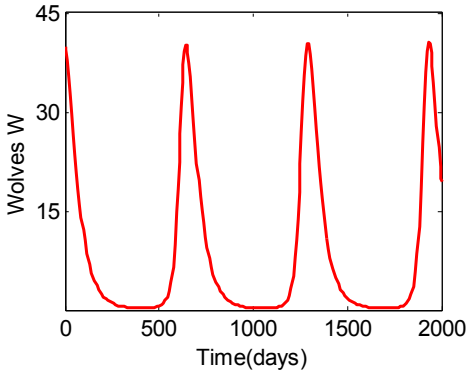

Figure 8: Numerical solutions of the Lotka-Volterra system with initial values of $R = 000$ and $W = 0$.

As a consequence of the cyclic orbits of Figure 7b the rabbit and wolf populations track each other over time. By plotting in Figure 9 both the rabbit and wolf populations on the same set of axes this phenomenon is clearly discernable.

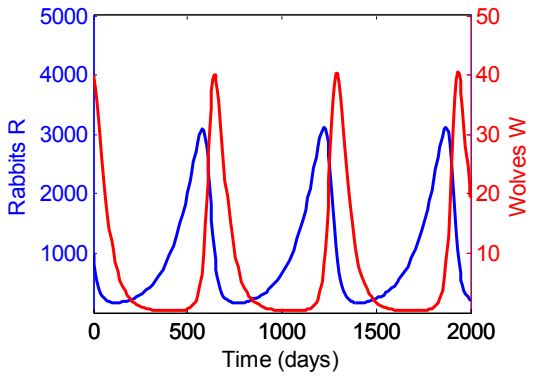

Figure 9: Superimposing the solutions to the Rabbit and Wolf populations. Note that they track each other over time.

The Lotka-Volterra model is a relatively simple model; however, when tested against ecological data, it does seem to display the qualitative behaviour that has been observed in certain predator-prey systems. As an example, one can view in Figure 10 records of the Canadian Lynx and Snowshoe Hare populations between 1845 and 1935 obtained from

the records of the Hudson's Bay Company in Canada which traded animal furs. One finds that the qualitative behaviour, in terms of the coupled oscillations of the predator-prey populations, predicted by the Lotka-Volterra model does actually occur in nature.

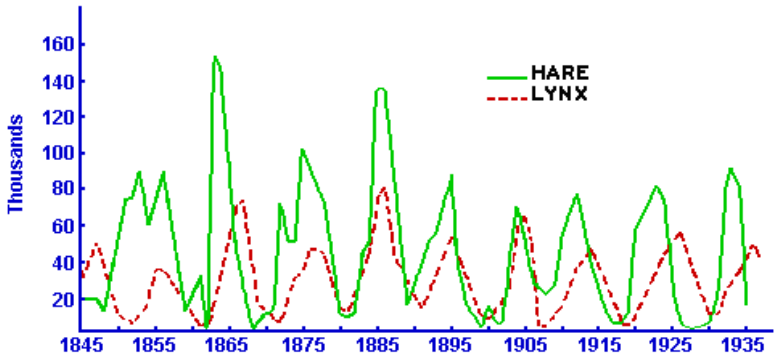

Figure 10: Ecological data of lynx-hare predator-prey system. One finds that the coupled oscillations shown in solutions to the Lotka-Volterra system are indeed found in nature [147].

The numerical solutions of the Lokta-Volterra equations, and all other models presented in this dissertation, were obtained by implementing explicit Runge-Kutta methods. Consider the initial value problem for a system of ordinary differential equations given as $y'(x) = f(x, y(x))$ for $a \leq x \leq b$ where we are given $y(a)$. The Runge-Kutta method [9] produces approximations $\hat{y}_n$ to $y(x_n)$ for $a = x_0 < x_1 \ldots < x_n = b$. Each step from x_n to x_{n+1} involves two approximations to $y(x_{n+1})$, namely $\hat{y}_{n+1}$ and y_{n+1}. The approximations are of the following form

$$\hat{y}_{n+1} = \hat{y}_n + \sum_{i=1} \hat{} \quad (11a)$$

$$y_{n+1} = \hat{y}_n + \sum_{i=1} \quad (11b)$$

where

$$k_1 = f(x_n, \hat{y}_n) \quad (11c)$$

$$k_i = f(x_n + c_i h, \hat{y}_n + h\sum_{j=}^{i-} a_{i\,j} k_j), \quad i = ,3,\ldots,s \tag{11d}$$

and

$$c_i = \sum_{j=1}^{i-1} a_{i,j}, \quad i = ,3,\ldots,s. \tag{11e}$$

To specify a particular Runge-Kutta method one needs to specify the integer s, i.e. the number of stages, and the coefficients $a_{i,j}$ for $1 \le \le \le$ and b_i for $i = ,2,..s$. In this dissertation the Runge-Kutta (4,5) pair of Dormand-Prince [39] and Runge-Kutta (2,3) pair of Bogacki and Shampine [8] were used. The Dormand-Prince pair works well as a general purpose ordinary differential equation (ODE) solver whereas the Bogacki-Shampine pair is better suited for stiff ODEs. These routines were run in MATLAB® where they are programmed as built in functions. Although all the models in this dissertation were solved by numerical techniques, we point out as a matter of interest that, analytical techniques to solve similar sets of equations do exist, for example c.f. the works of M.C. Nucci [41, 102, 131] where the analytical treatment of similar models is given.

Chapter 6

HIV-Immune System Models

Having worked through the formulation and analysis of the Lotka-Volterra predator-prey system, one can now think of developing a similar predator-prey model for the interaction of HIV virions with the human immune system cells. As was previously noted, the immune system cells interacting with HIV virions can be modelled as a predator-prey system due to the fact that one subset of the population is killed off by another subset of the population. To begin with one can look at a simple model of HIV and immune system interaction commonly referred to in the literature as the basic HIV model.

6.1. Basic HIV-Immune System Model

The basic HIV model [64, 98, 115, 141] describes immune system cells interacting with HIV virions. The model contains three variables. These variables denote the populations of the uninfected immune cells (T), infected immune cells (T^i) and the HIV virions (V). The model's equations are

$$\frac{dT}{dt} = \lambda - dT - \beta TV \tag{12a}$$

$$\frac{dT^i}{dt} = \beta TV - aT^i \tag{12b}$$

$$\frac{dV}{dt} = kT^i - uV\,. \tag{12c}$$

Eqn. (12a) gives the change in the uninfected immune cell population. The first and second terms of this equation represent source and death terms where uninfected cells are

replenished at a constant rate, λ, and die at a rate, d, proportional to its population. The third term is a loss due to infection term where virions encounter uninfected cells and infect them at a rate β proportional to both populations.

Eqn. (12b) gives the change in the infected immune cell population. The first term is carried over from eqn. (12a) and represents an increase in infected cells due to infection. The second term represents the natural death of infected cells which die at a rate a proportional to its population.

Eqn. (12c) gives the change in the HIV virion population. The first term is a source term in which virions are produced from infected cells at a rate k proportional to the infected cell population. The second term is a natural death term where virions die at a rate u proportional to their population.

A diagrammatic illustration [100] of the dynamics that are modelled by eqns. (12a) – (12c) is shown in Figure 11.

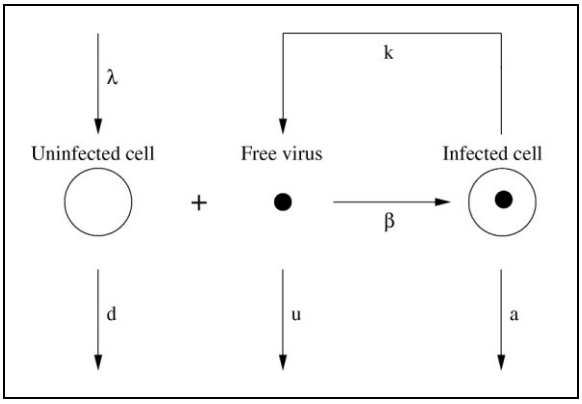

Figure 11: Schematic illustration of the basic HIV-immune system model [100].

6.1.1. Conditions for Infection

We now consider the mechanism by which infection occurs as modelled by the basic HIV model. When a small amount of HIV virions is added to the system, the virions infect the

uninfected cells, thus producing newly infected cells, which in turn produce new virions. This process can repeat itself leading to a chain reaction. The chain reaction can either go one of two ways, it can either be self-sustaining or it can die out. Whether it is successful in sustaining itself depends on a quantity called the basic reproductive ratio (R_0) [10, 11, 100]. The basic reproductive ratio is defined as the average number of secondary infected cells generated by a single infected cell at the beginning of an infection.

For the basic HIV-immune system model $R_0 = \frac{k\lambda\beta}{adu}$. R_0 can be understood in an intuitive manner [101], as illustrated in Figure 12, by noting that $\frac{k}{a}$ is the burst size, which gives the total number of virions produced from any one infected cell, $\frac{\lambda}{d}$ is the preinfection ($T^i = 0$ and $V = 0$) equilibrium density of uninfected cells, β is the rate of infection per unit time and $\frac{1}{u}$ is the average life-span of an HIV virion [10, 101].

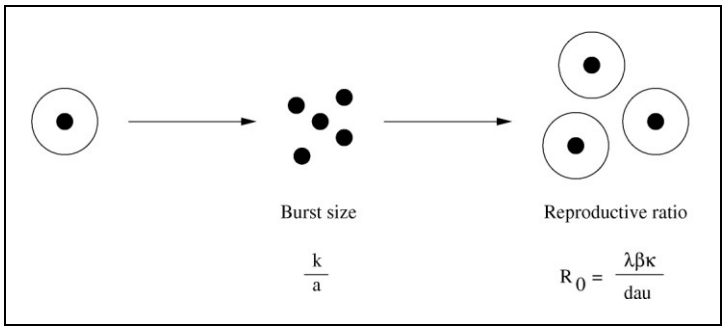

Figure 12: Schematic illustration of the initial proliferation process [101].

If $R_0 < 1$, then on average at the start of infection any one infected cell generates less than one newly infected cell, which means the infection is not able to sustain itself and eventually dies out, with the uninfected cell population converging to its preinfection

equilibrium value, given by eqn. 13(a). Conversely, if $R_0 > 1$, then on average at the beginning of infection any one infected cell generates more then one newly infected cell, which means the infection is able to take off and after some time converges to its equilibrium value, given by eqn. 13(b).

$$T = \frac{\lambda}{d}, \quad T^i = 0, \quad V = 0 \tag{13a}$$

$$T = \frac{\lambda}{R_0 d}, \quad T^i = (R_0 - 1)\frac{ud}{\beta k}, \quad V = (R_0 - 1)\frac{d}{\beta}. \tag{13b}$$

6.1.2. Simulations

One can investigate the dynamical behaviour of the basic HIV model shown in Figure 13, where two simulations were carried out, one for $R_0 < 1$, and another for $R_0 > 1$. Figure 13 serves to confirm, respectively, that, when $R_0 < 1$, the infection cannot sustain itself and soon dies out; and, when $R_0 > 1$, the infection takes off and there is an exponential increase in viral load.

Parameter values used in the simulation are $\lambda = 10^5$, $d = 0.1$, $a = 0.5$, $k = 100$, $u = 5$, $\beta = 2 \times 10^{-7}$ for $R_0 > 1$; the initial conditions are $T_o = \frac{\lambda}{d} = 10^6$, $T_o{}^i = 0$ and $V_0 = 100$ [101]. To satisfy $R_0 < 1$ put $\beta = 2 \times 10^{-8}$.

When $R_0 < 1$, one observes from the graph of the HIV virion population shown in Figure 13a and the graph of the infected cell population shown in Figure 13b that the infection is unable to sustain itself and dies off. In addition there is no discernable change in the uninfected cell population shown in Figure 13c. One notes that the simulated equilibrium values are in agreement with the values predicted by eqn. 13 (a).

Column I: R_0=0.8

Column II: R_0=8

a.

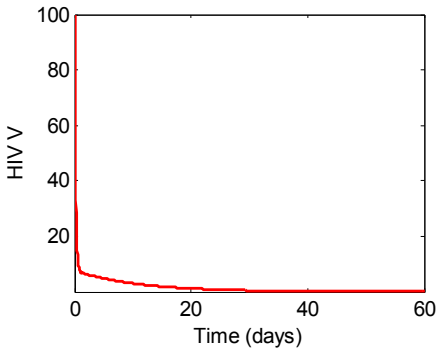

d.

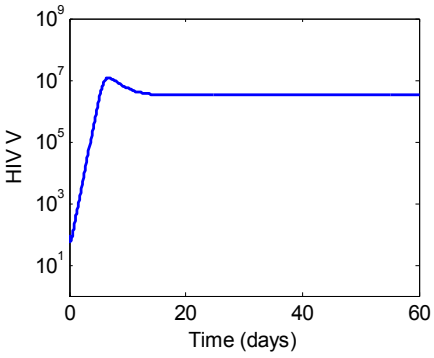

b.

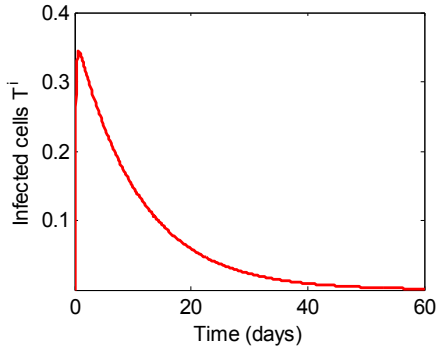

e.

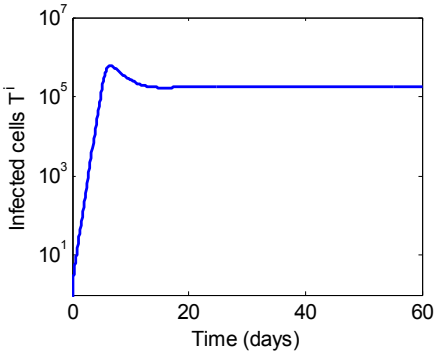

c.

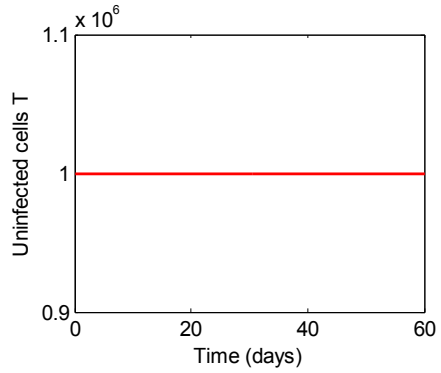

f.

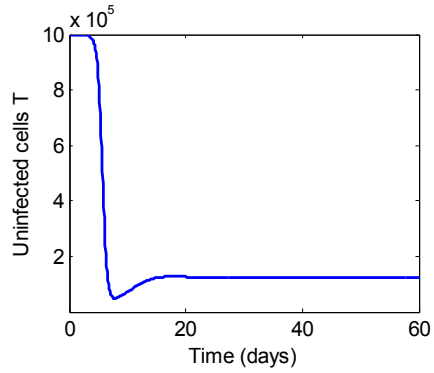

Figure 13: Simulations of the basic HIV model for two regimes of R_0 values: Column I, $R_0 < 1$, and Column II, $R_0 > 1$. Column I shows that HIV infection dies out when $R_0 < 1$ and Column II shows that HIV infection takes off when $R_0 > 1$.

When $R_0 > 1$, one finds that at the start of infection there is an exponential increase in the levels of the HIV virion and infected cell populations, as seen in Figures 13d and 13e respectively, where each population peaks before subsequently levelling off to their equilibrium values. The uninfected cell population initially stays approximately constant before it declines to a minimum value and subsequently recovers to its equilibrium value, see Figure 13f. The qualitative dynamics portrayed by the basic HIV-immune system model are typical of primary HIV infection [74, 86, 101, 127] in HIV-positive individuals. At very least the basic HIV model is able to give one some idea of the type of qualitative dynamics one would expect during primary HIV infection. The equilibrium values of $T = 1.25 \times 10^5$, $T^i = 1.75 \times 10^5$, and $V = 3.5 \times 10^6$ obtained by the numerical simulations confirm the predictions of eqn. 13(b).

6.1.3. Analysis and Implications

During primary HIV infection it has been suggested that the observed decline in viral load of up to 2-3 orders of magnitude after the viral load peaks is due to antibody and cellular immune responses [30, 81, 101, 105]. Intriguingly, although the basic HIV model does not include the specific involvement of an immune response, the model does reflect the decline in viral load and infected cells during persistent infection. Witten and Perelson [141] illustrated that in terms of the basic HIV model one can argue that, if the immune response played a role in lowering the level of viral load, its contribution would need to be small or constant. To illustrate their point they modelled the rate of death of infected cells a as having two components by expressing it as $a = a_0 + a_X X$. The two components, a_0 and $a_X X$, that contribute to the death rate are each respectively due to viral cytopathic effects and cytotoxic T-lymphocyte (CTL) immune responses [12, 107]. In the cytotoxic T-lymphocyte immune response term X denotes CTL and a_X denotes the contribution to the rate of death of infected cells per CTL. From $a = a_0 + a_X X$, which gives the total rate of death of infected cells, one sees that in order for a to be

approximately constant either $a_X X$ is small relative to a_0 or is itself approximately constant. During chronic infection one could easily envisage a constant immune response; however, during primary infection a CTL immune response is generated and correlates temporally with the decline in viremia [12, 81]. Hence it is surprising that the basic HIV model which has a constant death rate of infected cells can account for dynamics displayed in primary HIV infection. The reason that the basic HIV model displays a decline in viral load from its peak is due to a target cell limitation implying that there is a running out of susceptible cells [108].

For most HIV infected individuals, following the resolution of the acute primary HIV infection, viral load reaches a set-point and becomes relatively stable over a period of time. A set-point is achieved due to the fact that a balance is reached between the viral replication rate and the viral clearance rate. The level at which the set-point equilibrates after primary acute HIV infection is important since an individual with a higher set-point viral load has a greater risk of more rapidly progressing towards AIDS [92].

6.2. Basic HIV Model with Treatment

By modifying the basic HIV-immune system model one is able to include the effects of antiretroviral therapy into the model. The modification is performed by noting that reverse transcriptase (RT) inhibitors block the ability of HIV to infect a cell successfully. Protease inhibitors (PI) cause the production of noninfectious viral particles (V_{ni}).

Applying these therapeutic mechanisms to the existing structure of the basic HIV-immune system model one obtains the following set of equations [141].

$$\frac{dT}{dt} = \lambda - dT - (1-\varepsilon_{RT})\beta T V_i \tag{14a}$$

$$\frac{dT^i}{dt} = (1-\varepsilon_{RT})\beta T V_i - aT^i \tag{14b}$$

$$\frac{dV_i}{dt} = (1-\varepsilon_{PI})kT^i - uV_i \tag{14c}$$

$$\frac{dV_{ni}}{dt} = \varepsilon_{PI}kT^i - uV_{ni} \ . \tag{14d}$$

where ε_{RT} and ε_{PI} represent the respective efficacies of the reverse transcriptase and protease inhibitors. For a perfect inhibitor, one that is a 100% effective, $\varepsilon = 1$. The action of the protease inhibitor serves to divide the HIV virion population into infectious and noninfectious viral particles. The levels of infectious and noninfectious HIV virion populations are denoted by V_i and V_{ni} respectively. The total number of free virions is given as $V = V_i + V_{ni}$.

Perelson *et al* [107] were able to show that, if a 100% effective protease inhibitor (initially drug resistance effects are not discernable) is administered to an HIV-positive individual at steady state with viral load V_0 and one assumes that over the period of interest the uninfected cell population (T) remains constant, the viral load decay obeys the equation

$$V(t) = V_0 \exp(-ut) + \frac{uV_0}{u-a}\left[\frac{u}{u-a}\{\exp(-at) - \exp(-ut)\} - at\exp(-ut)\right]. \tag{15}$$

By using nonlinear least squares regression to fit eqn. (15) to clinical data, estimates were obtained for the parameters a and u. Estimates for the average life-time of an infected cell and the average life-time of a free virus particle are then obtained by noting that these are each given by $\frac{1}{a}$ and $\frac{1}{u}$ respectively. One can then proceed to calculate the half-life

of infected cells and free virions, which are each given by $t_{½} = \frac{\ln 2}{a}$ and $t_{½} = \frac{\ln 2}{u}$ respectively. Moreover estimates of the total virion production and clearance rates can be obtained by noting that at steady state the production rate of virions must equal its clearance rate uV, c.f. eqn. (12c). Thus it is possible to estimate virion production rates by using the previously obtained estimate of u and the pretreatment viral concentration V_0.

Once the necessary mathematical underpinning had been developed, the researchers then obtained clinical date from a group of five infected individuals who were administered Ritonavir, a potent protease inhibitor. The total plasma concentration and fluid volume of each individual was estimated on the basis of the individual's body weight. The total daily virion production and clearance rates were then obtained using the previously outlined methods and found to be in the range 0.4×10^9 to 32.1×10^9 (mean 10.3×10^9) virions per day being released into the extracellular fluid. It was noted that this estimate is a minimum estimate since virions that are not released into the extracellular fluid are not included in the estimate.

This work demonstrates that the latent stage of HIV disease progression is not a static process. The model reveals the enormous turn-over rates of around 10^{10} HIV virions per day in the human body. Clearly there are major dynamical processes that are taking place in the background even though one might not have thought this to be the case since the levels of HIV prognostic markers seem to be relatively stable. This is a good example of how mathematical modelling can be utilised to increase our understanding of the biological processes that occur during HIV disease progression.

6.3. Late versus Early Treatment

Before the advent of combination therapy, such as HAART, there has been much debate with regards to the particular stage of disease progression at which AZT monotherapy

should be initiated. A literature review revealed that there seemed to be conflicting results, with some advocating early treatment (200-500 $CD4^+$ T cells per mm^3 of blood) [45, 60, 84, 120, 136], whereas others advocate late treatment (< 200 $CD4^+$ T cells per mm^3 of blood) [28, 64]. In order to seek clarity on this matter a mathematical model was developed by Kirschner and Webb [76]. Results from their simulations agree well with the Concorde Study [24] which was set up to investigate the relative merits of late versus early treatment of HIV with AZT monotherapy. The study, which was conducted by the British Medical Research Council and the French National AIDS Research Agency, examined 1749 asymptomatic HIV-positive people in the United Kingdom, Ireland, and France. The Concorde study has shown that early treatment of HIV patients with AZT monotherapy does not necessarily produce a more favourable prognosis [24, 76].

6.3.1. Model Development

Developing mathematical models like the Kirschner-Webb model are important in order to gain a qualitative understanding of AIDS chemotherapy. One can test different strategies of drug administration in terms of timing, dose and frequency with such models. The qualitative results that the model yields would be able to help us gain insight into optimising the drug administration regime one would use in a clinical setting.

The Kirschner-Webb model was developed from the known mechanisms of interaction of HIV and the immune system, including the effects of AZT monotherapy. The population dynamics that the model simulates occur in a single compartment. This compartment is taken to be the peripheral blood. By modelling a single compartment one ensures that there are no flows from outside compartments and that the equations are scaled appropriately. The model is as follows.

Table 1: Variables and Parameters

Dependent Variables		Initial values
T	Uninfected T cell population	$1000\,\mathrm{mm}^{-3}$
T^i	Infected T cell population	$0.0\,\mathrm{mm}^{-3}$
V	HIV virion population	$1.0\times10^{-3}\ \mathrm{mm}^{-3}$
Parameters and Constants		**Values**
$s(t)$	Source of new T cells from the thymus	$0.5s_1 + \frac{0.5s_2}{c_1 + V(t)}$
c_1	Half saturation constant for T cell growth	$1\,\mathrm{mm}^{-3}$
s_1	Source of new T cell in absence of infection	$10\ \mathrm{mm}^{-3}\ \mathrm{day}^{-1}$
s_2	Rate of change in T cell supply	$10\ \mathrm{mm}^{-3}\ \mathrm{day}^{-1}$
μ_T	Death rate of uninfected T cell population	$0.02\ \mathrm{day}^{-1}$
μ_{T^i}	Death rate of infected T cell population	$0.24\ \mathrm{day}^{-1}$
k_V	Rate T cells become infected by free virus	$2.4\times10^{-5}\ \mathrm{mm}^3\ \mathrm{day}^{-1}$
k_T	Rate $CD8^+$ T cells kill virus	$7.4\times10^{-4}\ \mathrm{mm}^3\ \mathrm{day}^{-1}$
r	Maximal proliferation of T cell population	$0.01\ \mathrm{day}^{-1}$
N	Number of free viral particles produced by bursting infected cells	1000
C	Half saturation constant of the proliferation process	$100\,\mathrm{mm}^{-3}$
b	Half saturation constant of the external viral source	$10\,\mathrm{mm}^{-3}$
g_V	Growth rate of the external viral source other than T cells (e.g. macrophages)	$5 - 20\ \mathrm{day}^{-1}$

$$\frac{dT(t)}{dt} = s(t) - \mu_T T(t) + r\frac{T(t)V(t)}{C+V(t)} - k_V T(t)V(t) \tag{16a}$$

$$\frac{dT^i(t)}{dt} = k_V T(t)V(t) - \mu_{T^i} T^i(t) - r\frac{T^i(t)V(t)}{C+V(t)} \tag{16b}$$

$$\frac{dV(t)}{dt} = Nr\frac{T^i(t)V(t)}{C+V(t)} - k_T T(t)V(t) + \frac{g_V V(t)}{b+V(t)}. \tag{16c}$$

Eqn. (16a) describes the change in the T cell population. The equation's first term is a source term for new T cells from the thymus. HIV can infect thymocytes (T cell precursors); therefore, the source term is represented as a decreasing function of viral load. The function, which is given by $s(t) = 0.5s_1 + \frac{0.5s_2}{c_1 + V(t)}$, has been shown to be a good first approximation [77]. The next term is a natural loss term due to the finite life-span of T cells. This is followed by a T cell stimulation term representing the stimulation of T cells to proliferate in the presence of virus. Since T cells do not grow without bound, a saturation term of the Michaelis-Menten type, which is believed to encompass the desired effects [76], was used to represent this process. The final term represents the loss of T cells due to infection by HIV.

Eqn. (16b) describes the change in the infected T cell population. The first term, which is a gain due to infection term, carries over from the loss term in eqn. (16a). Next there is a loss term due to the finite life-span of infected T cells. This is followed by a Michaelis-Menten type loss term due to cytolysis of infected cells during the proliferation process.

Eqn. (16c) describes the change in the HIV virion population. The first term, which is a gain term, carries over from the cytolysis loss term in eqn. (16b) with factor N in front. The factor N represents the burst size, that is, the average number of virions produced from a single infected cell. This is followed by a loss term due to specific immune response, namely $CD8^+$ T cells killing the virus. The final term is a gain term of the Michaelis-Menten type which represents growth of virus from other infected cells, for

example, macrophages and thymocytes. This term also implicitly accounts for the natural death of virions. If an explicit natural death term, such as $-\mu_V V$, is included, an additional steady state arises which has negative values making it invalid. Furthermore the virions that die naturally do not affect the dynamics of the model since they do not have a chance to infect T cells and therefore no longer play a role in the interaction process.

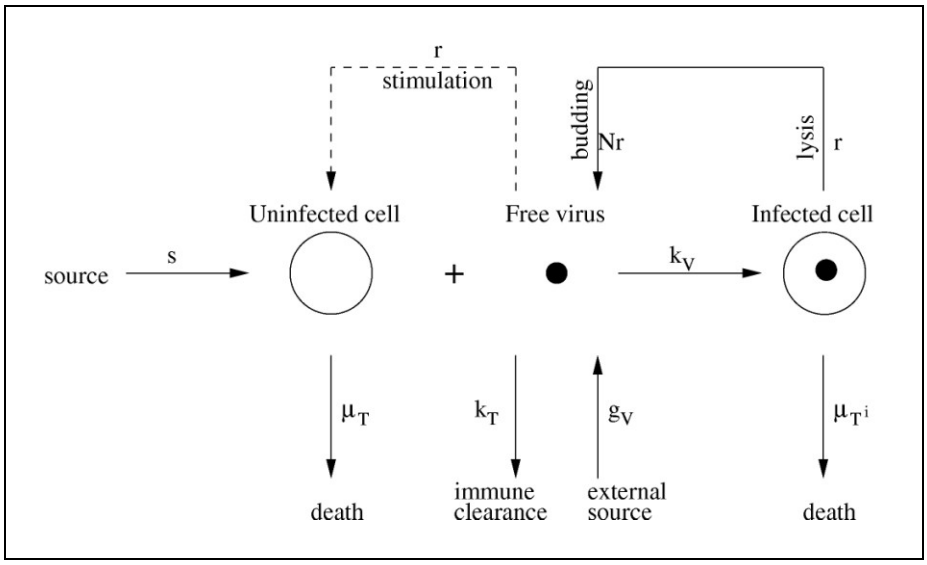

Figure 14: A schematic illustration of the Kirschner-Webb model [76].

6.3.2. Model Simulation

Simulations were run for different values of the external viral source growth rate g_V. It was observed that by changing the values of g_V one could simulate the different stages of disease progression. Primary infection and the infected steady state is shown in Figures 15a – 15c with $g_V = 5$. The progression towards AIDS is shown in Figures 15d – 15f with $g_V = 20$. Finally by gradually increasing the external viral source from $g_V = 5$ to $g_V = 20$ the complete course of HIV infection is shown in Figures 15g – 15i.

Column I: $g_V = 5$ **Column II: $g_V = 20$** **Column III: g_V increased from $g_V = 5$ to $g_V = 20$**

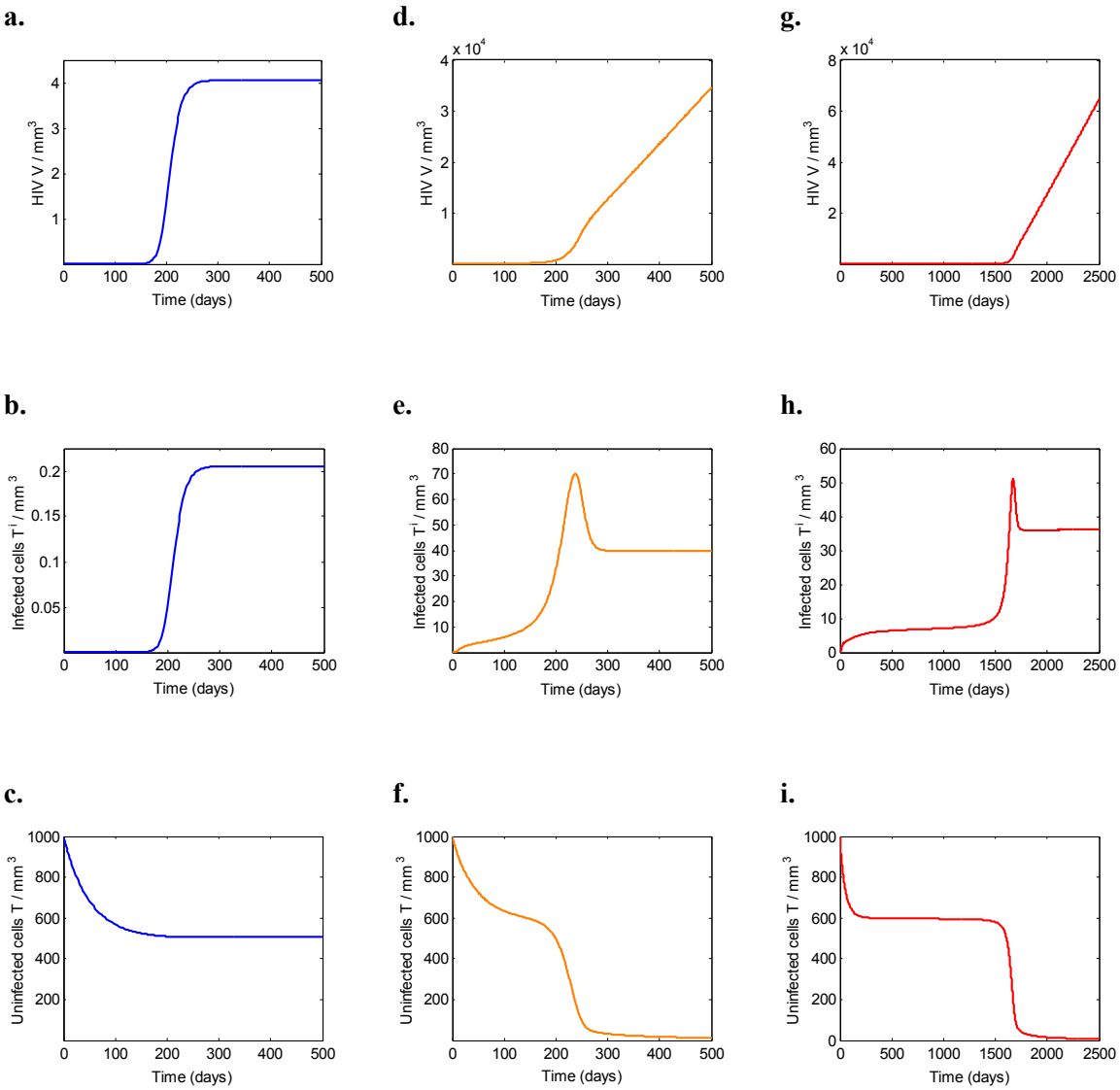

Figure 15: Simulations of the Kirschner-Webb model for three different regimes of g_V. When $g_V = 5$, Column I simulates the HIV infected steady state. When $g_V = 20$, Column II simulates the progression to AIDS. By increasing g_V over time from $g_V = 5$ to $g_V = 20$, Column III simulates the entire course of HIV infection.

Figures 15a – 15c, which simulate the primary and latent stage of HIV infection, show numerical solutions of the model for $g_V = 5$. The model does to some extent display typical qualitative behaviour associated with primary and latent infections. For primary infection there is initially an increase in virion and infected cell count while the T cell count experiences a decline. Thereafter all populations settle to set-point values as expected during the latent stage of the disease. The model, however, does not display the initial spike in viral load that one would associate with primary infection, as some other models that are reviewed below do.

In Figures 15d – 15f, which simulate the progression to AIDS, the external viral source growth rate is increased to $g_V = 20$. This increase may be due to factors such as mutations or increased efficiency in viral production. During this phase one typically finds that there is a steep increase in the viral load accompanied by equally dramatic decrease in the T cell population, just as the simulations of the model suggest.

Figures 15g – 15i simulate the entire course of HIV infection by increasing the external viral source growth rate from $g_V = 5$ to $g_V = 20$ over time. Note that the steep decrease in the T cell population and steep increase in the viral load at day 1500, signaling the onset of AIDS, occurs over the period of a year.

6.3.3. Bifurcation Analysis

We have seen that the external viral source growth rate plays an important role in the dynamics of the model. By increasing g_V the model is able to simulate the collapse of the immune system, representing the onset of AIDS. Figure 15a shows that for $g_V = 5$ the viral load stabilises to a positive constant; however, Figure 15d shows that for $g_V = 20$ the viral load grows linearly without bound. Clearly a qualitative change takes place in the dynamics of the model as g_V is increased. In order to understand the changes that occur to the qualitative behaviour of the system, one can do a bifurcation analysis of the

system. We begin our analysis by examining the steady state solutions for the system. For simplification of analysis assume that the T cell source, given by $s(t) = 0.5s_1 + \frac{0.5s_2}{c_1 + V(t)}$ in eqn. (16a), is approximated by a constant denoted by s. In addition let steady state values be denoted by an over-bar. Putting eqns. (16a) – (16c) equal to zero and rearranging terms one obtains eqns. (17a) – (17c) respectively.

$$s = \mu_T \overline{T} - r\frac{\overline{T}\,\overline{V}}{C + \overline{V}} + k_V \overline{T}\,\overline{V} \tag{17a}$$

$$\overline{T}^{i} = \frac{k_V \overline{T}\,\overline{V}}{\mu_{T^i} + r\overline{V}/(C + \overline{V})} \tag{17b}$$

$$Nr\frac{\overline{T}^{i}\overline{V}}{C + \overline{V}} = k_T \overline{T}\,\overline{V} - \frac{g_V \overline{V}}{b + \overline{V}}. \tag{17c}$$

Substitution of eqn. (17b) into eqn. (17c) yields

$$Nr\frac{\overline{V}^2 k_V \overline{T}}{\mu_{T^i}(C + \overline{V}) + r\overline{V}} = k_T \overline{T}\,\overline{V} - \frac{g_V \overline{V}}{b + \overline{V}}. \tag{18}$$

Making $\overline{T}$ the subject in eqns. (17a) and (18) and equating, one obtains

$$\frac{s}{\mu_T - r\overline{V}/(C + \overline{V}) + k_V \overline{V}} = \frac{g_V/(b + \overline{V})}{k_T - Nr\overline{V}k_V/(\mu_{T^i}(C + \overline{V}) + r\overline{V})}. \tag{19}$$

Cross multiplication of eqn. (19) gives

$$\begin{aligned} &g_V[\overline{V}^2 k_V + \overline{V}(Ck_V + \mu_T - r) + C\mu_T][\overline{V}(r + \mu_{T^i}) + C\mu_{T^i}] \\ &= s(c + \overline{V})(b + \overline{V})[\overline{V}(k_T\mu_{T^i} + k_T r - Nrk_V) + k_T\mu_{T^i}C]. \end{aligned} \tag{20}$$

Clearly eqn. (20) entails solving a cubic for $\overline{V}$ in terms of the parameter values given in Table 1. Nevertheless the bifurcation analysis performed by varying g_V in Figures 16a – 16c reveals that at most there are only two real steady state values of $\overline{V}$ for the given parameter values. We have specifically chosen to vary g_V since this parameter may vary between different individuals and also between the different stages in disease progression. By plotting bifurcation diagrams for each of the model's populations, where g_V is varied between 5 and 20 as it had been in the simulations shown in Figure 15, one is able to gauge the extent of the qualitative changes that the system undergoes.

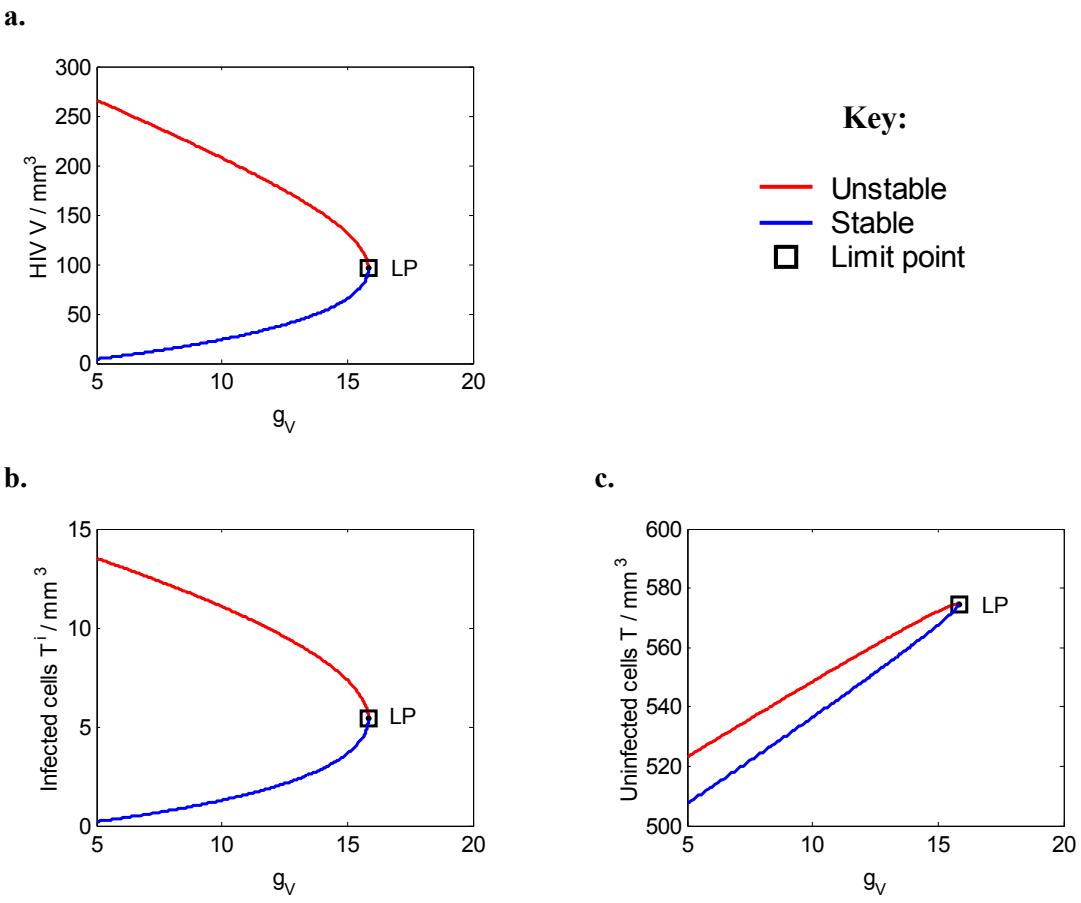

Figure 16: Bifurcation diagrams of the Kirschner-Webb model created by varying g_V from 5 to 20. The diagram shows that the system has at most two real-valued solutions, with one being stable and the other being unstable. A saddle-node bifurcation occurs at $g_V \approx 15.8$.

One sees from Figure 16 that a saddle-node bifurcation (limit point) occurs at about $g_V = 15.8$. It is at this point that the two steady state solutions of the system, one stable and the other unstable merge into a single solution.

One is now in the position to plot a two-parameter bifurcation diagram by varying N, the number of free viral particles produced by bursting infected cells. This two-parameter bifurcation diagram gives the g_V and N values at which a saddle-node bifurcation takes place. The reason for varying N in addition to g_V is that N is also an important parameter which governs the qualitative behaviour of the system and, like g_V, N has a fair amount of uncertainty associated with it.

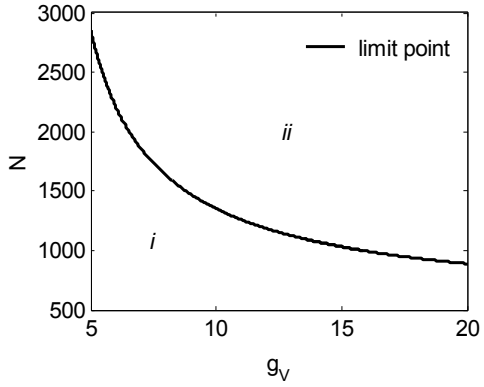

Figure 17: Two-parameter bifurcation diagram for the Kirschner-Webb model with the growth rate of external viral source g_V vs. the number of virions produced from cell bursting N. In region *i* positive steady-state equilibrium values for all three populations are attained, signifying chronic HIV infection. In region *ii* the viral load grows linearly without bound, signaling the onset of AIDS.

The qualitative behaviour of the system for the regions *i* and *ii* are described as follows. In region *i* positive steady-state values for all three populations are attained when they asymptotically converge to the single stable node of the system. This behaviour is exhibited in Figures 16a – 16c for values of $g_V < 15.8$, where the system converges to the steady state values denoted by the blue portion of the graphs. In region *ii* the T cell population converges to 0, the infected T cell population converges to a positive constant;

however, the HIV population grows linearly without bound. This type of qualitative behaviour signifies the onset of AIDS and is consistent with the Center for Disease Control's Definition for AIDS and AIDS-related complexes [76]. The simulations shown in Figures 15d – 15f demonstrate this behaviour. The fact that the HIV population grows without bound in region *ii* means that this regions does not attain any steady state solutions. This behaviour can be seen in Figures 16a – 16c for values of $g_V > 15.8$, where branches for the steady state solutions of the system do not extend beyond $g_V = 15.8$.

6.3.4. Finding R_0

All simulations of the model that have been run thus far have only been of HIV infections that were able to sustain themselves. This is indicative of basic reproductive ratios that are greater than 1 ($R_0 > 1$). One is able to find the analytical value of R_0 by doing a linearised stability analysis of the uninfected steady state. A threshold condition for the uninfected steady state becoming unstable and the infected steady state assuming stability yields the analytical value of R_0. The uninfected steady state has 0 populations for both HIV and infected T cells. Using eqns. (16a) – (16c) to solve for the uninfected steady state values, one obtains

$$\overline{T} = \frac{s}{\mu_T},\ \overline{T}^i = 0 \text{ and } \overline{V} = 0. \tag{21}$$

The Jacobian ($\mathbf{J}$) for the system at the uninfected steady state is

$$\mathbf{J} = \begin{pmatrix} -\mu_T & 0 & r\overline{T}/C - k_V\overline{T} \\ 0 & -\mu_{T^i} & k_V\overline{T} \\ 0 & 0 & g_V/b - k_T\overline{T} \end{pmatrix}. \tag{22}$$

The characteristic equation is given by

$$\begin{aligned}\det\begin{pmatrix} -\mu_T-\lambda & 0 & r\overline{T}/C-k_V\overline{T} \\ 0 & -\mu_{T^i}-\lambda & k_V\overline{T} \\ 0 & 0 & g_V/b-k_T\overline{T}-\lambda \end{pmatrix} \\ =(\mu_T+\lambda)(\mu_{T^i}+\lambda)(g_V/b-k_T\,\overline{T}-\lambda) \\ =0.\end{aligned} \tag{23}$$

The three eigenvalues of the system are

$$\lambda_1=-\mu_T,\ \lambda_2=-\mu_{T^i}\ \text{and}\ \lambda_3=g_V/b-k_T\,\overline{T}\ . \tag{24}$$

For the system to be locally asymptotically stable in the uninfected steady state, one requires that the eigenvalues of eqn. (24) be all negative. This is clearly the case for the first two; however, in order for the third eigenvalue to be negative, one requires

$$g_V/b-k_T\,\overline{T}<0\ \text{ or equivalently }\ g_V/\overline{T}\,k_Tb<1. \tag{25}$$

If $g_V/\overline{T}\,k_Tb>1$, then the uninfected steady state loses stability and the infected steady state becomes stable, which implies that

$$R_0=g_V/\overline{T}\,k_Tb\,. \tag{26}$$

By substituting $\overline{T}=s/\mu_T$ and using parameter values of Table 1 in R_0, one finds that, if $g_V>3.7$, we have $R_0>1$ and, when $g_V<3.7$, we have $R_0<1$. The Bifurcation diagrams created by varying g_V between 0 and 5 shown in Figures 18a – 18c confirm that when $g_V>3.7$, a sustainable HIV infection is achieved, that is, the blue branches of the HIV virion and infected cell populations are both positive thereby indicating positive

steady-state solutions for these populations. However, when $g_V < 3.7$, the blue branches of the HIV virion and infected cell populations are both zero which is indicative of an uninfected steady state.

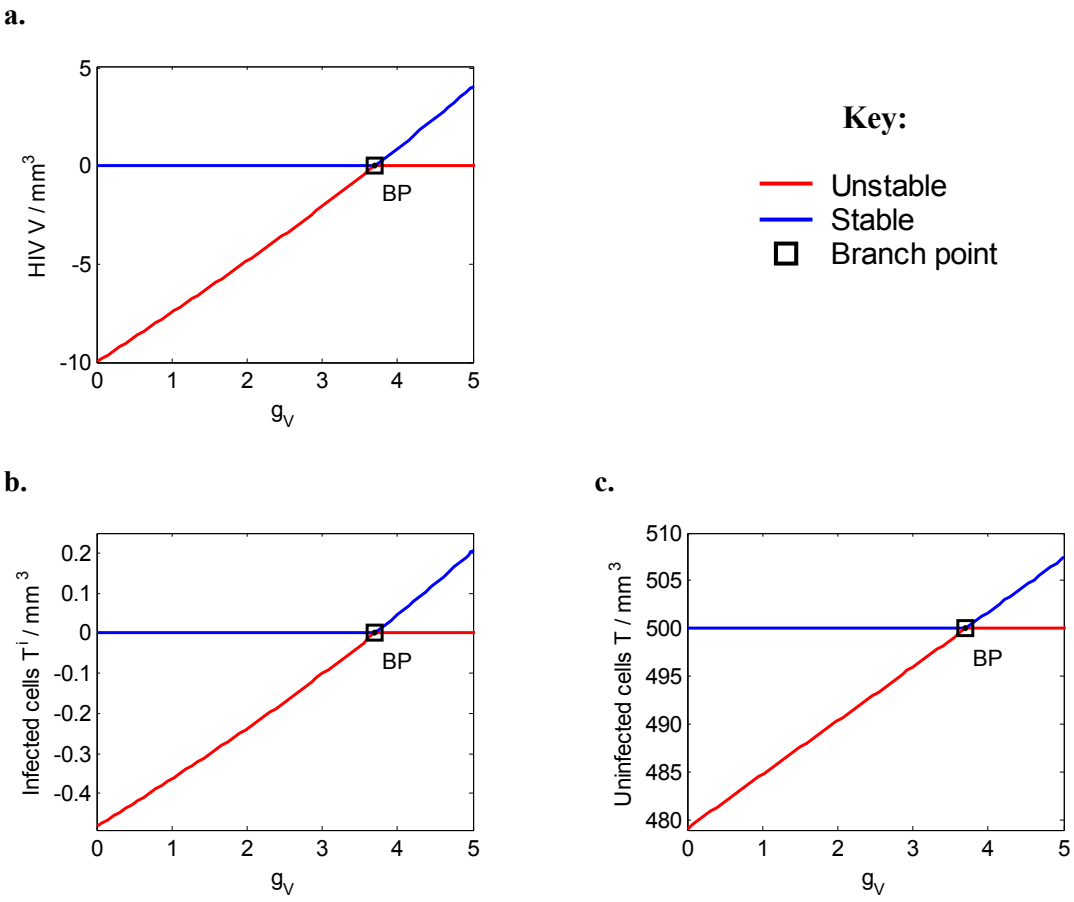

Figure 18: Bifurcation diagram of Kirschner-Webb model created by varying g_V from 0 to 5. The diagram confirms that, when $g_V < 3.7$, we have $R_0 < 1$ and the system converges to the uninfected steady state. Conversely, when $g_V > 3.7$, we have $R_0 > 1$ and the system converges to an HIV infected steady state.

6.3.5. Model with AZT Monotherapy

Using the Kirschner-Webb model one is able to obtain guidelines to the question that was initially posed at the beginning of the section, that is, is early treatment of HIV with AZT monotherapy more beneficial than late treatment? In order for the model to tackle this question it needs to be slightly modified to allow for AZT monotherapy. We recall that

AZT is a reverse transcriptase inhibitor and it therefore blocks the ability of HIV to successfully infect a cell. Thus the $k_V T(t)V(t)$ term in eqns. (16a) and (16b) is modified by introducing a factor $(1-\varepsilon_{RT})$ in front of the term. As was the case in eqns. (14a) and (14b), ε_{RT} values can range from 0 to 1 and represents the efficacy of AZT to inhibit the ability of HIV to successfully infect a cell. $\varepsilon_{RT}=1$ represents a perfect inhibitor. The model modified to include AZT monotherapy is given as follows [76]

$$\frac{dT(t)}{dt} = s(t) - \mu_T T(t) + r\frac{T(t)V(t)}{C+V(t)} - (1-\varepsilon_{RT})k_V T(t)V(t) \tag{27a}$$

$$\frac{dT^i(t)}{dt} = (1-\varepsilon_{RT})k_V T(t)V(t) - \mu_{T^i} T^i(t) - r\frac{T^i(t)V(t)}{C+V(t)} \tag{27b}$$

$$\frac{dV(t)}{dt} = Nr\frac{T^i(t)V(t)}{C+V(t)} - k_T T(t)V(t) + \frac{g_V V(t)}{b+V(t)}. \tag{27c}$$

Suppose that for a patient taking AZT for the first time it is initially 100% effective, that is, the virus had not been exposed to the drug long enough for the effects of resistance to be discernable. In addition assume that the patient takes the drug continuously so that before the effects of the drug wears off the patient is administered another dose of the drug.

Comparing simulation results for early and late treatment shown in Figure 19, one finds that during the late treatment regime the individual's T cell count remains elevated for a longer period of time, in excess of 100 days relative to the early treatment regime, before it starts to display signs of collapsing. This comparison is clearly shown in Figure 20 by superimposing the T cell counts of each of the regimes. The results of the simulation therefore do not advocate early treatment over late treatment and is thus in good agreement with the findings of the Concorde study [24]. Also notable was the model's ability to demonstrate the importance of HIV chemotherapy by showing that only a minimal amount of treatment was necessary to perturb the system from collapsing towards AIDS.

Column I: Early continuous therapy **Column II: Late continuous therapy**

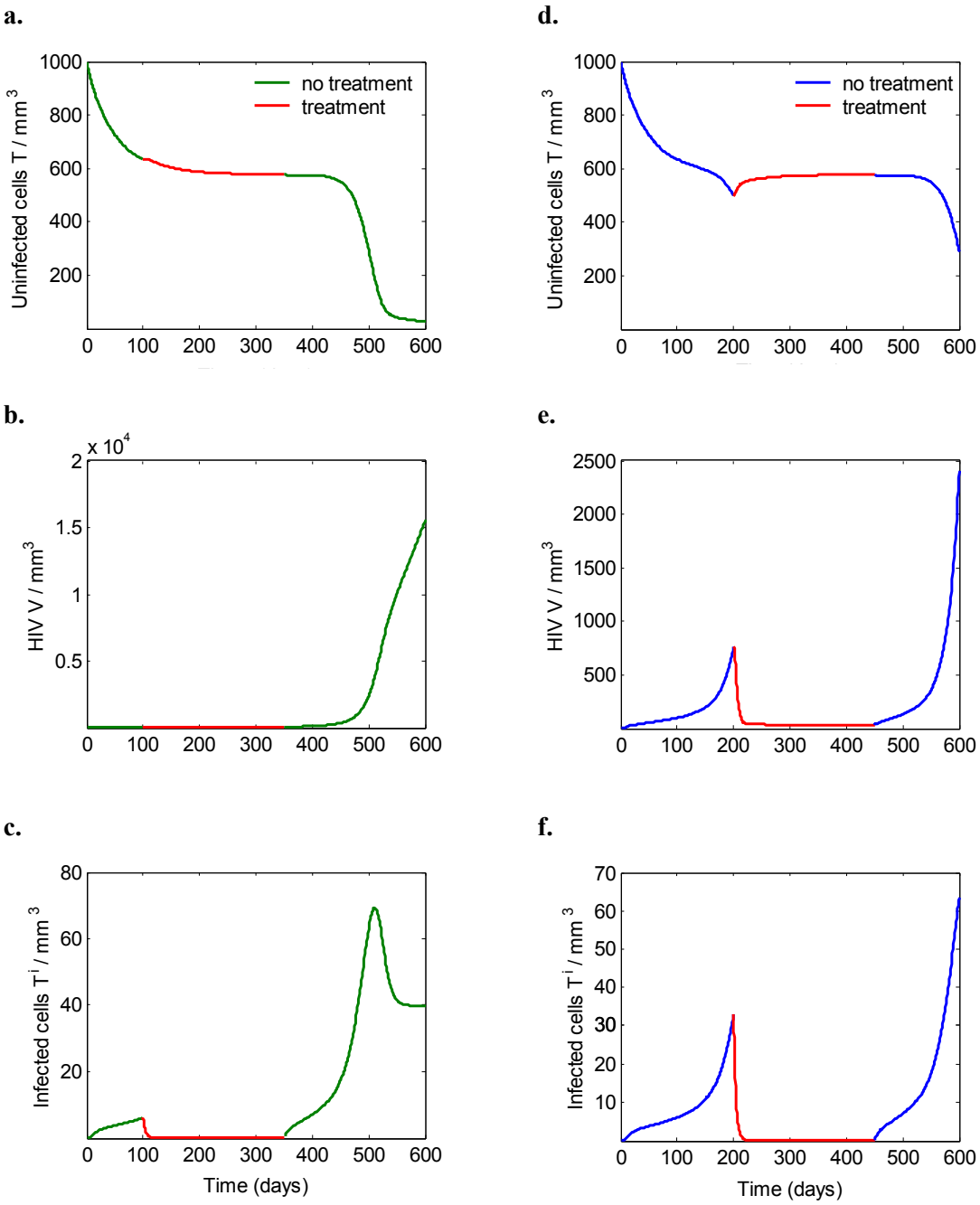

Figure 19: Simulations of early continuous and late continuous AZT monotherapy treatment. Early continuous treatment is simulated by administering therapy for 250 days beginning on the 100th day after the immune system starts collapsing towards AIDS. Late continuous treatment is simulated by administering therapy for 250 days beginning on the 200th day after the immune system starts collapsing towards AIDS. Administering treatment for only 250 days is done merely for simulation purposes and has no medical significance as such. Initial conditions and parameter values used to run the simulations are given in Table 1 with g_V=20.

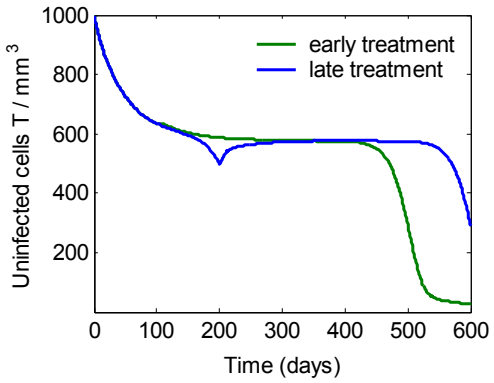

Figure 20: Superimposing T cell counts for early and late treatment regimes. For late treatment, T cell count remains elevated for a longer period of time, in excess of 100 days relative to the early treatment regime.

Chapter 7

HIV-TB Coinfection Model

One of the central themes of this dissertation is to study the interaction between HIV, TB and the immune system of the coinfected individual. Such a study is very relevant in the context of Sub-Saharan Africa, where there are high rates of coinfection exacerbated by the fact that each infection promotes disease progression in the other thereby increasing morbidity and mortality, c.f. section 4.3.

7.1. Model Development

Due to the endemic nature of HIV-TB coinfection in Sub-Saharan Africa it would be beneficial to have models that study the interaction of HIV, TB and the human immune system in order to gain insights into the dynamics of these interactions. Nevertheless, after a literature search had been conducted, only one such model was found. The model, which was developed by Kirschner [75], is given by the following set of equations

$$\frac{dT(t)}{dt} = \lambda_T(t) - \mu_T T(t) + r_T T(t)\left[\frac{(V(t)+\gamma_b(t))}{(\sigma + V(t)+\gamma_b(t))}\right] - k_1 V(t)T(t) \tag{28a}$$

$$\frac{dM(t)}{dt} = \mu_M[M_0 - M(t)] - k_2 M(t)V(t) + M(t)[k_M^2 V(t) + k_M^1 T_b(t)] \tag{28b}$$

$$\frac{dV(t)}{dt} = N_V(t)[N_1 k_1 T(t) + N_2 g_V M(t)] - N_V(t)[k_3 T(t) + k_4 M(t)] - \mu_V V(t) \tag{28c}$$

$$\frac{dT_b(t)}{dt} = r_{T_b} T_b(t)\left[1 - \frac{\gamma_b(t)}{K}\right] - \mu_{T_b} T_b(t) - \gamma_b(t)[k_5 T(t) + k_6 M(t)]. \tag{28d}$$

Table 2: Variables and Parameters

Dependent Variables		Initial values
T	Uninfected T cell population	$1500\,\mathrm{mm}^{-3}$
M	Macrophage population	$85\,\mathrm{mm}^{-3}$
V	HIV virion population	$1.0\times\ 0^{-3}\ \mathrm{mm}^{-3}$
T_b	M. tuberculosis population	$1.0\,\mathrm{mm}^{-3}$
Parameters and Constants		Values
μ	Death rate of uninfected T cell population	$0.007\ \mathrm{day}^{-1}$
$\mu_{\cdot\cdot}$	Death rate of macrophage population	$0.003\ \mathrm{day}^{-1}$
$\mu_{\cdot}$	Death rate of HIV virion population	$2.4\ \mathrm{day}^{-1}$
$\mu_{\cdot}$	Death rate of M. tuberculosis population	$0.5\ \mathrm{day}^{-1}$
k_1	Rate $CD4^+$ T cells become infected by free virus	$2.4\times\ 0^{-5}\ \mathrm{mm}^3\ \mathrm{day}^{-1}$
k_2	Rate macrophages become infected by free virus	$2.0\times\ 0^{-6}\ \mathrm{mm}^3\ \mathrm{day}^{-1}$
g_V	Rate macrophages produce virus	$1.0\times\ 0^{-6}\ \mathrm{mm}^3\ \mathrm{day}^{-1}$
k_3	Rate $CD8^+$ T cells kill virus	$7.4\times\ 0^{-4}\ \mathrm{mm}^3\ \mathrm{day}^{-1}$
k_4	Rate macrophages kill virus	$7.4\times\ 0^{-4}\ \mathrm{mm}^3\ \mathrm{day}^{-1}$
k_5	Rate T cells clear *M. tuberculosis*	$0.5\ \mathrm{mm}^3\ \mathrm{day}^{-1}$
k_6	Rate macrophages clear *M. tuberculosis*	$0.5\ \mathrm{mm}^3\ \mathrm{day}^{-1}$
r_T	Maximal proliferation of the T cell population	$0.02\ \mathrm{day}^{-1}$
r_{T_b}	Maximal proliferation of the *M. tuberculosis* population	$1.0\ \mathrm{day}^{-1}$
r_M	Recruitment rate of macrophage population	$2.5\times\ 0^{-7}\ \mathrm{day}^{-1}$
N_1	Number of free virus produced by infected T cells	100 – 1000
N_2	Number of free virus produced by macrophages	100 – 1000
C	Half saturation constant for the proliferation process	$1000\,\mathrm{mm}^{-3}$
K	Carrying capacity for the M. tuberculosis population	$1000\,\mathrm{mm}^{-3}$
M_0	Equilibrium value for the macrophage population	$100\,\mathrm{mm}^{-3}$

Once again the model dynamics are assumed to take in a single compartment, where this time the compartment is taken to be the lymph tissue. Model parameters for HIV in Table 2 are obtained from peripheral blood data; however, the lymph and periphery are generally assumed to be in parallel [62]. The model uses four variables to describe the different population dynamics. $T(t)$ represents the armed CD4+ and CD8+ T cell populations at time t in days, $M(t)$ represents the macrophage population, $V(t)$ represents the HIV virion population and $T_b(t)$ represents the *M. tuberculosis* population**.** The model is explained as follows.

Eqn. (28a) represents the change in the T cell population. This equation models the change in the T cell population in a manner analogous to eqn. (16a), c.f. Section 6.3.1. for a term-by-term explanation, with the only difference being in the third term where T cells are stimulated to proliferate by the presence of both virus and bacteria instead of virus alone.

Eqn. (28b) represents the change in the macrophage population. The inclusion of an equation representing macrophagic dynamics is important for the following reasons. Macrophages play an important role in the pathogenesis of TB [44], infected macrophages act as a reservoir for HIV by slowly budding new viral particles [54, 104] and infected macrophages can infect $CD4^+$ cells through the presentation of antigen [2, 85]. The first term of eqn. (28b) represents the birth-death process for macrophages. This is followed by a term representing the loss of macrophages due to infection of by HIV virions. The final term represents the increase in the population of macrophages due to macrophagic recruitment and stimulation in response to the presence of pathogen.

We note from eqn. (28a) and (28b) that although macrophages and T cells are both immune system cells their production are not modelled as parallel processes. The production of T cells is modelled via a Michaelis-Menten type response term which depends on the antigenic stimulation due to both HIV and TB and has a single recruitment rate, i.e. r_T. Modelling T cell production in this way is believed to encompass

the desired effects [76]. Macrophagic production, on the other hand, is bilinear with the antigenic stimulation due to HIV being distinct from that due to TB with each having a different rate of production, i.e. r_M^1 and r_M^2 respectively. The production of macrophages is modelled in this way since macrophagic production due to antigenic stimulation is not as yet fully understood. Therefore by using a bilinear type response term one allows for the possibility that production rates due to antigenic stimulation by HIV could well be different from that due to TB.

Eqn. (28c) represents the change in the HIV virion population. The first term is a virion source term. The first part of the first term represents the increase in virion population due to virion production by infected T cells. It carries over from the loss due to infection term of eqn. (28a) with an additional factor N_1 in front to account for the virion burst size. The term's second part represents the increase in virion population due to the virion production by infected macrophages. Similarly it too is a carry over term. It carries over from the macrophage loss due to infection term of eqn. (28b) with an additional factor N_2 for the macrophage burst size. Observe that, when this term carries over, the parameter k_2 changes to g_V. This is done because macrophage infection is not well understood; therefore it is necessary to allow for the possibility that the virion production rate (g_V) could be different than the virion infection rate (k_2). The second term of the equation is a loss term. It represents a decline in virion population due to immune clearance in that $CD8^+$ T cells and macrophages clear or kill HIV virions and infected cells. The final term of the equation represents the clearance of viral particles due to death since HIV virions have a finite life-span.

The final equation of the model, eqn. (28d), represents the change in the *M. tuberculosis* population. The first term of the equation represents bacterial growth in the form of a logistic growth term with carrying capacity denoted by the constant K. Next there is a clearance term due to death of bacilli as a result of *M. tuberculosis* having a finite life-span. The final term represents the immune clearance of *M. tuberculosis* by T cells and macrophages.

The aim of the immune system-HIV-TB model is to capture the dynamics that take place during the primary infection and asymptomatic period of disease progression, that is to say, the simulation is run until it reaches its steady state, where the steady-state represents the asymptomatic stage. There are four different permutations of steady states that the model can exhibit. These are the uninfected steady-state (no HIV or TB infection), HIV-infected steady-state (only HIV infection), TB-infected steady-state (only TB infection), and the coinfected steady-state (both HIV and TB infection). The simulation is run for each in turn.

7.2. Simulations

7.2.1. Uninfected Steady-State

Setting HIV and TB to zero, Figure 21 shows simulations of the uninfected state. Numerical solutions of the T cell and macrophage populations are seen to converge to positive steady-state values. One can easily verify from eqns. (28a) and (28b) that in the absence of infection steady-state solutions for T cells and macrophages are S_T/μ and M_0 respectively. The simulation is started with initial conditions slightly away from the steady-state values in order to demonstrate the nature of convergence for both populations.

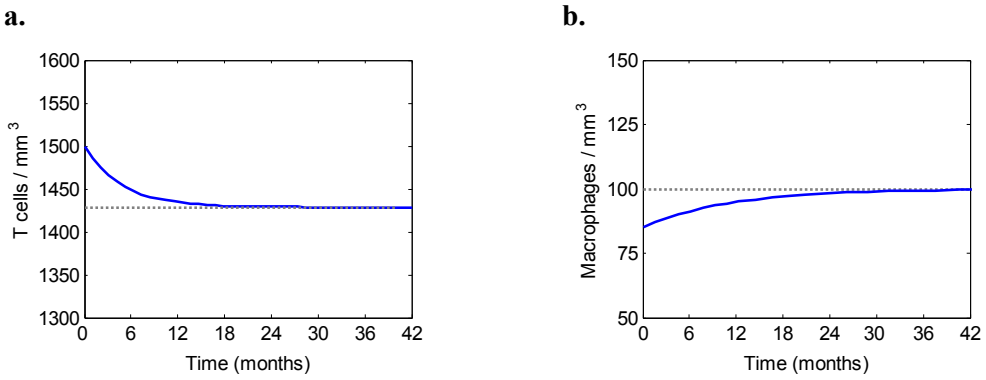

Figure 21: Simulations of the uninfected state (no HIV or TB infection). The model is seen to converge to its steady-state values, which when solved analytically are given by S_T/μ for the T cell population and M_0 for the macrophage population.

7.2.2. HIV Infected Steady-State

Setting TB to zero, the population graphs of Figure 22 for the numerical solution of the HIV infected steady-state shows that the model is able to approximate the primary and asymptomatic stage (quasi steady-state stage) of HIV infection. In a clinical setting during initial infection we find a large spike in viral load that is short lived; thereafter the immune system brings the viral load down and it settles to a quasi steady-state. Typically the spike's maximum occurs between 10^3 and 10^5 virons per mm^3. Once viral load stabilises, there is great variation amongst individuals as to what level it stabilises; nevertheless it usually settles in the range 10 to 100 virons per mm^3 and subsequently increases with disease progression. On inspection of Figure 22a one finds that the HIV population graph displays the qualitative and quantitative dynamics described above. The spike of the viral load graph peaks at $5.8\times\ 0^4$ virions per mm^3 and its set-point value is 88 virions per mm^3. Similarly, the qualitative behaviour of the T cell count and macrophage population, Figures 22b and 22c respectively, are also as one would expect them to be in that at the beginning there is a decline in the T cell count and macrophage population due to loss from initial HIV infection; however, subsequently to this there is an increase in each population as a result of antigenic stimulation of an immune response followed by both populations settling down to their set-point values.

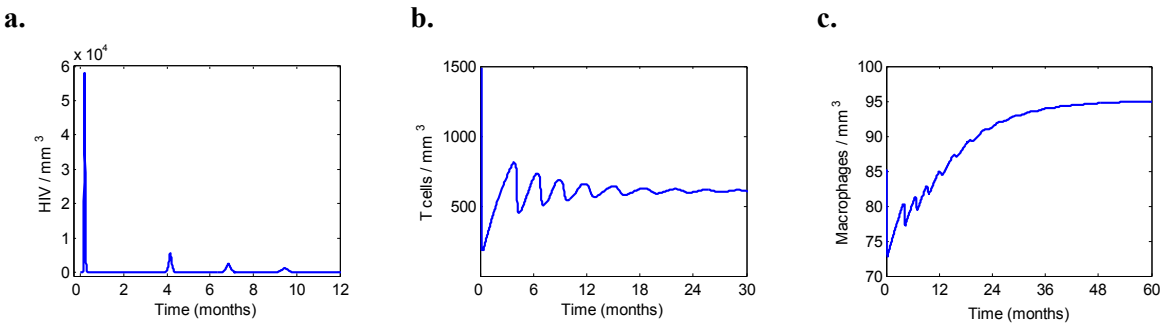

Figure 22: Simulations of the HIV infected state (HIV but no TB infection). After initial HIV infection there is a short-lived spike in the viral load; thereafter it settles down to its steady-state value. The T cell and macrophage populations initially experience a decline due to the HIV infection, but thereafter they experience an increase due to antigenic stimulation of the immune system before settling down the their set-point values. These dynamics, as displayed by the model, are typical of the qualitative behaviour of HIV infection before the onset of the immune system collapse.

7.2.3. TB Infected Steady-State

Setting HIV to zero, we find that the population graphs of Figure 23 for the TB infected state show that the T cell, macrophage, and *M. Tuberculosis* populations all progress to positive steady-state values. The TB bacteria population's positive steady-state value is indicative of chronic TB infection.

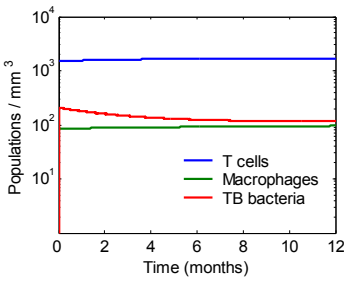

Figure 23: Simulations of the TB infected state (TB but no HIV infection). The TB bacteria population progresses to a set-point value of 115 TB bacteria per mm^3, thereby establishing a chronic TB infection.

7.2.4. Coinfected Steady-State

Simulations for coinfection are shown in Figure 24. When both diseases are present, one can clearly see the adverse effects that TB infection has on an HIV-positive person. This is shown by the plot of the HIV population in Figure 24a where the set-point value is approximately 250 virons per mm^3, as compared with 88 virons per mm^3 seen in the graph of HIV alone in Figure 22a. As was noted in section 4.3, an increased viral load is a very worrying sign indeed as it is used as a prognostic indicator for the speed of the onset of AIDS. The increase in viral load shown by the model simulations are due to an increase in susceptible cells (T cells and macrophages) which HIV virions can infect. As was previously discussed, a limitation in susceptible cells does limit the set-point of the viral load [108]. Thus an increase in susceptible cells increases the set-point of the viral load. The increase in T cells and macrophages are a result of increased antigenic stimulation from both the HIV and TB infections, as opposed to just one disease alone.

However, in a clinical setting the increase in viral load during coinfection might also be due to the overworked immune system having to simultaneously fight off two diseases instead of just HIV.

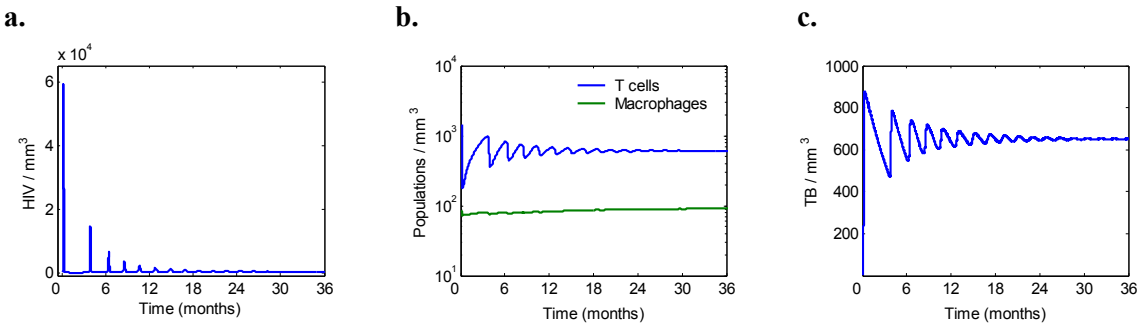

Figure 24: Simulations of the coinfected state (both HIV and TB infection). Coinfection with HIV and TB produces a greater viral load set-point, thus increasing the speed of the onest of AIDS.

Chapter 8

Modelling Coinfection Treatment

In South Africa HIV-positive individuals tend only to be diagnosed after the asymptomatic period of HIV infection when the immune system is collapsing and the individual is most likely to be coinfected with TB. Generally medical practitioners do not prescribe both antiretroviral and TB treatment concurrently. Antiretrovirals on their own have significant side-effects. Combining antiretroviral treatment with TB treatment escalates these adverse side-effects due to the overlapping toxicity profiles of both drug regimes and the large number of pills required to treat for each disease [35]. Moerover, drug-drug interactions could also lead to suboptimal therapeutic results [16]. Due to the severity of the side effects of the combined medications, strict adherence to the drug intake regime by coinfected individuals might be compromised. This could lead to grave implications for both diseases. Drug resistant strains of TB and HIV could develop and the rate of HIV disease progression would be significantly increased, signaling the earlier onset of AIDS.

The Centre for the AIDS Programme of Research in South Africa (CAPRISA) has commenced the START trial (STarting Anti-Retroviral Therapy). These trials are designed to resolve the question, when would the optimal point in time be to commence antiretroviral treatment in coinfected individuals? Researchers are still uncertain as to whether the best time to start antiretroviral treatment for HIV-TB coinfected individuals is at the beginning, the peak, or after the completion of the TB treatment phase. Clearly for reasons previously outlined one would hope to treat for HIV after completing TB treatment; however, this treatment strategy might not always be feasible. When disease progression for both infections is in advanced stages, death could result from either one of the diseases. One hopes that at the completion of the START trials there are clear guidelines established on how to treat such situations.

8.1. Model Development

In addition to clinical trials, by developing a mathematical model for HIV-TB coinfection which includes treatment, one can obtain clues as to what the most effective treatment strategies are likely to be. The development of such a model was undertaken during this dissertation. It was noted that there are certain desirable features that the model should possess. It should be able to simulate HIV infection and TB infection independently, as well as being able to simulate coinfection. The model should be able to simulate the treatment of HIV by both treatment mechanisms, that is protease inhibition and reverse transcriptase inhibition. We have seen that the coinfection model of Section 7.1 was able to simulate infection with each disease separately, as well as coinfection, and the HIV treatment models of Sections 6.2 and 6.3.5 incorporated features for modelling treatment with reverse transcriptase and protease inhibitors. Thus it would be prudent to combine the desirable mathematical structures of these models when constructing a model to stimulate the treatment of coinfection. In addition to the above we need to add TB treatment mechanisms, in terms of the bacteriostatic and bactericidal action of TB drugs. A new coinfection model was developed to successfully combine the desirable features of the previous models. This model has the ability of being easily modified to accept HIV and TB treatment (as we show below). Firstly we present the coinfection model excluding its treatment mechanisms. This new model is as follows

$$\frac{dT(t)}{dt} = {}_{T}(t) - \mu\ T(t) + {}_{2}T(t)\left[\frac{V(t) + {}_{b}(t)}{C + {}_{}(t) + {}_{b}(t)}\right] - {}_{V}T(t)V(t) \tag{29a}$$

$$\frac{dT^{i}(t)}{dt} = k_{V}T(t)V(t) - \mu_{,}\ T^{i}(t) - rT^{i}(t)\left[\frac{V(t)}{C + V(t)}\right] \tag{29b}$$

$$\frac{dM(t)}{dt} = \mu_{,,}\left[M_{0} - M(t)\right] - {}_{2}M(t)V(t) + M(t)\left[{}^{2}_{M}V(t) + {}^{1}_{M}T_{b}(t)\right] \tag{29c}$$

$$\frac{dM^{i}(t)}{dt} = {}_{2}M(t)V(t) - \mu_{,,i}M^{i} \tag{29d}$$

$$\frac{dV(t)}{dt} = \sqrt{}g_{VT}T^{i}(t) - {}_{T}T(t)V(t) + \sqrt{}_{2}g_{V}M^{i}(t) - {}_{4}M(t)V(t) - {}_{t}V(t) \qquad (29e)$$

$$\frac{dT_b(t)}{dt} = {}_{T_b}T_b(t)\left(K - {}_{b}(t)\right) - \mu_{\ }T_b(t) - {}_{b}(t)\left({}_{5}T(t) + {}_{6}M(t)\right). \qquad (29f)$$

We once again assume that the model dynamics take place in a single compartment, the lymph tissue. For the sake of continuity the variables used to describe the six populations employ the same notation as the previous models. $T(t)$ represents the T cell population at time t in days, $T^{i}(t)$ represents the HIV infected T cell population, $M(t)$ represents the macrophage population, $M^{i}(t)$ represents the HIV infected macrophage population, $V(t)$ represents the HIV virion population, and $T_b(t)$ represents the *M. tuberculosis* population. Model parameters are listed in Tables 1 and 2. The model is described as follows.

Eqns. (29a), (29c), and (29f) use the mathematical structure found in the coinfection model of Section 7.1, where term-by-term descriptions for each of the equations are given. Similarly eqn. (29b) can be found in the HIV model of Section 6.3.1.

Eqn. (29d) represents the change in the infected macrophage population. Its first term, which comes from the macrophagic loss due to HIV infection term in eqn. (29c), is carried over as a source term. The second term represents the natural death of macrophages due to finite life-span.

Eqn. (29e) gives the change in the HIV virion population. The first term is a source term that represents budding of virions from infected T cells with the rate that infected T cells produce virus denoted by g_{VT} and the burst size denoted by N. The second term comes from eqn. (16c) Section 6.3.1. The third is a source term that represents virion budding from infected macrophages with the rate that infected macrophages produce virus denoted by g_V and the burst size denoted by N_2. The fourth and fifth terms come from eqn. (28c) Section 7.1.

From the discussion above one notes that this new model has been developed by using many of the structures found in models that were reviewed earlier in this dissertation. The sole purpose of developing a new model in this way is to allow it to accept treatment for HIV and TB so that the different treatment scenarios that arise when treating for HIV-TB coinfection can be tested. It is shown below that this model can easily facilitate the therapeutic mechanisms used to simulate both HIV and TB treatment.

However, before any treatment strategies are tested one has firstly to ensure that the model is able to simulate disease progression accurately. The model is evaluated by comparing its results to the published models that were presented earlier, where a discussion of these models' ability to simulate disease progression had already been undertaken and established. Due to the fact that the model was developed by using many of the structures of existing models, it is shown that in many cases the model reduces to and thus displays several of the desirable features of the existing models.

As an initial test one can show that in the absence of any pathogens the model displays steady-state values for T cells and macrophages that are consistent with the Kirschner coinfection model of Section 7.1. This is done by noting that on inspection of eqns. (29a) – (29f) one recognises that in the uninfected state the model reduces to the uninfected state of the Kirschner model. The model dynamics for the uninfected state are displayed in Figures 21a and 21b. Similarly for the TB-infected state this new model also reduces to the Kirschner model. Model dynamics for the TB-infected state are shown in Figure 23.

Moreover in the HIV-infected state eqns. (29a) – (29f) share similarities to the HIV model of Section 6.3.1. The difference between the two is that this new model has an added equation, eqn. (29d), used to represent infected macrophagic dynamics. Numerical simulation of the new model for Primary and asymptomatic HIV infection is shown in Figures 25.

8.2. Model Simulations

8.2.1. Primary and Asymptomatic HIV Infection

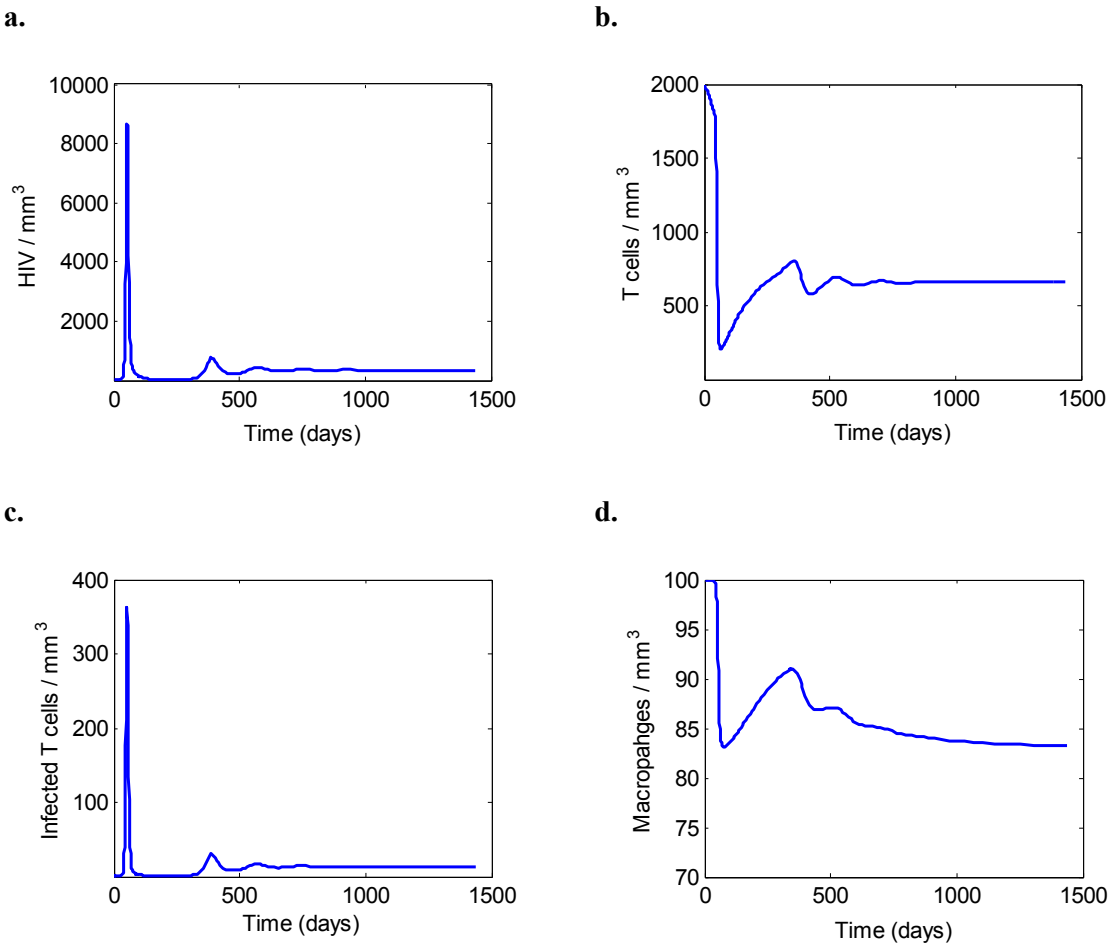

Figure 25: Simulations of the Primary and asymptomatic stage of HIV infection. The qualitative and quantitative dynamics displayed is in keeping with the general clinical observations of HIV disease progression.

The numerical simulations shown in Figure 25, depicting primary and asymptomatic infection for the HIV infected state, show that the model is able to approximate virus dynamics according to what clinical records suggest (see Section 7.2.2.). One finds that the viral load does display the characteristic initial short-lived spike; thereafter it settles down to its steady-state value depicting the onset of the asymptomatic stage of infection. The T cell and infected T cell populations' qualitative dynamics are also in good

agreement with what happens clinically in that during primary infection there is a dip in the T cell population and a spike in the infected T cell population. Thereafter the T cell population increases due to antigenic stimulation and the infected T cell population decreases due to specific immune responses and possible target cell limitation, whereupon they then settle down to their set-point values signalling the onset of the asymptomatic stage of infection.

Furthermore examining the model quantitatively we have noted previously that according to clinical records of viral load the spike should peak in the range 10^3 – 10^5 virons per mm^3 and the set-point value should settle in the range 10 – 100 virons per mm^3. Figure 25a shows that the simulation's viral quantitative dynamics does also agree with these clinical observations.

8.2.2. Complete Course of HIV Infection

Since we have now established the model's ability to simulate primary and asymptomatic stages of disease progression, one can test subsequent stages of disease progression. Typically after a few years of the asymptomatic stage of infection the immune system inevitably starts to collapse resulting in the onset of AIDS. The reasons for the immune system collapsing are not fully understood by immunologists; however, there is much ongoing biological research to determine the cause. Using the present model one can simulate the immune system collapse by assuming that the virion production rates of infected T cells (g_{VT}) and macrophages (g_V) are increased over the period of a year [76]. This could be caused by mutations, increased efficiency in virion production or the immune system's inability to contain virion production any longer due to, for example, large numbers of latently infected cells becoming active.

The complete course of HIV infection is shown in Figure 26. After an asymptomatic period of a few years, in this case five years into the infection, the viral production rate of both infected T cells and macrophages are simultaneously increased over the following year. This simulates the immune system collapsing, thereby signalling the onset of AIDS.

Figure 26 shows the immune system collapsing from the 1800th day (5th year) onward. Towards the end of the 2160th day (6th year) both the T cell count and macrophage population are descending steeply while the viral load experiences a similarly dramatic ascent. These dynamics, as displayed by the model, are typical of the generalised clinical observations of the HIV disease progressing towards AIDS with the eventual collapse of the immune system.

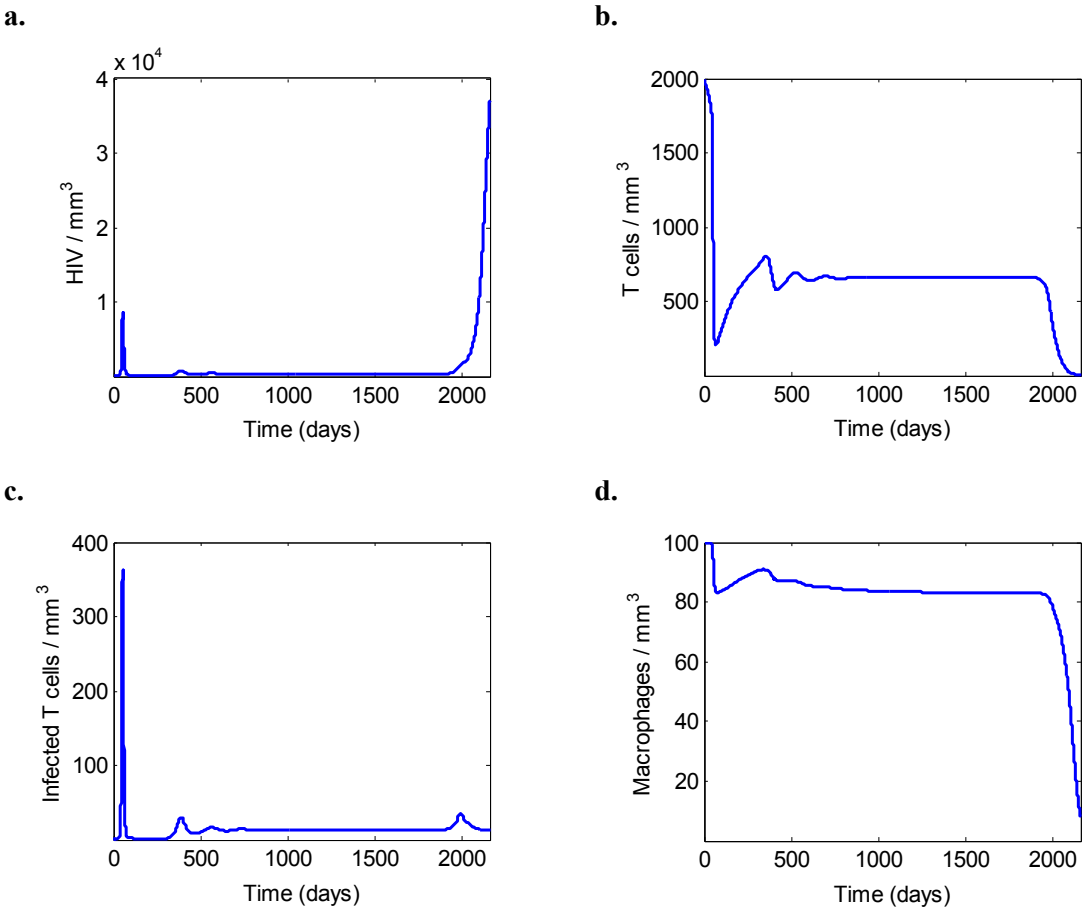

Figure 26: Simulations of the complete course of HIV infection. By the 5th year the immune system begins to display signs of collapsing, thus signaling the onset of AIDS. Towards the end of the 6th year the immune system is almost totally eroded resulting in full-blown AIDS and possibly even death.

8.2.3. HIV-TB Coinfection

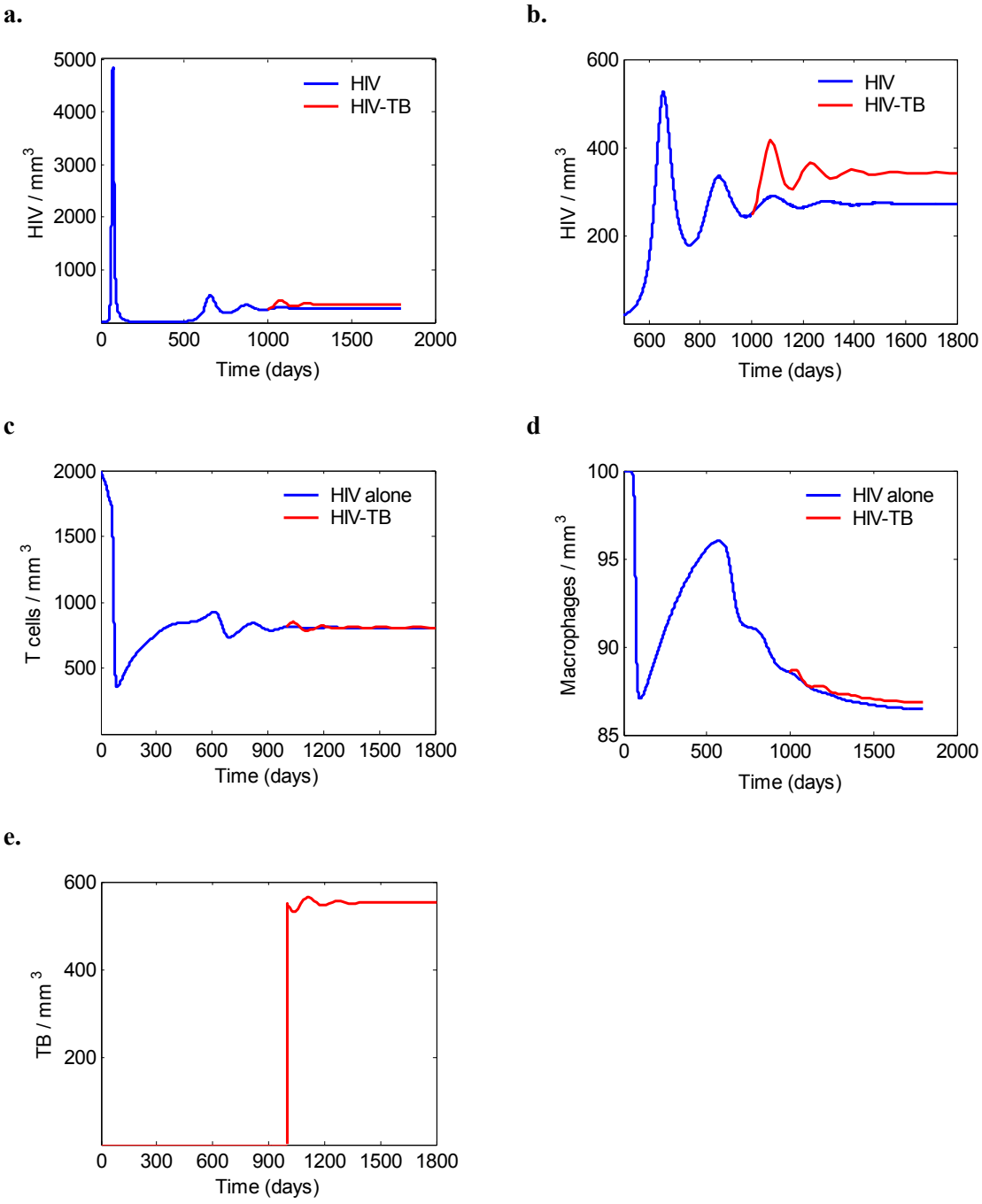

Figure 27: Simulations of the HIV-TB coinfection. The model is able to demonstrate that HIV-TB coinfection results in a higher set-point viral load when compared to HIV infection alone.

It has been noted earlier that an HIV-TB coinfected individual is more likely to progress rapidly toward AIDS than the person who has HIV alone. One of the factors that are indicative of rapid disease progression is the viral load. In general a higher viral load correlates with an increased likelihood of rapidly progressing towards AIDS. One way to test the model's ability to display realistic clinical characteristics is to test whether TB infection in an HIV-positive individual does indeed increase the viral load which would thereby cause the immune system to collapse in a shorter amount of time.

Figure 27 simulates HIV-TB coinfection by introducing TB into the system on the 1000^{th} day, about two and three quarter years, into HIV infection. Figures 27a and 27b show that coinfection results in an associated increase in viral load. The set-point viral load for HIV alone is about 282 virions per mm^3. This is compared to 341 virions per mm^3 for HIV-TB coinfection, which represents an increase of 25% in the viral load of the coinfected individual over the HIV-infected individual. The coinfected individual's higher viral load would normally result in the immune system collapsing in a shorter amount of time. As has been discussed in Section 7.2.4, the higher viral load is due to the fact that there are more susceptible cells (macrophages and T cells) for HIV virions to infect. Figures 27c and 27d show that T cell and macrophage populations are slightly higher for HIV-TB coinfection than for HIV infection alone. This is as expected since the introduction of another pathogen, TB, into the system stimulates T cells and macrophages to increase their numbers in order to fight off the additional diseases. However, the already overworked immune system struggles to keep TB in check. From figure 27e one finds that the bacterial levels rapidly increase before settling to its set-point value establishing chronic TB infection.

8.3. Modelling Treatment

Having evaluated the model to ensure that it simulates the dynamics of HIV-TB coinfection in a realistic manner, we are now able to tackle the fundamental reason for building the HIV-TB coinfection model, which is to use the model to test the different

treatment strategies for coinfection. We add treatment mechanisms to the coinfection model, eqns (29a) – (29f), in the following way.

We firstly consider the treatment of HIV. One recalls that HIV chemotherapy uses protease and reverse transcriptase inhibitors. Protease inhibitors cause the formation of noninfectious virions. Consequently eqn. (29e), which models the HIV virions population, is divided by the therapeutic action of protease inhibition into two subpopulations. These subpopulations are the infectious HIV virions (V_i), and the non-infectious HIV virions (V_{ni}), where the total virion population is given by $V = V_i + V_{ni}$. The action of protease inhibitors is modelled by including $(1-\varepsilon_{PI})$ in front of the infectious HIV virions source terms, and ε_{PI} in front of the noninfectious HIV virions source terms. ε_{PI} ranges from 0 to 1 with $\varepsilon_{PI} = 1$ simulating a 100% effective protease inhibitor.

The second class of anti-HIV drugs, reverse transcriptase inhibitors, inhibits the HIV virion's ability to infect successfully immune system cells such as T cells and macrophages. Thus the HIV infection terms of eqn. (29) for macrophages and T cells, $k_V T(t)V(t)$ and $k_2 M(t)V(t)$ respectively, are modified by appending $(1-\varepsilon_{RT})$ in front. ε_{RT} ranges from 0 to 1 with $\varepsilon_{RT} = 1$ simulating a 100% effective protease inhibitor.

Now turning our attention to the anti-TB drugs we recall that their therapeutic mechanisms of action were their bacteriostatic and bactericidal action. Bacteriostatic drugs inhibit the growth of the bacterial population and are therefore modelled by including $(1-\varepsilon_B)$ in front of the logistic growth term of eqn. (29f). ε_B ranges from 0 to 1 with $\varepsilon_B = 1$ simulating a 100% effective growth inhibitor. Bactericidal drugs actively kill the bacterial population and are therefore modelled by appending β_B to the bacterial death term of eqn. (29f), where $\beta_B \geq 0$. $\beta_B = 0$ has a 0% efficacy, but this increases as β_B is increased.

Applying the antiretroviral and TB-dug therapeutic mechanisms to eqn. (29) yields a new HIV-TB coinfection model with treatment.

$$\frac{dT(t)}{dt} = {}_T(t) - \iota\, T(t) - 1 - {}_{\cdot T})k_V T(t)V_i(t) + r_2 T(t)\left[\frac{V_i(t)+V_{ni}(t)+T_b(t)}{C+V_i(t)+V_{ni}(t)+T_b(t)}\right] \tag{30a}$$

$$\frac{dT^i(t)}{dt} = 1 - {}_{\cdot T})k_V T(t)V_i(t) - {}_{\cdot i}T^i(t) - rT^i(t)\left[\frac{V_i(t)+V_{ni}(t)}{C+V_i(t)+V_{ni}(t)}\right] \tag{30b}$$

$$\frac{dM(t)}{dt} = \iota\, M_0 - M(t) - 1 - {}_{\cdot T})k_2 M(t)V_i(t) + M(t)\left[{}^2_M(V_i(t)+{}_{ni}(t)) + {}^1_M T_b(t)\right] \tag{30c}$$

$$\frac{dM^i(t)}{dt} = (1 - {}_{\cdot T})k_2 M(t)V_i(t) - {}_{\cdot i}M^i \tag{30d}$$

$$\frac{dV_i(t)}{dt} = 1-\varepsilon_{\cdot I})Ng_{VT}T^i(t) - {}_T T(t)V_i(t) + 1 - {}_{\cdot I})N_2 g_V M^i(t) - {}_4 M(t)V_i(t) - \iota\, V_i(t) \tag{30e}$$

$$\frac{dV_{ni}(t)}{dt} = \varepsilon_{\cdot I}Ng_{VT}T^i(t) - {}_T T(t)V_{ni}(t) + {}_{\cdot I}N_2 g_V M^i(t) - {}_4 M(t)V_{ni}(t) - \iota\, V_{ni}(t) \tag{30f}$$

$$\frac{dT_b(t)}{dt} = 1 - {}_{\cdot b})r_{T_b}T_b(t)\left(K - {}_b(t)\right) - {}_{\cdot b}\mu_{\cdot b}T_b(t) - {}_b(t)\left[{}_5 T(t) + {}_6 M(t)\right] \tag{30g}$$

We can now use this model to test the different coinfection treatment scenarios for treating HIV-TB coinfected individuals. Initially we test simultaneous treatment of HIV and TB. We then simulate treating for TB first and once that is completed treating for HIV. By using the TB first HIV second treatment strategy there are two different scenarios that can be tested, these are: the commencement of treatment early on during the immune system collapse and the commencement of treatment late into the immune system collapse. Such a simulation is relevant since some individuals would be able to commence treatment early due to already having been diagnosed HIV-positive before the symptomatic stages of HIV disease progression. Treatment can typically begin with the first signs of an AIDS-related complex such as TB. Others, mainly in developing countries, are not aware of their HIV status until late into their immune system collapse. Thus treatment commences much later. Concluding the simulations for HIV-TB treatment, the final simulation that is tested treats HIV first and then TB. This treatment strategy is not practical (see section 8.3.4.), but is included to demonstrate the ability of mathematical models to test situations that would otherwise not be feasible.

8.3.1. Simultaneous HIV-TB Treatment

Having already pointed out that treating HIV and TB simultaneously is generally not recommended, we note that the simulations for concurrent treatment shown in Figure 28 considers only the levels of the various populations that constitute the immune system-HIV-TB model and does not take into account adverse side-effects or drug-drug interactions.

On inspecting the simulations for the simultaneous treatment of HIV and TB shown in Figure 28 one finds that, when both drug regimes are administered concurrently, the best results in terms of decreasing viral and bacterial loads and increasing immune system cells are obtained, as compared to treating TB then HIV shown in Figures 30 and 31 respectively.

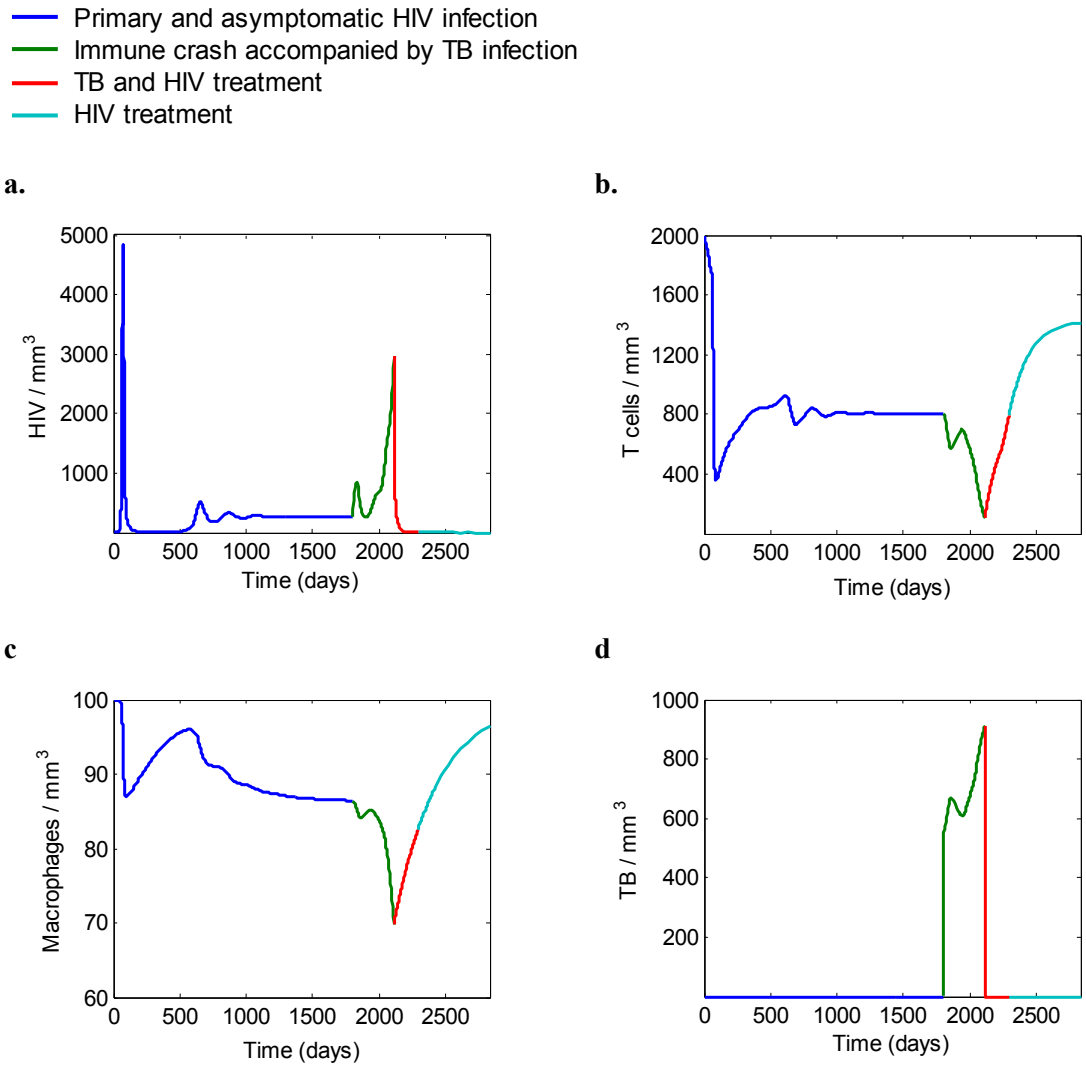

Figure 28: Simulations of the simultaneous treatment of HIV and TB. The viral load is brought down to undetectable levels by the 27th week of treatment; nevertheless, HIV treatment has to be continued indefinitely. The TB treatment course lasts 6 months by which time TB infection is eliminated from the system.

In Figure 28a the antiretroviral treatment commences on day 2112 when the viral load is 2961 virions per mm^3 and decreases the viral load to undetectable levels (< 0.05 virions per mm^3) by day 2301. This represents a time frame of 27 weeks. Current guidelines for antiretroviral therapy suggest that viral load should be brought down to undetectable levels by between 16–24 weeks [109]. Thus the simulations time frame of 27 weeks is realistic especially when considering that initially the individual was HIV-TB coinfected and had a high viral load.

On examining Figure 28d one finds that as a result of TB treatment the TB bacteria are decreased to levels very close to zero in a short space of time. Thus one might be tempted to cease TB treatment as soon as this happens. In practice TB treatment is carried out for 180 days so as to ensure all traces of the bacteria, no matter how minute, are killed. As an example one sees from the simulation of the premature cessation of TB treatment shown in figure 29 that even when the TB bacterial population is reduced to almost zero and TB treatment is stopped, an almost instant rebound in the bacterial population does occur. Therefore it is necessary to complete the entire 180 days of the anti-TB drug course.

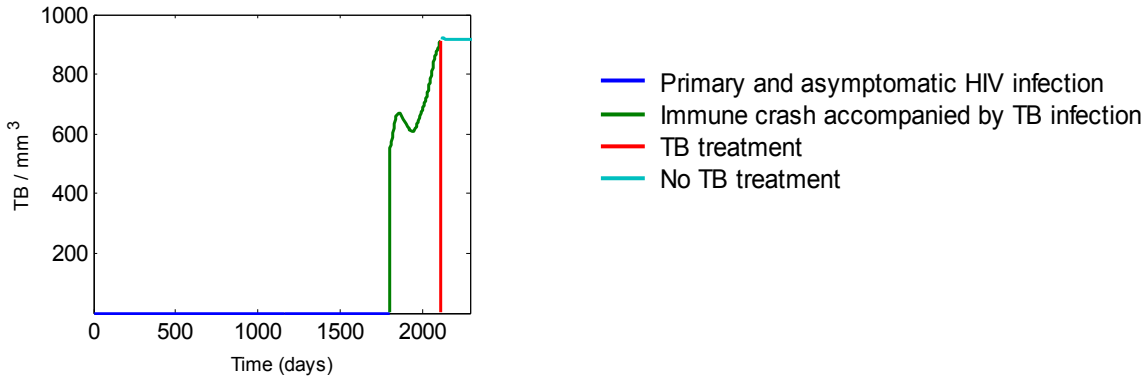

Figure 29: Simulation of premature cessation of TB treatment. One finds that TB treatment rapidly brings the bacterial levels close to zero; however, if treatment is stopped prematurely, a rebound in the TB infection occurs just as rapidly.

8.3.2. Treating TB then HIV: Advanced Stages of Immune Collapse

When treating coinfected individuals most medical practitioners recommend treating for TB first and then HIV so as to minimise the compounded side effects and drug-drug interactions between the antiretroviral and antibacterial drugs. Figures 27a and 27b show that, when TB is introduced into the body, the HIV viral load increases. One can now use the model to test if the converse is true, that is, by treating TB does the HIV viral load decrease? If this be the case, it might not be necessary to treat both HIV and TB simultaneously, thus sparing the coinfected individual from any compounded side effects and drug-drug interactions that might result from simultaneous treatment.

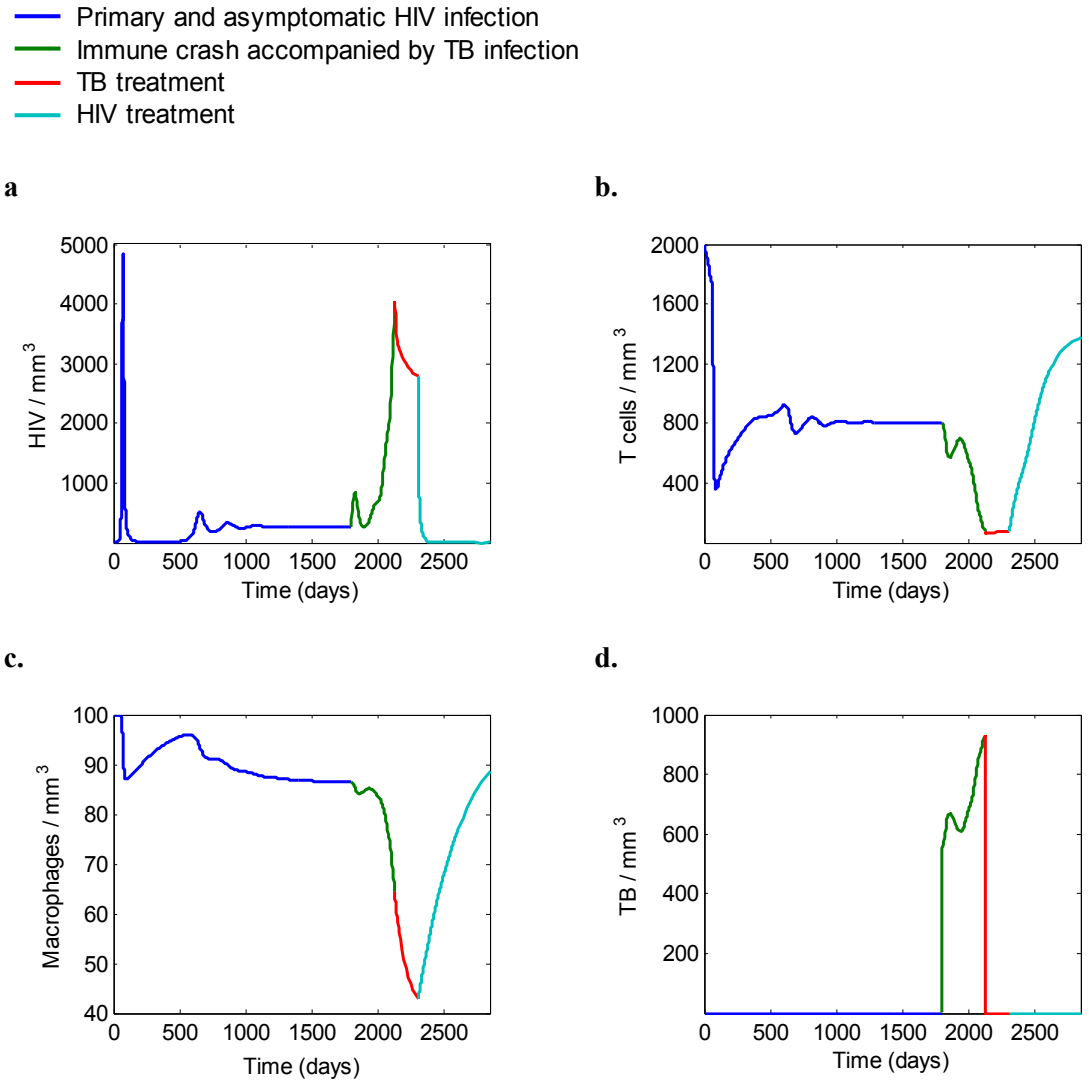

Figure 30: Simulations of treating TB then HIV at advanced stages of immune system collapse. One finds that treating TB first does indeed decrease the viral load and halts T cell decline. However, since treatment started late into the immune system collapse, this might not be enough to ensure the coinfected individual's survival.

Figure 30 shows simulations of treating of TB then HIV, where treatment is commenced at advanced stages into the immune system collapse when the T cell count is 72 T cells per mm^3 and the viral load is 4005 virions per mm^3. One finds that treating TB does indeed decrease the viral load. The viral load decreases from about 4005 to 2897 virions per mm^3. Moreover Figure 30b shows (red portion of graph where there is a flat plateau) that the T cell population halts its decline and stabilises during TB treatment.

Nevertheless the TB drugs do not help to increase significantly the T cell count. The patient is left with a T cell count of around 77 T cells per mm^3 after TB treatment where the pretreatment level was 72 T cells per mm^3. A viral load of 2897 per mm^3 and a T cell count of 77 per mm^3 are indeed dangerous and could result in death. Here the TB drugs alone are not enough to ensure the patient's survival and in this case the medical practitioner might have no choice but to treat for both diseases, complications resulting from simultaneous treatment notwithstanding.

In Figure 30 treatment was only commenced very late into the immune system collapse. Nevertheless we have seen that TB treatment does decrease the viral load as well as stabilise the T cell count, thus preventing it from falling any further. One might hypothesise that, if we treat TB early in the immune system collapse, for example, when the T cell count just dips under 200 per mm^3, it might not be necessary to treat for both diseases, thereby avoiding any complication arising from simultaneous treatment. We test this hypothesis in the simulations shown in Figure 31.

8.3.3. Treating TB then HIV: Early Stages of Immune Collapse

Figure 31 shows the results of simulating the commencement of TB treatment during early stages in the immune system collapse. Viral load and T cell count at the beginning of TB treatment are 1935 virions and 198 T cells per mm^3 respectively. Figure 31b shows that, when TB is treated early on during the immune system collapse, in this case when the T cell count dips just below 200 per mm^3, the TB treatment is able to halt the T cell decline and stabilise the T cell level (red portion of Figure 31b where there is a flat plateau) at 198 T cells per mm^3 by the end of the TB treatment period. A similar situation is observed for the viral load shown in Figure 31a. Here the TB treatment results in stabilising the viral load and keeping it relatively steady at about 1137 virions per mm^3. A viral load of 1137 virions per mm^3 and a T cell count of 198 per mm^3 are much safer levels compared to those observed in the treatment of TB at advanced stages of the immune system collapse, which were 2897 virions per mm^3 and 77 T cells per mm^3 respectively. A comparison of the early versus late commencement of TB treatment

shows that the late treatment has an associated viral load that is approximately 60.8% greater than early treatment and a T cell count that is about 61.1% less than early treatment. Consequently, if the patient is in the early stages of the immune system collapsing, medical practitioners might deem it unnecessary to expose patients to complications arising from treating both HIV and TB simultaneously and treat only for TB.

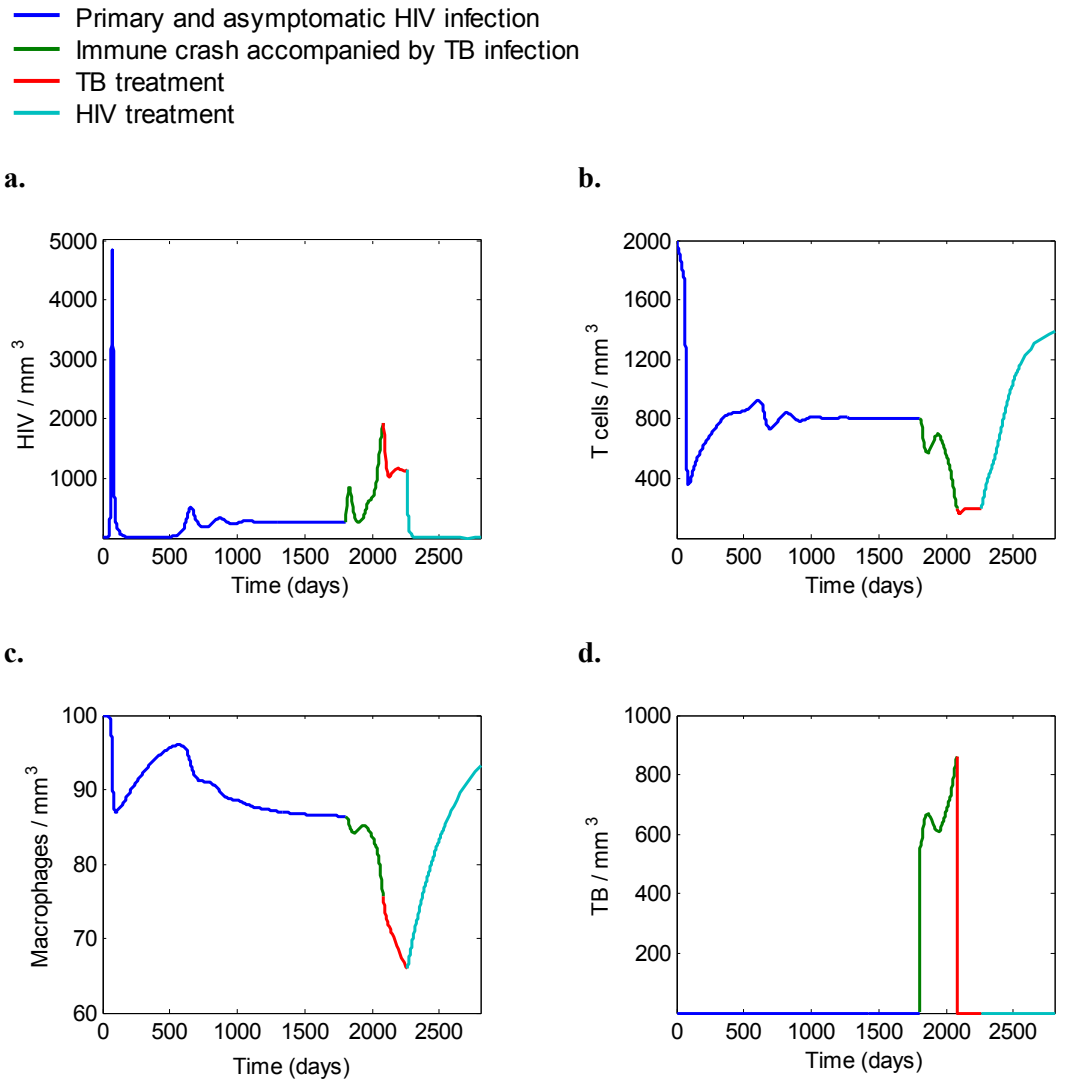

Figure 31: Simulations of treating TB then HIV at early stages of immune system collapse. By treating TB at early stages of the immune system collapse, one is able to halt the decline in T cells and lower the viral load to acceptable levels so that concurrent HIV-TB treatment would not be necessary.

8.3.4. Treating HIV then TB

An interesting simulation that can be performed is treating HIV first and then TB. Such experiments show the utility of developing mathematical models, which allows us the opportunity to experiment with simulations that are not clinically practical. All simulations so far have treated TB first as this is the method utilised by CAPRISA to run their START trials. CAPRISA adopts this method for the following reason. One might hypothesise that by treating HIV first the immune system might recover sufficiently to hold off the possible danger that TB poses to the coinfected individual; however, once HIV treatment has commenced one cannot suspend the treatment of HIV to treat TB since this might promote the evolution of mutant strains of HIV. This would serve only to further jeopardise the coinfected individual. Thus, if one commences by treating for HIV first, one has to treat for TB while treating for HIV and would therefore still be faced with the compounded side effects and drug-drug interactions of combining HIV and TB treatment. The only realistic hope one has of negating the possibility of simultaneous treatment is to treat for TB first. Nevertheless, even though treating HIV first is not practical in a clinical setting, by using the model one can simulate this treatment strategy.

Simulations of the treatment of HIV in an HIV-TB coinfected individual are shown in Figure 32. One observes in Figure 32a that when antiretroviral treatment is initiated on day 2112 the viral load is decreased to below 0.05 virions per mm^3 by day 2298. From Figures 32b and 32c one finds that by the 2298^{th} day the T cell count and macrophage population recover substantially and the individual reverts once more to the asymptomatic stage of disease progression. Figure 32d shows that the immune system is again able to suppress the *M. tuberculosis* population and keep it at a low level.

From the dynamics observed in Figure 32 one sees that treating HIV first in an HIV-TB coinfected individual could be a very desirable strategy. With new HIV drugs in the developmental phase that target different treatment mechanisms than the ones being currently used there might just be some hope of implementing this treatment strategy since one might treat HIV initially with one class of HIV drugs, then treat TB and

thereafter treat HIV once again with a different class of HIV drugs. By using the different classes of HIV drugs before and after TB treatment one could possibly reduce the risk of HIV-drug resistance.

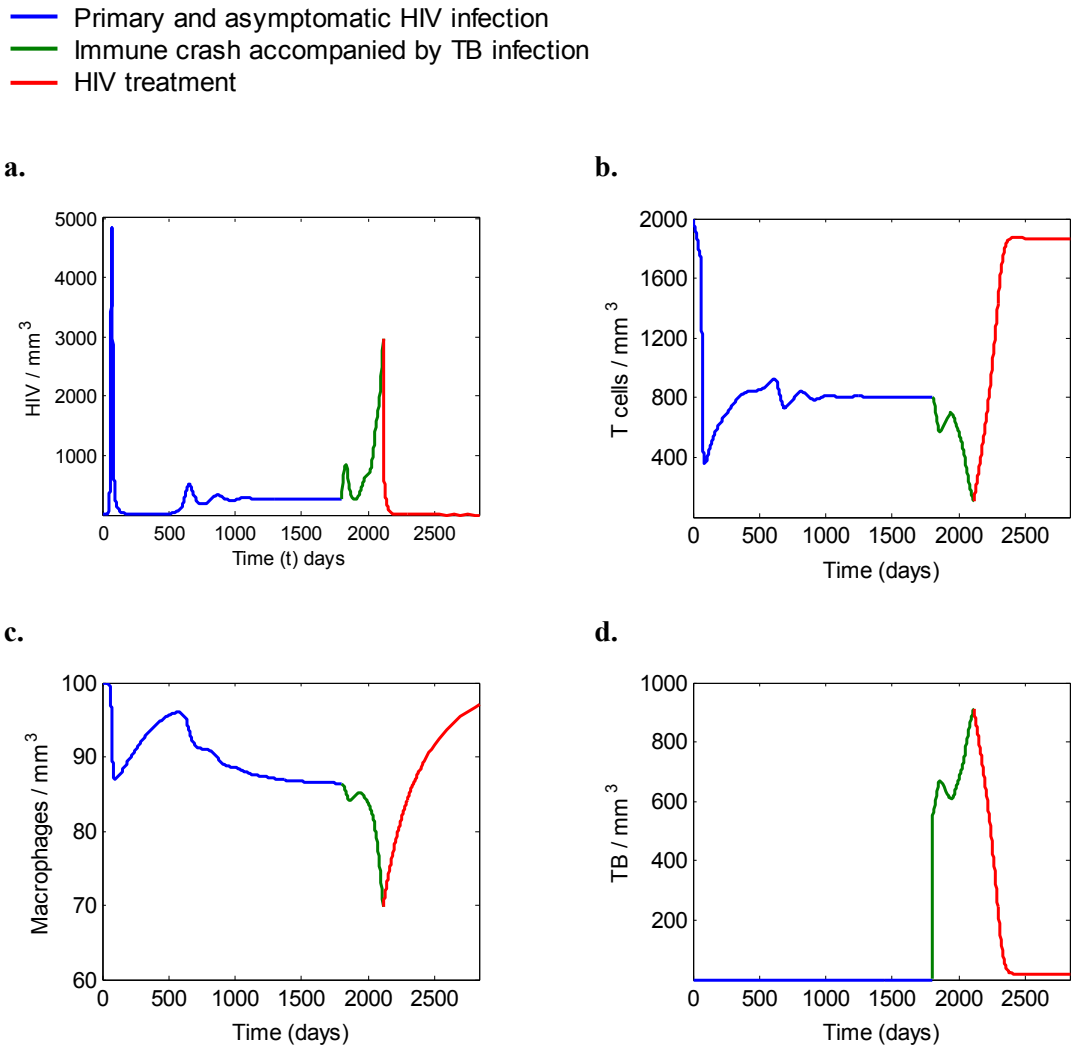

Figure 32: Simulations of treating HIV in an HIV-TB coinfected individual. By treating HIV first one is able to bring down the viral load and allow immune reconstitution to take place. Once the immune system has recovered it is able to once again suppress the TB infection.

Chapter 9

Conclusion

Medical practitioners are often faced with the question, when should one treat for TB in HIV coinfected individuals? The significance of this question is great enough to warrant medical trials in attempting to answer it. As we have noted, HIV-TB coinfection poses a considerable problem in Sub-Saharan Africa. It is therefore of utmost importance that we understand the dynamics involving the treatment of HIV-TB coinfection.

Bearing these facts in mind this dissertation was undertaken. After a review of the scientific literature many examples of HIV models were found, several of these models also included treatment mechanisms for anti-HIV drugs. However, with regards to mathematical models of HIV-TB coinfection only one model was found even though coinfection is endemic in Sub-Saharan Africa. This model did not include any treatment mechanisms for HIV or TB, but did offer a framework on which a model with treatment mechanisms could be built.

In order to facilitate mechanisms for anti-HIV treatment into the model, one was able to draw on the large array of existing HIV treatment models. Since no treatment models for TB could be found, one had to model TB treatment according to the known mechanisms of interaction of anti-TB drugs. The challenge that lay ahead was manipulating all these separate constituent elements to develop an HIV-TB coinfection model which included treatment mechanisms for both diseases. Once this had been achieved one was then in a unique position to be able to offer insights and predictions purely from simulations into the different treatment strategies used to treat coinfection. Although clinical trials rightfully are at the core of medical research of this nature, model simulations do offer certain advantages. Model simulations are far less time intensive and require fewer resources in terms of funding and personnel to run.

The dissertation culminated with the development of a coinfection model with treatment mechanisms, which was presented in Chapter 8. One could now test the different scenarios of coinfection treatment and offer some suggestions for optimising treatment strategies. The model simulations of Section 8.3.2. demonstrated that, if one treats HIV-TB co-infection at advanced stages of the immune system collapsing towards AIDS, treating initially for TB alone might not be enough to allow sufficient immune reconstitution to ensure the individual's survival. In this case it might be necessary to simultaneously treat for both diseases even though the combination of the two drug regimes might have undesirable consequences. Nevertheless the model simulations of Section 8.3.3. show that there are situations when the simultaneous treatment of coinfection might not be necessary. These simulations revealed that if an individual is co-infected during relatively early stages of the immune system collapsing one might treat for TB alone before treating for HIV. In addition there were other useful features that the model was able to demonstrate, for example, the model showed in Section 8.3.2. that, if TB treatment is not carried out for the complete six month course, TB infection can rebound even if the infection seems to be cleared when the individual ceases treatment. Model simulation of Section 8.3.4. showed that, if one could treat for HIV first without treating for TB, the immune system would recover sufficiently to allow the coinfected individual the opportunity to stop HIV treatment and treat for TB alone. However, after TB treatment is completed and HIV treatment is started once again, the emergence of resistance to anti-HIV drugs could worsen the individual's prognosis. Nevertheless a possible solution to this problem was offered in that one could use different types (having different therapeutic mechanisms) of anti-HIV drugs before and after TB treatment.

The results above serve to illustrate that mathematical models are useful tools when applied to medical and biological settings. Previously it was through the use of a mathematical model in HIV/AIDS research that a major breakthrough in understanding the dynamics of the disease during the latent stage of infection was achieved. Contrary to popular belief at the time the model was able to counter-intuitively demonstrate that viral dynamics are not static during asymptomatic stage of infection. In fact HIV virions are

being produced and cleared at the astonishing rate of 10 billion virions per day. Similarly the model that was developed during this dissertation was able to offer some useful insights even if they were very much in keeping with what one would intuitively expect. Since the model was built from known biological interactions, results that reinforce one's intuition do serve the purpose of enhancing one's confidence of its validity.

Mathematical modelling offers a rigorous method of building a conceptual framework when attempting to understand the dynamics of a disease. Clearly there is a great need for the interdisciplinary collaboration between mathematicians, immunologists and even computational scientists. As a result of the staggering infection rates and numbers of people who have been previously infected with HIV, there is a lot of quantitative data that has been amassed over the years. This data can be used to calibrate model parameters and test model hypotheses. These models can in turn be used to make predictions for disease progression and improve our understanding of disease dynamics. Disease modelling is currently a very active field of research with many interesting and challenging possibilities for future work.

References

1. Adamson C.S. and Jones I.M. 2004. The molecular basis of HIV capsid assembly – five years of progress. *Rev. Med. Virol.* **14**, 107–121.

2. Aquaro S., Calio R., Balzarini J., *et al*. 2002. Macrophages and HIV infection: therapeutical approaches toward this strategic virus reservoir. *Antiviral Res.* **55**, 209–225.

3. Barre-Sinoussi F. 1996. HIV as the cause of AIDS. *Lancet* **348**, 31–35.

4. Barre-Sinoussi F., Chermann J.C., Rey F., *et al.* 1983. Isolation of a T-lymphotropic retrovirus from a patient at risk for acquired immune deficiency syndrome (AIDS). *Science* **220**, 868–871.

5. Bass J.B. Jr., Farer L.S., Hopewell P.C., *et al.* 1994. Treatment of tuberculosis and tuberculosis infection in adults and children: American Thoracic Society and the Centers for Disease Control and Prevention. *Am. J. Respir. Crit. Care Med.* **149**, 1359–1374.

6. Blattner W.A. 1991. HIV epidemiology: past, present, future. *FASEB J.* **5**, 2340–2348.

7. Blumberg H.M., Burman W.J., Chaisson R.E., *et al.* 2003. American Thoracic Society/Centers for Disease Control and Prevention/Infectious Diseases Society of America: treatment of tuberculosis. *Am. J. Respir. Crit. Care Med.* **167**, 603–662.

8. Bogacki P. and Shampine L. F. 1989. A 3(2) pair of Runge-Kutta formulas. *Appl. Math. Letters* **2**, 1–9.

9. Bogacki P. and Shampine L. F. 1996. An Efficient Runge-Kutta (4,5) Pair. *Computers Math. Applic.* **32**, 15–28.

10. Bonhoeffer S., Coffin J.M. and Nowak M.A. 1997. Human immunodeficiency virus drug therapy and virus load. *J. Virol.* **71**, 3285–3288.

11. Bonhoeffer S., May R.M., Shaw G.M., *et al.* 1997. Virus dynamics and drug therapy. *Proc. Natl. Acad. Sci. USA* **94**, 6971–6976.

12. Borrow P., Lewicki H., Hahn B.H., *et al.* 1994. Virus-specific $CD8^+$ cytotoxic T-lymphocyte activity associated with control of viremia in primary human immunodeficiency virus type 1 infection. *J. Virol*. **68**, 6103–6110.

13. Boyle M. and Senior K. 2002. *Human Biology*. Harper Collins, London.

14. Brum G., Mckane L. and Karp G. 1995. *Biology Fundamentals*. John Wiley & Sons, New York.

15. Bukrinskaya A., Brichacek B. and Mann A. 1998. Establishment of a functional human immunodeficiency virus type 1 (HIV-1) reverse transcription complex involves the cytoskeleton. *J Exp Med.* **188**, 2113–2125.

16. Burman W.J. and Jones B.E. 2001. Treatment of HIV-related tuberculosis in the era of effective antiretroviral therapy. *Am. J. Respir. Crit. Care Med.* **164**, 7–12.

17. Campbell E.A., Korzheva N., Mustaev A., *et al.* 2001. Structural mechanism for rifampicin inhibition of bacterial RNA polymrase. *Cell* **104**, 901–912.

18. Chan D., Fass D., Berger J., *et al.* 1997. Core structure of gp41 from the HIV envelope glycoprotein. *Cell* **89**, 263–273.

19. Chinen J. and Shearer W.T. 2002. Molecular virology and immunology of HIV infection. *J. Allergy. Clin. Immunol.* **110**, 189–98.

20. Chiu I.-M., Yaniv A., Dahlberg J.E., *et al.* 1985. Nucleotide sequence evidence for relationship of AIDS retrovirus to lentiviruses. *Nature* **317**, 366–368.

21. Ciuffia A. and Bushmana F.D. 2006. Retroviral DNA integration: HIV and the role of LEDGF/p75. *Trends Genet*. **22**, 388–395.

22. Coffin J.M. 1995. Exploring the mysteries of the retrovirus. *Science Year 1995*, 122–137.

23. Coffin J.M. 1995. HIV population dynamics in vivo: implications for genetic variation, pathogenesis, and therapy. *Science* **267**, 483–489.

24. Concorde Coordinating Committee 1994. MRC/ANRS randomised double-blind controlled trial of immediate and deferred zidovudine in symptom-free HIV infection. *Lancet* **343**, 871–881.

25. Connor R.I., Mohri H., Cao Y., *et al.* 1993. Increased viral burden and cytopathicity correlate temporally with $CD4^+$ T-lymphocyte decline and clinical progression in human immunodeficiency virus type 1-infected individuals. *J. Virol.* **67**, 1772–1777.

26. Conti L., Fantuzzi L., Del Corno M., *et al.* 2004. Immunomodulatory effects of the HIV-1 gp120 protein on antigen presenting cells: implications for AIDS pathogenesis. *Immunobiology* **209**, 99–115.

27. Corbett E.L., Watt C.J., Walker N., *et al.* 2003. The growing burden of tuberculosis: global trends and interactions with the HIV epidemic. *Arch. Intern. Med.* **163**, 1009–1021.

28. Cox P.H., Martin M.A., Styer C.M., *et al.* 1990. Outcomes of treatment with AZT of patients with AIDS and symptomatic HIV infection. *Nurse Pract.* **15**, 36–43.

29. Curtis H. 1985. *Biology 4th edition*. Worth Publishers, New York.

30. Daar E.S., Moudgil T., Meyer R.D., *et al.* 1991. Transient high levels of viremia in patients with primary human immunodeficiency virus type 1 infection. *N. Engl. J. Med.* **324**, 961–964.

31. Daley C.L., Small P.M., Schecter G.F., *et al.* 1992. An outbreak of tuberculosis with accelerated progression among persons infected with the human immunodeficiency virus. An analysis using restriction-fragment-length polymorphisms. *N. Engl. J. Med.* **326**, 231–235.

32. Dalgleish A.G., Beverly P.C.L., Clapham P.R., *et al.* 1984. The CD4 (T4) antigen is an essential component of the receptor for the AIDS retrovirus. *Nature* **312**, 763–767

33. De Boer R.J. and Perelson A.S. 1998. Target cell limited and immune control models of HIV infection: a comparison. *J. Theor. Biol.* **194**, 201–214.

34. De Cock K.M., Coulibaly I.M. and Lucas S.B 1992. Tuberculosis and HIV infection in sub-Saharan Africa. *J. Amer. Med. Assoc.* **268**, 1581–1587.

35. Dean G.L., Edwards S.G., Ives N.J, *et al.* 2002. Treatment of tuberculosis in HIV-infected persons in the era of highly active antiretroviral therapy. *AIDS* **16**, 75–83.

36. Deng H., Liu R., Ellmeier W., *et al.* 1996. Identification of a major co-receptor for primary isolates of HIV-1. *Nature* **381**, 661–666.

37. Deng L., Mikusova K., Robuck K.G., *et al.* 1995. Recognition of multiple effects of ethambutol on metabolism of mycobacterial cell envelope. *Antimicrob. Agents Chemother.* **39**, 694–701.

38. Doranz B.J., Baik S.S., and Doms R.W. 1999. Use of a gp120 binding assay to dissect the requirements and kinetics of human immunodeficiency virus fusion events. *J. Virol.* **73**, 10346–10358.

39. Dormand J. R. and Prince P. J. 1980. A family of embedded Runge-Kutta formulae. *J. Comp. Appl. Math.* **6**, 19–26.

40. Dye C., Scheele S., Dolin P., *et al.* 1999. Consensus statement. Global burden of tuberculosis: estimated incidence, prevalence, and mortality by country. WHO global surveillance and monitoring project. *J. Amer. Med. Assoc.* **282**, 677–686.

41. Edwards M. and Nucci M.C. 2006. Application of Lie group analysis to a core group model for sexually transmitted diseases. *J. Nonlinear Math. Phys.* **13**, 211–230.

42. Enserink M. 2001. Driving a stake into resurgent TB. *Science* **293**, 234–235.

43. Epp S.S. 1995. *Discrete Mathematics with Applications 2nd Edition.* Brooks/Cole, California.

44. Fenton M.J. and Vermeulen M.W. 1996. Immunopathology of tuberculosis: roles of macrophages and monocytes. *Infect. Immun.* **64**, 683–690.

45. Fischl M.A., Richman D.D., Hansen N., *et al.* 1990. The safety and efficacy of AZT in the treatment of subjects with mildly symptomatic HIV type 1. *Ann. Int. Med.* **112**, 727–737.

46. Flynn J.L. 2004. Mutual attraction: does it benefit the host or the bug? *Nat. Immunol.* **8**, 778–779.

47. Freed E. O. 1998. HIV-1 Gag proteins: diverse functions in the virus life cycle. *Virology* **251**, 1–15.

48. Furuta R.A., Wild C.T., Weng Y., *et al.* 1998. Capture of an early fusion-active conformation of HIV-1 gp41. *Nat. Struct. Biol.* **5**, 276–279.

49. Gallo R. and Montaigner L. 2002. Prospects for the future. *Science* **298**, 1730–1731.

50. Gallo R., Salahuddin S.Z., Popovic M., *et al.* 1984. Frequent detection and isolation of cytopathic retroviruses (HTLV-III) from patients with AIDS and at risk for AIDS. *Science* **224**, 500–503.

51. Gallo S.A., Finnegan C.M., Viard M., *et al.* 2003. The HIV Env-mediated fusion reaction. *Biochim. Biophys. Acta* **1614**, 36–50.

52. Gao F., Bailes E., Robertson D.L., *et al.* 1999. Origin of HIV-1 in the chimpanzee Pan troglodytes troglodytes. *Nature* **397**, 436–441.

53. Gelderblom H.R., Hausmann E.H., Ozel M., *et al.* 1987. Fine structure of human immunodeficiency virus (HIV) and immunolocalization of structural proteins. *Virology* **156**, 171–176.

54. Gendelman H.E., Orenstein J.M., Baca L.M., *et al*. 1989. The macrophage in the persistence and pathogenesis of HIV infection. *AIDS* **3**, 475–495.

55. Glatthaar E. 1991. *Tuberculosis*. Academica, Pretoria.

56. Glickman G.S. and Jacobs W.R. Jr. 2002. Microbial pathogenesis of Mycobacterium tuberculosis: dawn of a discipline. *Cell* **104**, 477–485.

57. Goletti D., Weissman D., Jackson R.W., *et al.* 1996. Effect of Mycobacterium tuberculosis on HIV replication: role of immune activation. *J. Immunol*. **157**, 1271–1278.

58. Goto T., Nakai M. and Ikuta K. 1998. The life-cycle of human immuno-deficiency virus type 1. *Micron* **29**, 123–138.

59. Gottlinger H.G. 2001. The HIV-1 assembly machine. *AIDS* **15 suppl. 5**, S13–S20.

60. Graham N.M., Zeger S.L., Park L.P., *et al.* 1992. The effects on survival of early treatment of HIV infection. *N. Engl. J. Med.* **326**, 1037–1042

61. Grant A.D., Djomand G. and De Cock K.M. 1997. Natural history and spectrum of disease in adults with HIV/AIDS in Africa. *AIDS* **11 suppl. B**, S43–S54.

62. Haase A.T., Henry K., Zupancic M., e*t al*. 1996. Quantitative image analysis of HIV-1 infection in lymphoid tissue. *Science* **284**, 985–989.

63. Hahn B.H., Shaw G.M., De Cock K.M., *et al.* 2000. AIDS as a zoonosis: scientific and public health implications. *Science* **287**, 607–614.

64. Hamilton J.D., Hartigan P.M., Simberkoff M.S., *et al.* 1992. A controlled trial of early vs. late treatment with AZT in symptomatic HIV infection. *N. Engl. J. Med.* **326**, 437–443.

65. Henderson L.E., Sowder R.C., Copeland T.D., *et al.* 1990. Gag precursors of HIV and SIV are cleaved into six proteins found in the mature virions. *J. Med. Primatol.* **19**, 411–419.

66. Herz A.V.M., Bonhoeffer S., Anderson R.M., *et al.* 1996. Viral dynamics in vivo: limitations on estimates of intracellular delay and virus decay. *Proc. Natl. Acad. Sci. USA* **93**, 7247–7251.

67. Hill C.P., Worthylake D., Bancroft D.P., *et al.* 1996. Crystal structures of the trimeric human immunodeficiency virus type 1 matrix protein: implications for membrane association and assembly. *Proc. Natl. Acad. Sci. U.S.A.* **93**, 3099−3104.

68. Houben E.N., Nguyen L., and Pieters J. 2006. Interaction of pathogenic mycobacteria with the host immune system. *Curr Opin Microbiol.* **9**, 76–85.

69. Hu Y., Coates A.R., and Mitchison D.A. 2006. Sterilising action of pyrazinamide in models of dormant and rifampicin-tolerant Mycobacterium tuberculosis. *Int. J. Tuberc. Lung Dis.* **10**, 317–322.

70. Hui J., Gordon N. and Kajioka R. 1977. Permeability barrier to rifampin in mycobacteria. *Antimicrob. Agents Chemother.* **11**, 773–779.

71. Jindani A, Dore C.J. and Mitchison D.A. 2003. Bactericidal and sterilizing activities of antituberculosis drugs during the first 14 days. *Am. J. Respir. Crit. Care Med.* **167**, 1348–1354.

72. Jonassen T.O., Stene-Johansen K., Berg E.S., *et al.* 1997. Sequence analysis of HIV-1 group O from Norwegian patients infected in the 1960s. *Virology* **231**, 43–47.

73. Kassa E., Rinke de Wit T.F., Hailu E., *et al.* 1999. Evaluation of the World Health Organization staging system for HIV infection and disease in Ethiopia: association between clinical stages and laboratory markers. *AIDS* **13**, 381–389.

74. Kaufmann G.R., Cunningham P., Kelleher A.D., *et al.* 1998. Patterns of viral dynamics during primary human immunodeficiency virus type 1 infection. *J. Infec. Dis.* **178**, 1812–1815.

75. Kirschner D. 1999. Dynamics of co-infection with M. tuberculosis and HIV-1. *Theoret. Popul. Biol.* **55**, 94–109.

76. Kirschner D. and Webb G.F. 1996. A model for treatment strategy in the chemotherapy of AIDS. *Bull. Math. Biol.* **58**, 367–390.

77. Kirschner D., Mehr R. and Perelson A. 1998. The role of the thymus in adult and pediatric HIV-1 infection. *J. AIDS Human Retrov.* **18**, 95–109.

78. Kliger Y., Peisajovich S.G., Blumenthal R., *et al.* 2000. Membrane-induced conformational change during the activation of HIV-1 gp41. *J. Mol. Biol.* **301**, 905–914.

79. Koch R. 1932. The etiology of tuberculosis. *Am. Rev. Tuberc.* **25**, 285–323.

80. Korber B., Muldoon M., Theiler J., *et al.* 2000. Timing the ancestor of the HIV-1 pandemic strains. *Science* **288**, 1789–1796.

81. Koup R.A., Safrit J.T., Cao Y., *et al.* 1994. Temporal association of cellular immune responses with the initial control of viremia in primary human immunodeficiency virus type 1 syndrome. *J. Virol.* **68**, 4650–4655.

82. Kuznetsov Y. G., Victoria J. G., Robinson W. E., *et al.* 2003. Atomic force microscopy investigation of human immunodeficiency virus (HIV) and HIV-infected lymphocytes. *J. Virol.* **77**, 11896–11909.

83. Lemey P., Pybus O.G., Wang B., *et al.* 2003. Tracing the origin and history of the HIV-2 epidemic. *Proc. Natl. Acad. Sci. U.S.A.* **100**, 6588–6592.

84. Lenderking W.R., Gelber R.D., Cotton D.J., *et al.* 1994. Evaluation of the quality of life associated with zidovudine treatment in asymptomatic human immunodeficiency virus infection. *N. Engl. J. Med.* **330**, 738–743.

85. Lewis C.E. and Mcgee J. 1992. *The Macrophage*. IRL Press, Oxford.

86. Little S.J., McLean A.R., Spina C.A., *et al.* 1999. Viral dynamics of acute HIV-1 infection. *J. Exp. Med.* **190**, 841–850.

87. Lotka A.J. 1925. *Elements of Physical Biology*. Williams & Wilkins, Baltimore.

88. Lukashov V.V. and Goudsmit J. 1997. Evolution of the human immunodeficiency virus type 1 subtype-specific V3 domain is confined to a sequence space with a fixed distance to the subtype consensus. *J. Virol.* **71**, 6332–6338.

89. Massiah M.A., Starich M.R., Paschall C., *et al.* 1994. Three-dimensional structure of the human immunodeficiency virus type 1 matrix protein. *J. Mol. Biol.* **244**, 198–223.

90. Melamud A., Kosmorsky G.S. and Michael S.L. 2003. Ocular ethambutol toxicity. *Mayo Clin. Proc.* **78**, 1409–1411.

91. Mellors J.W., Kingsley L.A., Rinaldo C.R., *et al.* 1995. Quantitation of HIV-1 RNA in plasma predicts outcome after seroconversion. *Ann. Intern. Med* **122**, 573–579.

92. Mellors J.W., Munoz A., Giorgi J.V., *et al.* 1997. Plasma viral load and $CD4^+$ lymphocytes as prognostic markers of HIV-1 infection. *Ann. Intern. Med.* **126**, 946–954.

93. Morgan D., Mahe C., Mayanja B., *et al.* 2002. HIV-1 infection in rural Africa: is there a difference in median time to AIDS and survival compared with that in industrialized countries? *AIDS* **16**, 597–603.

94. Morse D., Brothwell D.R. and Ucko P.J. 1964. Tuberculosis in ancient Egypt. *Am. Rev. Respir. Dis.* **90**, 524–541.

95. Munoz A., Sabin C.A. and Phillips A.N. 1997. The incubation period of AIDS. *AIDS* **11 suppl. A**, S69–76.

96. Munoz A., Wang M.-C, Bass S., *et al.* 1989. Acquired immunodeficiency syndrome (AIDS)-free time after human immunodeficiency virus type 1 (HIV-1) seroconversion in homosexual men. *Am. J. Epidemiol.* **130**, 530–539.

97. Nakata K., Rom W., Honda Y., *et al.* 1997. Mycobacterium tuberculosis enhances human immunodeficiency virus-1 replication in the lung. *Am. J. Respir. Crit. Care Med.* **155**, 996–1003.

98. Nerlich A.G., Haas C.J., Zink A., *et al.* 1997. Molecular evidence for tuberculosis in an ancient Egyptian mummy. *Lancet* **350**, 1404.

99. Nielsen M.H., Pederson F.S. and Kjems J. 2005. Molecular strategies to inhibit HIV-1 replication. *Retrovirology* **2**, 10–15.

100. Nowak M.A. and Bangham C.R.M. 1996. Population dynamics of immune responses to persistent viruses. *Science* **272**, 74–79.

101. Nowak M.A. and May R.M. 2000. *Virus Dynamics: Mathematical Principles of Immunology and Virology*. Oxford University Press, Oxford.

102. Nucci M.C. 1997. The role of symmetries in solving differential equations. *Mathl. Comput. Modelling* **25**, 181–193.

103. Oni A.A. 2005. Education: an antidote for the spread of HIV/AIDS. *J. Assoc. Nurses AIDS Care* **16**, 40–48.

104. Orenstein J.M., Fox C. and Wahl S.M. 1997. Macrophages as a source of HIV during opportunistic infections. *Science* **276**, 1857–1861.

105. Pantaleo G., Demarest J.F., Schacker T., *et al.* 1997. The qualitative nature of the primary immune response to HIV infection is a prognosticator of disease progression independent of the initial level of plasma viremia. *Proc. Natl. Acad. Sci. USA* **94**, 254–258.

106. Peisajovich S.G., Blank L., Epand R.F., *et al.* 2003. On the interaction between gp41 and membranes: the immunodominant loop stabilizes gp41 helical hairpin conformation. *J. Mol. Biol.* **326**, 1489–1501.

107. Perelson A.S., Neumann A.U., Markowitz M., *et al.* 1996. HIV-1 dynamics in vivo: virion clearance rate, infected cell life-span, and viral generation time. *Science* **271**, 1582–1586.

108. Phillips A.N. 1996. Reduction of HIV concentration during acute infection: independence from a specific immune response. *Science* **271**, 497–499.

109. Phillips A.N., Miller V., Sabin C., *et al*. 2001. Durability of HIV-1 viral suppression over 3.3 years with multi-drug antiretroviral therapy in previously drug-naive individuals. *AIDS* **15**, 2379–2384.

110. Popovic M., Sarngadharan M.G., Read E., *et al.* 1984. Detection, isolation, and continuous production of cytopathic retroviruses (HTLV-III) from patients with AIDS and pre-AIDS. *Science* **224**, 497–500.

111. Poulsen A.-G., Aaby P., Jensen H., *et al.* 2000. Risk factors for HIV-2 seropositivity among older people in Guinea-Bissau. A search for the early history

of HIV-2 infection. *Scand. J. Infect. Dis.* **32**, 169–175.

112. Preston B.D., Poiesz B.J., and Loeb L.A. 1988. Fidelity of HIV-1 reverse transcriptase. *Science* **242**, 1168–1171.

113. Raman K., Rajagopalan P. and Chandra N. 2005. Flux balance analysis of mycolic acid pathway: Targets for anti-tubercular drugs. *PLoS Comput. Biol*. **1**, e46.

114. Raulin J. 2002. Human immunodeficiency virus and host cell lipids. Interesting pathways in research for a new HIV therapy. *Prog. Lipid Res.* **41**, 27–65.

115. Reid A., Scano F., Getahun H., *et al.* 2006. Towards universal access to HIV prevention, treatment, care, and support: the role of tuberculosis/HIV collaboration. *Lancet Infect. Dis.* **6**, 483–495.

116. Revilla T. and Garcia-Ramos G. 2003. Fighting a virus with a virus: a dynamic model for HIV-1 therapy. *Math. Biosci.* **185**, 191–203.

117. Roberts J.D., Bebenek K. and Kunkel. T.A. 1988. The accuracy of reverse transcriptase from HIV-1. *Science* **242**, 1171–1173.

118. Rozwarski D.A., Grant G.A., Barton D.H.R., *et al.* 1998. Modification of the NADH of the Isoniazid Target (InhA) from Mycobacterium tuberculosis. *Science* **279**, 98–102.

119. Rue S.M., Roos J.W., Tarwater P.M., *et al.* 2005. Phosphorylation and proteolytic cleavage of gag proteins in budded simian immunodeficiency virus. *J Virol* **79**, 2484–2492.

120. Ruedy J., Schechter M. and Montaner J.S.G. 1990. Zidovudine for early HIV infection: who, when and how? *Ann. Int. Med.* **112**, 721–722.

121. Salemi M., Strimmer K., Hall W.W., *et al.* 2001. Dating the common ancestor of SIVcpz and HIV-1 group M and the origin of HIV-1 subtypes using a new method to uncover clock-like molecular evolution. *FASEB J.* **15**, 276–278.

122. Sarngadharan M.G., Popovic M., Bruch L., *et al.* 1984. Antibodies reactive with human T-lymphotropic retroviruses (HTLV-III) in the serum of patients with AIDS. *Science* **224**, 506–508.

123. Schneider M.F., Gange S.J., Williams C.M., *et al.* 2005. Patterns of the hazard of death after AIDS through the evolution of antiretroviral therapy: 1984–2004. *AIDS* **19**, 2009–2018.

124. Simon V., Ho D.D., and Abdool Karim Q. 2006. HIV/AIDS epidemiology, pathogenesis, prevention, and treatment. *Lancet* **348**, 489–504.

125. Smith I. 2003. Mycobacterium tuberculosis pathogenesis and molecular determinants of virulence. *Clin. Microbiol. Rev.* **16**, 463–496.

126. South African Department of Health 2000. Practical guidelines for the South African tuberculosis control programme, 2000. Pretoria, South Africa.

127. Stafford MA, Corey L., Cao Y., *et al.* 2000. Modeling plasma virus concentration during primary HIV infection. *J. Theor. Biol.* **203**, 285–301.

128. Stewart J. 1998. *Calculus, concepts and contexts*. Brooks/Cole, Pacific Grove, CA.

129. Stilianakisa N.I. and Schenzlec D. 2006. On the intra-host dynamics of HIV-1 infections. *Math. Biosci.* **199**, 1–25.

130. Thomason A.R. and Warren E.I. 2005. Tuberculosis: a clinical review. *US Pharm.* **30**, HS-14–HS-22.

131. Torrisi V. and Nucci M.C. 2001. Application of Lie group analysis to a mathematical model which describes HIV transmission. In: The Geometrical Study of Differential Equations (J.A. Leslie and T.P. Hobart, Eds.), *Contemp. Math.* **285**, 11–20. Amer. Math. Soc., Providence.

132. Turner B.G. and Summers M.F. 1999. Structural biology of HIV. *J. Mol. Biol.* **285**, 1–32.

133. van Crevel R., Ottenhoff T.H.M. and van der Meer J.W.M. 2002. Innate immunity to Mycobacterium tuberculosis. *Clin. Microbiol. Rev.* **15**, 294–309.

134. Vidal N., Mulanga C., Bazepeo S.E., *et al.* 2005. Distribution of HIV-1 variants in the Democratic Republic of Congo suggests increase of subtype C in Kinshasa between 1997 and 2002. *J. Acquir. Immune Defic. Syndr.* **40**, 456–462.

135. Vidal N., Peeters M., Mulanga C., *et al.* 2000. Unprecedented degree of human immunodeficiency virus type 1 (HIV-1) group M genetic diversity in the Democratic Republic of Congo suggests that the HIV-1 pandemic originated in central Africa. *J. Virol.* **74**, 10498–10507.

136. Volberding P.A., Lagakos S.W., Grimes J.M., *et al.* 1994. The duration of zidovudine benefit in persons with asymptomatic HIV infection. *J. Amer. Med. Assoc.* **272**, 437–442.

137. Volkow P., Mohar A., Terrazas J.J., *et al.* 2002. Changing risk factors for HIV infection. *Arch. Med. Res.* **33**, 61–66.

138. Volterra V. 1926. Variazioni e fluttuazioni del numero d'individui in specie animali conviventi. *Mem. Acad. Lincei. Roma.* **2**, 31–113.

139. Wallis R.S. and Ellner J.J. 1994. Cytokine and tuberculosis. *J. Leukocyte Biol.* **55**, 676–681.
140. Winder F.G. and Collins P.B. 1970. Inhibition by isoniazid of synthesis of mycolic acids in Mycobacterium tuberculosis. *J. Gen. Microbiol.* **63**, 41–48.

141. Witten G.Q. and Perelson A.S. 2004. Modelling the cellular-level interaction between the immune system and HIV. *S. Afr. J. Sci.* **100**, 447–452.

142. World Health Organisation 1990. Interim proposal for a WHO staging system for HIV infection and disease. *Wkly Epidemiol Rec.* **65**, 221–224.

143. World Health Organisation 2003. Treatment of tuberculosis: Guidelines for national programmes. Geneva.

144. World Health Organisation 2004. Global tuberculosis control – surveillance, planning, financing. Geneva.

145. World Health Organisation 2006. Global tuberculosis control – surveillance, planning, financing. Geneva.

146. Wu L., Gerard N.P., Wyatt R., *et al.* 1996. CD4-induced interaction of primary HIV-1 gp120 glycoproteins with the chemokine receptor CCR-5. *Nature* **384**, 179–183.

147. www.math.duke.edu/education/webfeats/Word2HTML/Predator.html

148. Yerly S., Kaiser L., Race E., *et al.* 1999. Transmission of antiretroviral-drug-resistant HIV-1 variants. *Lancet* **354**, 729–733.

149. Zhang Y., Nakata K., Weiden M., *et al.* 1995. Mycobacterium tuberculosis enhances human immunodeficiency virus-1 replication by transcriptional activation at the long terminal repeat. *J. Clin. Invest.* **95**, 2324–2331.

150. Zhang Y., Permar S. and Sun Z. 2002. Conditions that may affect the results of Mycobacterium tuberculosis susceptibility testing to pyrazinamide. *J. Med. Microbiol.* **51**, 42–49.

151. Zhang Y., Wade M.W., Scorpio A., *et al.* 2003. Mode of action of pyrazinamide: disruption of Mycobacterium tuberculosis membrane transport and energetics by pyrazinoic acid. *J. Antimicrob. Chemother.* **52**, 790–795.

152. Zhenga Y.-H., Lovsina N. and Matija Peterlina B. 2005. Newly identified host factors modulate HIV replication. *Immunol. Lett.* **97**, 225–234.

153. Zhu P., Chertova E., Bess J. Jr., *et al.* 2003. Electron tomography analysis of envelope glycoprotein trimers on HIV and simian immunodeficiency virus

virions. *Proc. Natl. Acad. Sci. U. S. A.* **100**, 15812–15817.

154. Zhu P., Liu J., Bess J. Jr., *et al.* 2006. Distribution and three-dimensional structure of AIDS virus envelope spikes. *Nature* **441**, 817–818.

155. Zhu T., Korber B.T., Nahmias A.J., *et al.* 1998. An African HIV-1 sequence from 1959 and implications for the origin of the epidemic. *Nature* **391**, 594–597.

156. Zimhony O., Cox J.S., Welch J.T., *et al.* 2000. Pyrazinamide inhibits the eukaryotic-like fatty acid synthetase I (FASI) of Mycobacterium tuberculosis. *Nat Med* **6**, 1043–1047.